Envelope Retrofits for Enhancing Thermal Comfort in Indian Residences Against the Backdrop of Global Warming

THESIS

Submitted in partial fulfilment of the requirements for the degree of

DOCTOR OF PHILOSOPHY

by

RAHUL UKEY

2018PHXF0031P

Under the supervision of
Dr. Aakash Chand Rai

and co-supervision of
Prof. Shyam Sunder Yadav

BIRLA INSTITUTE OF TECHNOLOGY & SCIENCE, PILANI – 333031 (RAJASTHAN), INDIA
2023

……Dedicated to my
beloved family……

Birla Institute of Technology & Science, Pilani
Pilani Campus

CERTIFICATE

This is to certify that the thesis entitled "**Envelope Retrofits for Enhancing Thermal Comfort in Indian Residences Against the Backdrop of Global Warming**" submitted by Rahul Ukey, ID. No. 2018PHXF0031P for the award of PhD degree of the Institute embodies original work done by him under our supervision.

Signature (Co-Supervisor)

Prof. Shyam Sunder Yadav

Associate Professor,

Department of Mechanical Engineering,

BITS Pilani, Pilani campus

Date:

Signature (Supervisor)

Dr. Aakash Chand Rai

Assistant Professor,

Department of Mechanical Engineering,

BITS Pilani, Pilani campus, and

Department of Sustainable Energy Engineering,

IIT Kanpur

Date:

First and foremost, I would like to express my deep gratitude and sincere thanks to my PhD supervisors **Dr. Aakash Chand Rai** and **Prof. Shyam Sunder Yadav,** for their stimulating guidance and unwavering support throughout my research work. This thesis could not have attained its present form in content and presentation without their active interest, direction and help. I am extremely grateful to both guides, who have been tremendous mentors for me, for their consistent support to overcome the difficulties so that I could confidently march towards completion of the research work.

I am grateful to **Prof. V Ramgopal Rao**, Vice-Chancellor, and **Prof. Sudhir Kumar Barai**, Director, BITS Pilani, Pilani Campus, for giving me the opportunity to pursue my research work at the institute. I sincerely thank **Prof. M. B. Srinivas**, Dean, Academic – Graduate Studies & Research (AGSR), and **Prof. Shamik Chakraborty**, Associate Dean, AGSR, for their official support and encouragement. I thank **Prof. Srikanta Routroy** (Head of Department) and the entire faculty and staff of the Department of Mechanical Engineering, BITS-Pilani, Pilani Campus, for their kind, moral support, and assistance.

I would also like to thank the doctoral advisory committee (DAC) members **Prof. Mani Sankar Dasgupta**, Professor, Department of Mechanical Engineering, Pilani Campus, and **Dr. A R Harikrishnan**, Assistant Professor, Department of Mechanical Engineering, for sparing their valuable time in reviewing my thesis draft. I must acknowledge that their constructive criticisms and valuable suggestions have immensely helped in improving the quality of my PhD thesis report. I want to thank **Prof. Arun Kumar Jalan**, Convener, Departmental Research Committee, Associate Professor, Mechanical Engineering Department, Pilani Campus, who has provided valuable comments during the departmental poster presentation.

My thanks are extended to, my colleagues and co-researchers **Dr. Shailendra Panwar, Dr. Santosh Kumar Saraswat, Mr. Mukesh Budaniya, Mr. Rishi Parwnada, Mr. Chandrachud Bijay Vaswar Dash, Mr. Ashish Kumar Srivastava**, and **Mr. Ashish Khare** for providing moral support whenever I needed. I believe that all those who have helped me, directly or indirectly, will forgive me for my inability to name them here; however, I express my gratitude and indebtedness to them. I also express my gratitude to all staff members of BITS Pilani, Heat Transfer Laboratory, especially **Mr. Dhanna Ram Saini**, **Mr. Niranjan Saini, Mr. Umanath**, and **Late. Mr. Parvat Ram** for their efforts in assisting me in the experimental work.

Lastly, I owe my deep thanks to my parents, **Shri Gautam Ukey** and **Shreemati Ruplata Ukey,** and my sister, **Dr. Sanskrit Ukey,** and my wife, **Mrs. Pratiksha Ukey,** for their encouragement and unlimited support, which cannot be expressed in words. Without their countless sacrifices, I could not have completed my research work. My heartfelt appreciation goes to my loving son, **Advit Ukey**. I am deeply indebted to all the pains taken by them to make my dream come true. Thank you for giving me the confidence and courage to make my choices. I would also thank my uncles and aunts. Their constant love and care empowered me to accomplish my thesis and also ignited me to take on more challenges in my life Last but not least, I pray and thank the Almighty for showering HIS divine blessings and giving me inner strength and patience.

Rahul Ukey

Abstract

The increase in ambient temperatures caused by global warming is expected to have a substantial effect on the energy needed for heating and cooling (H/C) buildings. This issue is particularly alarming in India, where many residential buildings have been constructed without regard for energy efficiency, as there is currently no mandatory residential energy efficiency code. Addressing this issue is crucial for improving indoor comfort and reducing air conditioning energy usage in residential spaces. Envelope retrofit solutions are a cost-effective and practical way to improve thermal comfort and save energy. Consequently, researchers are actively exploring their potential to enhance indoor comfort.

This study assessed the impact of global warming on space H/C energy requirements in eight major Indian cities covering all of the county's climate zones. By using historical weather records and general circulation model outputs, we quantified the historical (1969–2017) and future (2018–2100) trends in annual mean temperatures together with heating and cooling degree days (HDDs and CDDs), which are well-known metrics for quantifying buildings' H/C requirements. The historical weather records of temperatures were primarily taken from India's Meteorological Department (IMD). On the other hand, the future projected temperatures were general circulation models. These mathematical models simulate the Earth's climate system using mathematical equations to characterize how energy and matter interact in different parts of the ocean, atmosphere, and land.

Furthermore, this study utilizes ordinary least square regression, Mann-Kendall test, and Theil-sen slope for the trends analysis. It was found that annual temperatures would be higher by 0.1–1.1 ℃ in the 2020s, by 0.6–2.8 ℃ in the 2050s, and by 1.0–4.6 ℃ in the 2080s, depending on the city and the emission scenario. Due to rising temperatures, CDDs would also increase by 2.9–22.9% in the 2020s, by 8.3–54.1% in the 2050s, and by 11.89–

83.0% in the 2080s; thus, increasing the cooling requirements by a similar amount. In contrast, HDDs would decrease by 8.1–30.3% in the 2020s, by 17.6–83.3% in the 2050s, and by 19.3–97.1% in the 2080s, thereby reducing the heating requirements.

Retrofitting residential buildings could substantially reduce the sector's energy and carbon footprint and provide significant economic benefits in the long run. Building retrofits must be urgently developed and promoted in India, where most residences are constructed without any consideration of energy efficiency due to the lack of a mandatory residential energy code.

However, building retrofits must be devised considering the local construction practices and climatic conditions since an improper retrofit can deteriorate the indoor environment and even increase the building's energy consumption. Therefore, through a year-long monitoring and simulation exercise, this investigation evaluated different envelope retrofit options for improving the thermal comfort conditions in a detached single-story houses in India's hot-semi arid climate zone. The results showed that the indoor environment in such a dwelling was comfortable for only 23% of the year. The comfort period could be increased by 6–19 percentage points by applying cool/super-cool roof paints. Slight comfort enhancements could also be obtained by insulating the roof or the envelope (roof and walls); however, insulating the walls alone deteriorated the comfort conditions. Overall, applying cool/super-cool roof paints was recommended over other options since they provide the maximum thermal comfort benefits and are low-cost and easy to implement.

Table of Content

Abbreviation/Symbol	Description
A	Constant
a	Linear intercept
AC	Air-conditioner
AELS	Absolute error in the linear slope
$\overline{AELS}$	Median value of AELS
ASHRAE	American society of heating, refrigerating, and air-conditioning engineers
ATC	Adaptive thermal comfort
AvgRH	Monthly average of the relative humidity
B	Constant
b	Slope value
$\hat{b}_{GCM}$	Predicated trend (slopes)
$\hat{b}_{Obs}$	Observed trend (slopes)
$\hat{b}_{TS}$	Theil-Sen slope
BRL	Boland–Ridley–Laurent
C	Constant
CDD	Cooling Degree Days
CVRMSE	Coefficient of variation of the root mean square error
D	Diameter of globe
DHI	Diffuse horizontal irradiance
DNI	Direct normal irradiance
E_{AELS}	Relative error in AELS
e_i	Error term
EPS	Expanded polystyrene
E_{RMSE}	Relative error in RMSE
GCM	General circulation model
GDDP	Global daily downscaled projections
GHG	Greenhouse gases
GHI	Global horizontal radiation
H/C	Heating and Cooling

HDD	Heating Degree Days
IMAC-R	Indian model for adaptive comfort-Residential
IMD	Indian meteorological department
ISHRAE	Indian society of heating, refrigerating, and air conditioning engineers
LPD	Liquid precipitation
LULC	Land-use/land-cover
m	Number of tied groups
MaxT	Monthly averages of the maximum outdoor air temperatures
M_i	Measured value
MinT	Monthly averages of the minimum outdoor air temperatures
N	Number of days in the year
n	Number of observations
NASA	National aeronautics and space administration
NMBE	Normalized mean bias error
N_i	Number of data points
NOAA	National oceanic and atmospheric administration
NEX	Earth exchange
OLS	Ordinary least square
PWMKTS	Prewhitening the time series followed by conducting the Mann-Kendall (MK) test and estimating the Theil-Sen (TS) slope
RCP	Representative concentration pathways
RH	Relative humidity
RMSE	Root mean square error
$\overline{RMSE}$	Median value of RMSE
S	Test statistic
S_i	Simulated value
T	Daily mean ambient temperature
t	Time
T_a	Indoor air temperature
T_{base}	Base temperature
T_{GCM}	Predicated daily mean temperature

T_g	Globe temperature
t_k	Number of ties in k^{th} groups
TMY	Typical meteorological year
T_{MRT}	Mean radiant temperature
T_{neut}	Neutral temperature
T_{obs}	Observed daily mean temperature
$T_{out\text{-}30d}$	30-day outdoor running mean temperature
T_{opt}	Operative temperature
V_a	Indoor air speed
WMO	World meteorological organization
$\bar{x}$	Represents the mean value in time series
x_i	Observations in the time series (i = 1,2,3….n)
x_{i-1}	Previous observations in the time series
y_i	Values in the time series
Z	Standard normal distribution
α	Solar absorptance
$\hat{\alpha}$	Lag-1 autocorrelation
β	Constant
ε	Thermal emittance
ε_d	Emissivity of the globe

Chapter 1:

Introduction

1.1 Research Motivation

In 2018 energy consumption in buildings accounted for around 30% of the total energy consumed worldwide, of which space heating and cooling (H/C) were responsible for 34% and 6%, respectively [1]. A similar situation can also be seen in India, where in 2018, buildings accounted for about 33% of the country's total energy consumption [2]. Of the energy consumed by Indian buildings, space cooling accounts for about 5% [3–5], while the heating energy consumption is likely to be relatively small (exact estimates unavailable) since most of the country experiences a warm climate. Thus, space H/C in buildings constitutes a significant portion of energy consumption globally and in India. The energy consumption in buildings is also responsible for about 28% of energy-related CO_2 emissions worldwide, which is the primary reason for global warming [2]. Due to global warming, the global mean surface temperatures for 2081–2100 are projected to be 0.3–4.8 °C higher (depending on the emission scenario) than those in 1986–2005 [6]. As global temperatures rise, the energy required for space cooling will increase, while the space heating requirements will decrease [7]. Thus, in India, where energy requirements for space cooling are much larger than those for space heating [8], global warming may substantially increase the energy consumption in buildings and the associated CO_2 emissions.

A changing climate coupled with rising household incomes and built-up areas has led to a staggering increase in the cooling needs of Indian residences [9,10]. This trend is expected to persist, with projections indicating that the residential sector's air-conditioning (AC) stock will double within fifteen years and quadruple within the next two decades [8]. Adding to the challenge, most of India's residential buildings were and continue to be constructed without consideration for energy efficiency, primarily due to the absence of mandatory residential

energy efficiency codes [11]. Consequently, the implementation of energy efficiency measures within India's residential buildings can significantly reduce this sector's energy and carbon footprint [12,13], offering substantial long-term cost savings [14]. A critical factor influencing indoor conditions in residential buildings is heat transfer through the building envelope, encompassing walls, roofs, and windows [15]. Therefore, optimizing the thermal characteristics of the envelope through appropriate retrofit techniques, such as insulation, thermal mass enhancements, and heat-reflective paints, can enhance indoor comfort conditions and reduce the reliance on active H/C systems.

1.2 Objective of the Study

This study had three major objectives:

- Assessing the impact of global warming on space H/C energy requirements in eight major Indian cities covering all the county's climate zones.
- Evaluating thermal comfort in detached single-story houses in India's hot semi-arid climate conditions.
- Comparing various envelope retrofit solutions for enhancing thermal comfort in detached single-story houses under hot semi-arid climate conditions.

1.3 Methodology

The different phases of the adopted methodology to achieve the objectives are as follows:

Phase–I: A comprehensive literature review was conducted on studies that were focused on quantifying the impact of climate change on energy consumption for building space conditioning in India. Furthermore, the literature review will focus on studies that investigate the performance of different envelope retrofit solutions to enhance indoor thermal comfort.

Phase–II: This study quantifies the impact of climate change on the H/C energy consumption in residential buildings in several major Indian cities. To achieve this, future climate predictions

for major Indian cities (covering all the climate zones of India) will be made under various GHG (greenhouse gases) emission scenarios by using appropriate general circulation models such as HadCM3, GFDL, CCSM, etc. Subsequently, future energy requirements for space conditions will be quantified by using the degree-day analysis.

Phase–III: In this stage of the study, year-long measurements of the weather and indoor environmental conditions have been taken in the room of a residential house located in Pilani, Rajasthan, India. These observations assessed the occupants' comfort levels in the room as it was in an “as-built” state. It is essential to evaluate the initial thermal comfort of the houses before considering any potential changes to the building envelope. The data obtained from the measurements offer characterization of outdoor weather data and valuable insights into the room's thermal environment and comfort conditions.

Phase–IV: An EnergyPlus model has been developed to predict the indoor environmental conditions within the monitored room. The EnergyPlus model was constructed using building materials, internal heat load, and monitored weather conditions data. These data inputs were essential for creating a robust and accurate representation of the monitored room's indoor environment over time. A rigorous calibration and validation process was undertaken to ensure the model's reliability and accuracy.

Phase–V: In this phase of the research, the validated model was used with different envelope retrofit solutions to evaluate the impact of different retrofit solutions (e.g., the application of cool roof paints and the insulation of walls and roof) on the room’s thermal comfort conditions.

1.4 Organization of Thesis

The thesis is organized into six chapters. Chapter 1 provides the introduction to the present thesis. A review of literature related to the impact of climate on H/C degree days and envelop retrofit solutions for improving thermal comfort is presented in Chapter 2. Based on the

literature on the impact of climate change and the mitigation of its effect on the thermal comfort potential of envelope retrofit solutions are analysed to identify research gaps, and the study's objectives are determined based on the existing knowledge and research gaps. In Chapter 3, the impact of global warming on buildings' H/C energy requirements in eight major Indian cities covering all of the county's climate zones is presented. Chapter 4 presents a year-long measurement of the weather and indoor conditions in the house's bedroom. It assesses thermal comfort conditions and heat transfer characteristics in the as-built state. In Chapter 5, the well-calibrated model was developed to compare different envelope retrofit options for improving the thermal comfort conditions in a detached single-story house in India's hot-semi arid climate zone through detailed thermal comfort measurements. Finally, Chapter 6 summarises the change in H/C degree day and identifies the most suitable envelope retrofit solution for detached single-storeyed houses in hot semi-arid climates to improve thermal comfort, the limitations of the present work, and the direction of future research.

Chapter 2:

Literature Review

2.1 Literature Review on Impact of Global Warming on H/C Energy Consumption in Buildings

The impact of global warming on the H/C energy consumption in buildings can either be estimated by conducting hourly energy simulation [16–18] or by using the degree-day method [7]. In the former approach, simulation programs (like EnergyPlus) are used to predict the energy requirements for space H/C of archetype buildings by modeling their thermal performance under current and future climatic conditions. The latter approach uses H/C degree-days (HDDs and CDDs), which are essentially summations of temperature differences (ambient temperature minus a base temperature) over time, as indicators for predicting energy requirements for space H/C. Although degree-days do not consider the effect of variables like relative humidity and wind speed that can influence buildings' H/C energy requirements, nevertheless, they remain excellent indicators for the same [19]. The degree-days approach stands out due to its simplicity, transparency, and repeatability that hourly energy simulations may not provide [20].

2.1.1 Historical HDD and CDD Trends

Several researchers have investigated past trends in degree-days in different regions worldwide by estimating the HDD and CDD values based on historical weather records [21–26]. For example, Rosa et al. [25] studied the changes in HDDs and CDDs in six cities in Italy from 1978 to 2013, covering all its climate zones. Their study found that HDDs decreased (by 2.6–17.1%, depending on the city) while CDDs increased (by 7.4–170%, depending on the city) in 2000–2013, as compared to their values in 1980–1993. Similarly, Christenson et al. [21] estimated the impact of climate warming on degree-days in Switzerland's four major cities during 1901–2003. Their investigation also showed that HDDs reduced by 11–18% while

CDDs increased by 50–170% during the study period, depending upon location and the base temperature used. A similar conclusion was obtained by Ortizbeviá et al. [23], who studied the trends in degree-days at 31 weather stations in Spain during 1970–2005. They reported decreasing trends (2.3–6%/decade) in HDDs at 21 stations, while no significant HDD trends were detected in the remaining stations. On the other hand, CDDs had increasing trends (5–40%/decade) at 23 stations, while no significant CDD trends were detected in the rest. On similar lines, Jiang et al. [22] studied variations in HDDs and CDDs at 51 weather stations in Xinjiang, China, from 1959 to 2004. They reported that HDDs exhibited decreasing trends (from −25.1 °Cd/decade to −312.1 °Cd/decade) in 49 stations, while no significant trend was detected in the remaining stations. The CDD trends ranged from −21.5 °Cd/decade to 38.4 °Cd/decade, with 29 stations showing positive trends, 18 showing no trends, and the remaining four showing negative trends.

2.1.2 Future HDD and CDD Trends

In addition to studying the historical degree-day trends, several investigations have also made predictions of future degree-days using future weather data obtained from climate simulation models [27–29]. For example, Isaac and Vuuren [30] estimated that due to climate change (3.7 ℃ increase in global temperature over the pre-industrial age value), global HDDs would reduce by 34%, while CDDs will increase by 70% in 2100, as compared to their values in 2100 assuming no climate change. A similar conclusion was obtained by Warren et al. [31], who reported that a 1–5 ℃ increase in global temperatures would decrease global HDDs by 14–18% and increase CDDs by 18–99%. Spinoni et al. [27] studied the impact of global warming on degree-days in Europe from 1981–2100 under two different representative concentration pathways (RCPs): RCP4.5 and RCP8.5. The RCPs are defined by the increase in 'radiative forcing' in the year 2100 relative to 1750 due to increasing greenhouse gas concentrations in the atmosphere, i.e., 4.5 W/m^2 for RCP4.5 and 8.5 W/m^2 for RCP8.5 [6].

Their study showed that in Europe from 1981 to 2100, HDDs would decrease by 49–84 °Cd/decade while CDDs would increase by 8–20 °Cd/decade, depending on the RCP. On similar lines, Petri and Caldeira [28] studied the variations in degree-days in 25 of the United States' most populous cities under the RCP8.5 emission scenario. Their study showed that depending on the location, HDDs would decrease by 28–99% while CDDs would increase by 12–650% in 2080–2099, as compared to those in 1981–2010. Ramon et al. [29] also obtained a similar conclusion by studying the impact of climate change on future degree days in Belgium under the RCP8.5 scenario. They reported that there would be a 27% decrease in HDDs and a 140% increase in CDDs in 2070–2098, over those in 1976–2004.

2.2 Literature Review on Envelop Retrofit Solutions

In residential buildings, the heat transfer through the building envelope (walls, roof, and windows) plays a dominant role in determining the building's indoor conditions [15]. Thus, modulating the envelope's thermal characteristics through suitable retrofit techniques (insulation, thermal mass, reflective paints, etc.) can enhance indoor comfort conditions and minimize the need for active H/C. Two cost-efficient envelope retrofit techniques particularly suitable for India's residential building stock and climate are: i) converting the roof to a cool/super-cool roof by applying heat-reflective paints [32] and ii) adding insulation on the roof and walls [33]. The applications of those techniques for residential buildings are discussed in the following sub-sections.

2.2.1 Cool/Super-cool Roof Applications in Residential Buildings

A conventional roof can be converted to a cool or super-cool roof by applying heat-reflective paints on its surface, such that its solar absorptance (α) is decreased while its thermal emittance (ε) is kept high. For example, a conventional gray roof has $\alpha \approx 0.7$ and $\varepsilon \approx 0.9$, a cool roof has $\alpha \leq 0.3$ and $\varepsilon \geq 0.75$ [34], and a super-cool roof has $\alpha \leq 0.05$ and $\varepsilon \geq 0.95$ [32,35]. Several

investigations have assessed the impact of cool/super-cool roofs on occupants' thermal comfort and AC energy savings in residential buildings [33,36–42], which are summarized in the following two paragraphs. For a comprehensive review of research on cool roof materials, their applications and challenges, the reader is referred to Tian et al. [32].

The studies that evaluated the energy and thermal comfort benefits of applying cool/super-cool roofs in residential buildings generally used a two-step procedure. Firstly, a building energy model was calibrated for the region and construction of interest by using standard test cases from the literature [43], or experimental data from test chambers [33,44,45], or real-world case studies [46–48]. Subsequently, the calibrated model was used to determine the impact of the cool/super-cool roof retrofit strategy for various conditions. For example, Kolokotroni et al. [37] monitored a typical single-story house in Jamaica (a tropical country) and reported that, with the application of cool roof paint, the internal ceiling surface temperature was reduced by an average of 6.8 °C and indoor air temperature by 2.3 °C. Those monitoring results were subsequently used to develop and calibrate building energy models, with country-specific construction practices, to assess the impact of cool roofs in other tropical countries (Ghana and Brazil). Similar studies conducted for other climate zones and construction practices have found that converting a conventional roof to a cool/super-cool roof reduces roof temperatures by 20–40 °C [36,41], thus leading to indoor air temperature reductions between 0.75–4 °C [45,49]. Decreased indoor air temperatures significantly enhance occupants' comfort in summer [33,36,37,39,41,50] and reduce AC energy consumption by 1–93% [33,39,49,51].

The results of such model-centric studies have also been confirmed by a few site-level measurements [37,40,52]. For example, Pisello et al. [52] conducted a two-year continuous monitoring campaign to evaluate the impact of a cool roof on a residential building in Italy. The building was monitored for an entire year in the original configuration and for another year with the cool roof. The results showed that the proposed cool roof solution produced substantial

thermal comfort benefits in summer and relatively small penalties in winter for residential buildings in temperate climates. Since cool/super-cool roofs lead to reduced roof heat gains, they are beneficial in lowering summer discomfort and AC energy consumption; however, they adversely impact comfort conditions and heating energy consumption in winter [49]. For example, implementing a cool roof in a typical single-story residence in Sydney decreased the cooling energy consumption but increased the heating energy consumption, thus leading to a net *increase* in the building's energy consumption by 6.6 kWh/m^2/year [41]. Similarly, due to cool roofs, a 1–5 kWh/m^2/year increase in energy consumption was reported for residences in Barcelona, Spain [39]. Thus, cool roofs are generally beneficial in those locations where cooling energy consumption dominates over heating energy consumption and seem suited for most parts of India [53,54].

2.2.2 Wall and Roof Insulation of Residential Buildings

Applying wall and roof insulation is another effective retrofit technique for residential buildings and forms the core of most energy-reduction policies worldwide [55,56]. Increasing wall and roof insulation levels significantly lower heat gains in summer and heat losses in winter, thus improving occupants' thermal comfort [33,57–59] and buildings' energy efficiency [33,57,59–62]. We provide a summary of those investigations in the following paragraphs. For a detailed review of the impact of insulation on building energy efficiency and thermal comfort, the reader is referred to [68–72].

Most investigations focusing on insulation as a retrofit strategy have also used the two-step simulation approach or on-site measurements, as discussed in the previous subsection. For example, a field study conducted on residential buildings in Mandi, India (with warm summers and cold winters) found that modern insulated houses were warmer in winter by 3–4 °C and cooler in summer by 1–3 °C than uninsulated ones [57]. Thus, envelope insulation significantly improved the thermal comfort conditions in both seasons. Similarly, an experimental study

conducted with test cubicles in Lleida, Spain, demonstrated up to 37% heating and 64% cooling energy reductions by applying wall insulation [59]. Simulation-based studies have also reported similar results, i.e., the annual heating and cooling energy consumption in detached residential dwellings was reduced by 11–30% with wall insulation [33,62] and by 16–20% with roof insulation [33,60].

However, increasing insulation levels have also been associated with enhanced summer overheating in dwellings in cold and mild climates [63–65,73]. For example, experiments conducted on a pair of semi-detached solid wall houses in the UK (with and without internal wall insulation) showed that the indoor temperatures in the main bedroom of the insulated house were about 1.5 °C higher than those in the uninsulated house [66]. Thus, wall insulation increased the overheating risk by 7.7 percentage points in the bedroom. Similar results were reported by a simulation-based study conducted on bungalows and single-story houses in London, i.e., wall insulation increased the indoor air temperature by 3 °C in summer [65]. Another simulation study using different residential building variants spread across multiple climates also found that higher insulation levels increase the overheating risk when windows are closed at night. However, higher insulation levels reduce overheating risk if windows can be opened at night [67]. Thus, the use of insulation needs to be carefully assessed for the construction practices, user behavior, and climate conditions.

2.3 Research Gaps and Novelty of the Present Study

The literature reviewed included impact of climate change on H/C degree days. The literature reveals that HDDs in the last century decreased while CDDs increased almost universally due to global warming. Similar trends in HDDs and CDDs are projected to continue in the future, leading to a decrease in the heating energy demand and an increase in the cooling energy demand of buildings. Thus, in India, where buildings' cooling requirements are much larger than heating requirements, global warming would substantially increase the building energy

consumption. However, there are few studies [74,75] that have quantified the impact of climate change on building energy consumption for space conditioning purposes in India.

In addition to that, the literature reviewed carried out for retrofitment practices to improve thermal comfort shows that envelope retrofits generally improve indoor thermal comfort and reduce air-conditioning energy consumption in residences. However, they should be applied carefully after considering the building characteristics and climatic conditions, and an improper application can even *increase* thermal discomfort and energy consumption. Thus, the present research was motivated by the immense potential of envelope retrofit solutions for improving thermal comfort conditions in Indian residences, together with the limited number of previous studies [42,57] that have assessed such solutions for Indian building practices and climatic conditions. The study was conducted to aid building retrofit programs in the region and made the following novel contributions to the field:

- Most previous studies on cool/super-cool roofs and insulation-based retrofits focus on heating and cooling energy savings in air-conditioned buildings or on occupants' thermal distress in summer. However, the effect of such retrofits on the year-round thermal comfort in non-air-conditioned buildings has not been well studied. This issue is crucial for India, where over 90% of households currently lack access to air-conditioning [8] and will experience severe thermal distress with rising global temperatures [76,77]. A proper application of cost-effective building retrofits can significantly improve indoor comfort in such houses, thus preventing their future shift and over-reliance on AC systems.
- The present study was the first to be conducted in India's composite climate zone (BSh according to the Köppen-Geiger climate classification system), measuring the year-round indoor and outdoor environmental conditions of a non-air-conditioned detached single-story house. Even though the composite zone includes some major Indian cities such as

New Delhi, Allahabad, Amritsar, Lucknow, etc., and a total population of about 0.4 billion people, the indoor environment of such buildings has not been well-studied.

- The study's climate also presents a unique challenge for devising building retrofits since the location experiences a long and harsh summer (~6 months) with dry and wet spells and a relatively short but severe winter (~4 months). Thus, the retrofit must operate over the hot-dry, warm-humid, and cold periods and significantly improve the building's indoor environment.
- The study evaluated two cost-effective envelope retrofit options (cool/super-cool roofs and insulation) for improving the thermal comfort conditions in such residences using a well-calibrated energy model. Overall, the results offer valuable physical insights into the heat transfer characteristics and thermal comfort conditions of such residences, along with identifying a suitable retrofit solution.

3.1 Methodology

To assess the impact of global warming on the H/C energy requirements in India, this investigation first selected eight representative Indian cities, for which the historical temperature records (from 1969 to 2017) were obtained from the Indian Meteorological Department (IMD). Since the IMD temperature data had missing values, those values were filled using other datasets. Next, this study obtained the future temperature projections (from 2018 to 2100) for the selected cities from the National Aeronautics and Space Administration (NASA) earth exchange (NEX) global daily downscaled projections (GDDP) dataset after identifying a GCM suitable for each city. Subsequently, the annual mean temperatures, HDDs, and CDDs for each city from 1969 to 2100 were calculated, and their linear trends were estimated. The complete methodology is summarized in Figure 3.1 and elaborated in the following sub-sections.

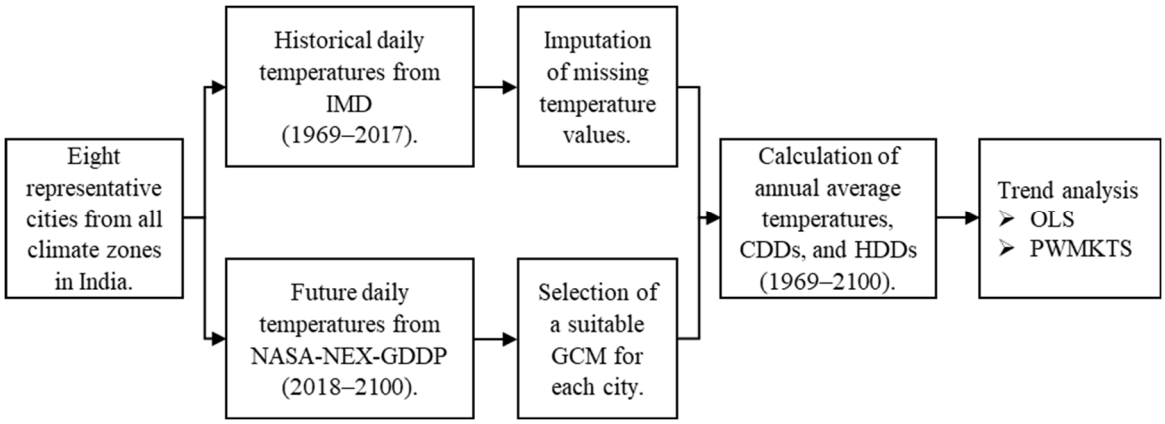

Figure 3.1: Flow chart of the methodology.

3.2 Selection of Representative Cities

In this study, eight representative cities covering all the country's climate zones were selected, as depicted in Figure 3.2. The total area of 4,812 square kilometers was encompassed by these chosen cities, supporting a population of 103 million. A detailed description of these

cities is provided in Table 3.1. Historical and future Cooling Degree Days (CDDs) were investigated for seven cities, as one city (Srinagar) had no cooling requirements. Conversely, Heating Degree Days (HDDs) were only studied for two cities (Delhi and Srinagar), as the others did not have significant heating requirements. By these carefully selected cities, a comprehensive analysis of India's climate was undertaken, spanning various climate zones. The aim of the research is to offer a holistic understanding of India's climate dynamics and their implications for energy consumption and urban planning.

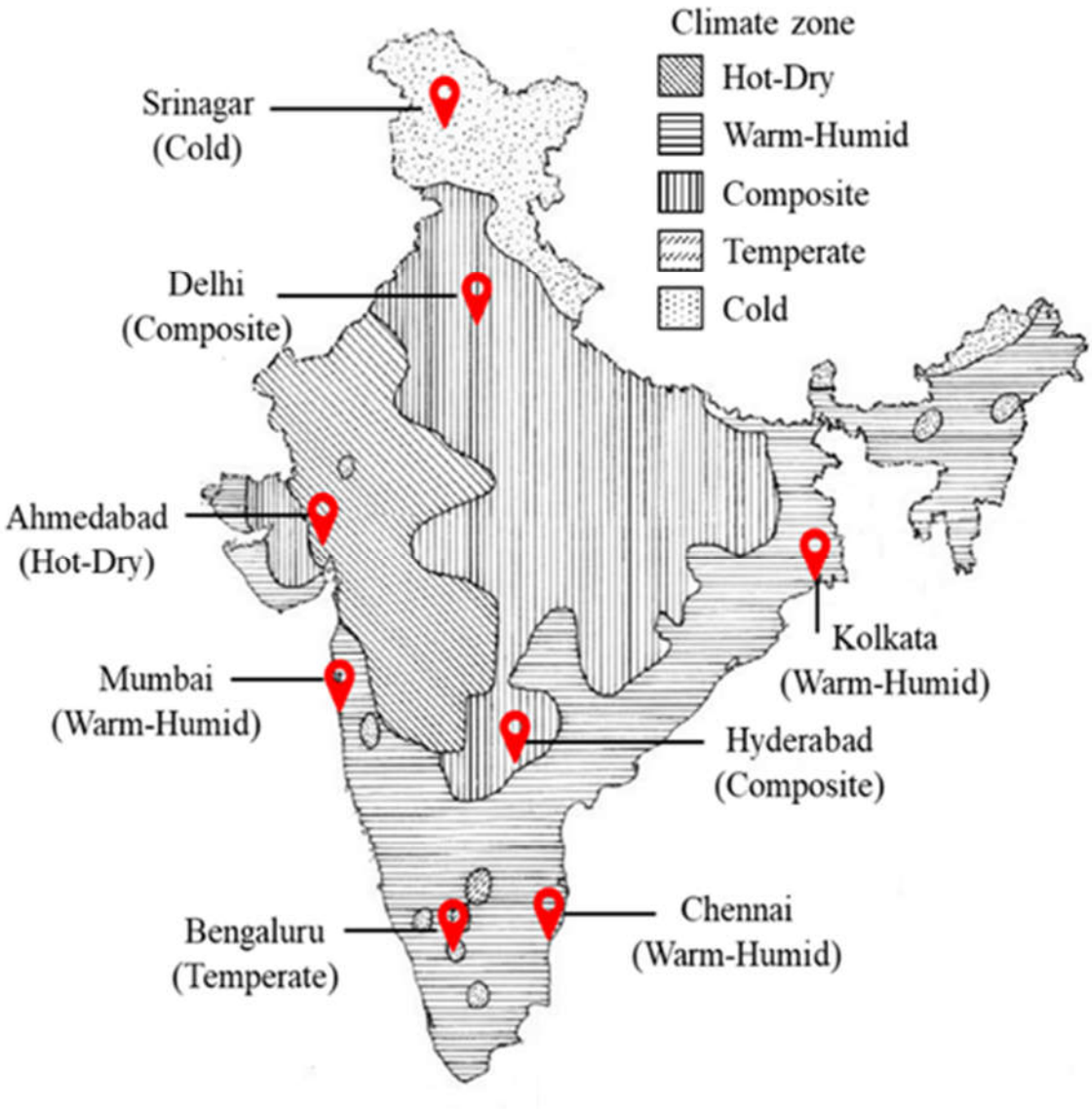

Figure 3.2: The selected cities covering all the climate zones of India. The climate classification map was taken from National Building Code of India [78].

Table 3.1: Description of the selected cities.

Climate zone	City	Description
Hot–Dry	Ahmedabad	Ahmedabad is a large metropolis located in the western part of India. Winters are short and mild, with the lowest monthly temperature being 12 °C, whereas summers are long and harsh, with maximum monthly temperatures reaching up to 42 °C.
Warm-Humid	Chennai Kolkata Mumbai	Chennai, Kolkata, and Mumbai are all coastal cities and the major metropolitan hubs of the country. The cities experience a very mild winter season with temperatures generally exceeding 15 °C throughout the day. Summers are hot and humid with maximum monthly temperatures ranging between 34–38 °C.
Composite	Delhi	Delhi is a major metropolitan area and the capital city of India. Winters are cold, with temperatures dropping routinely below 10 °C at night, while summers are hot with temperatures exceeding 40 °C during the day.
	Hyderabad	Hyderabad is a major metropolitan city located on the Telangana plateau in the southern part of the country. Winters are mild, with temperatures generally ranging between 15–30 °C, while summers are hot with temperatures exceeding 40 °C.
Temperate	Bengaluru	Bengaluru is another large metropolitan city in India. The city experiences a moderate climate with temperatures generally ranging between 16–34 °C throughout the year.
Cold	Srinagar	Srinagar is one of India's most populous city in the cold climate zone and lies in a valley region surrounded by the Himalayan mountains. Winters are cold, with temperatures dropping below 0 °C at night, while summers are mild, with the maximum daytime temperature being around 30 °C.

3.3 Calculation of HDD and CDD

This investigation calculated the annual HDDs and CDDs for the selected cities, as per the definition of the American Society of Heating, Refrigerating, and Air-conditioning Engineers (ASHRAE) [79]:

$$HDD = \sum_{i=1}^{N} (T_{base} - T)^{+} \quad \text{(Eq.3.1)}$$

$$CDD = \sum_{i=1}^{N} (T - T_{base})^{+} \quad \text{(Eq.3.2)}$$

where T is the daily mean ambient temperature, T_{base} the base temperature, and N the number of days in the year. The '+' superscript denotes that only positive values contribute to the degree-day calculations. In the above equations, the ambient temperature (T) was approximated as the arithmetic mean of the daily minimum and maximum temperatures, and the base temperature (T_{base}) was taken as 18 °C. An 18 °C base temperature value was used for calculating both HDDs and CDDs, as recommended for India by Bhatnagar et al. [80], based on detailed energy simulations of several building types located across the different climate zones of the country.

3.4 Historical Weather Data (1969–2017)

The degree-days for the years 1969–2017 were calculated from the daily values of minimum and maximum ambient temperatures obtained from IMD. IMD has been monitoring meteorological parameters in more than 500 stations in India for over a century, and releases weather data following stringent quality tests and pre-processing based on World Meteorological Organization (WMO) protocols [81]. However, IMD's temperature data had some missing values (0.2–4.5%, depending on the city). Those missing values were filled using the data obtained from the National Oceanic and Atmospheric Administration (NOAA), which maintains an archive of global historical climate data. IMD data was chosen as the primary data source, and NOAA was selected as the secondary source because IMD data exhibited lower missing values than the NOAA data. Even after combining both datasets, there were still some missing values (0.1–2.6%, depending on the city). The missing temperature values for the years 1969–2005 were taken as the arithmetic means of the temperature predictions given by 21 different general circulation models (GCM) under the 'historical' scenario (see details in Section 3.5). Since the historical scenario ends in 2005, the missing values from 2006–2017

were filled by data from TuTiempo.net, a website that provides access to WMO data. However, one or two temperature values were still missing for 2006–2017. Those values were filled by using linear interpolation since the consecutive missing values were less than five [82,83]. Finally, if the endpoint (31st December 2017) of the data was missing, it was filled by the previous day's value. Thus, by following this procedure, we obtained the complete ambient air temperature records for all eight cities from 1969 to 2017.

To assess the suitability of the procedure used for filling the missing values, in this study, the root mean square error (RMSE) in the daily mean ambient temperatures between the primary dataset (from IMD) and other datasets (from NOAA, mean GCM, or TuTiempo) was calculated, as reported in Table AI1 (Appendix-I). The RMSE values were calculated using all common data points available between the primary and secondary datasets, except for the TuTiempo data, for which we randomly selected 30 data points for RMSE calculation since the TuTiempo data had to be manually recorded for each day. Table AI1 shows that the RMSE values ranged between 0.46–2.67 for the different datasets, depending on the city. The RMSE values compared reasonably well with other imputation algorithms reported in the literature [84]. This study did not estimate the performance of the linear interpolation technique for missing value imputation since only 1–2 data points per city were filled by this method.

3.5 Future Weather Data (2018–2100)

For calculating future degree-days, daily predictions of ambient air temperatures were obtained from the NASA-NEX-GDDP dataset. This dataset (available at https://cds.nccs.nasa.gov/nex-gddp/) was developed from simulations conducted under the 5th phase of the coupled model inter-comparison project (CMIP-5) using 21 different GCMs, as given in Table AI2. The dataset contains statistically downscaled projections of the minimum and maximum ambient temperatures at a geospatial resolution of 0.25° × 0.25° (about 25 km

× 25 km) for RCP4.5 and RCP8.5 scenarios from 2005–2100. Note that RCP4.5 is a stabilization scenario with the total radiative forcing stabilizing at 4.5 W/m^2 in 2100, relative to 1750 [85]; while RCP8.5 is a scenario with very high greenhouse gas emissions leading to an increase in radiative forcing of 8.5 W/m^2 in 2100, relative to 1750 [86]. From the NEX-GDDP dataset, this study obtained the daily temperature predictions (minimum and maximum values) at four closest grid-points for a particular city, and then used bilinear interpolation for estimating the city's temperatures [17].

Since the NEX-GDDP dataset contained future temperature predictions from 21 different GCMs; therefore, choosing an appropriate GCM for making future temperature predictions was a non-trivial exercise. So, in this study first evaluated the performance of different GCMs by comparing their predictions under the 'historical' scenario with the corresponding observations (1969–2005) for all the eight cities. The historical scenario provides the modeled historical evolution of temperature using reconstructed historical forcing. Thus, temperature predictions under the historical run were evaluated by us for all eight cities by comparing them with their corresponding observed values using different GCMs.

This investigation calculated the RMSE values for each model for all cities by using the following equation:

$$RMSE = \sqrt{\sum_{i=1}^{N} \frac{(T_{GCM} - T_{Obs})^2}{N}} \qquad \text{(Eq. 3.3)}$$

where T_{GCM} and T_{Obs} are the predicted (by a particular GCM) and observed values of the daily mean temperature on the ith day, respectively, and N is the number of days (N = 13514 days for years 1969–2005).

This study also calculated the absolute error in predicting the historical temperature trends (linear slope) for each GCM by using the following equation:

$$AELS = \left|\hat{b}_{GCM} - \hat{b}_{Obs}\right| \quad \text{(Eq. 3.4)}$$

where AELS is the absolute error in the linear slope, $\hat{b}_{GCM}$ and $\hat{b}_{Obs}$ are the GCM predicted and observed trends (slopes) in annual mean temperature from 1969–2005, respectively, obtained from the ordinary least square (OLS) analysis given in Section 3.6.1.

Note that RMSE values quantify the errors in the daily mean temperatures predicted by each GCM, thus quantifying the model's performance for short time-periods, whereas the AELS values assess the model's long-term performance. To assess the model performances relative to each other, this study defined E_{RMSE} and E_{AELS} metrics, as suggested by Gleckler et al. [87]:

$$E_{RMSE} = \frac{RMSE - \overline{RMSE}}{\overline{RMSE}} \quad \text{(Eq. 3.5)}$$

$$E_{AELS} = \frac{AELS - \overline{AELS}}{\overline{AELS}} \quad \text{(Eq. 3.6)}$$

where E_{RMSE} and E_{AELS} are the relative errors in the RMSE and AELS values, respectively; $\overline{RMSE}$ and $\overline{AELS}$ are the median values and quantify the 'typical' model errors. By using 'median' rather than the 'mean,' this study clear out the possible problems arising from outliers in the dataset. The smaller the *E* value is for a model, the better is its performance compared to others. For example, if $E_{RMSE} = -0.1$ for a particular model, it demonstrates that the model's RMSE is 10% lower than that of the typical (median) model, which means that the model outperforms the typical model.

Figure 3.3 shows the relative error values (E_{RMSE} and E_{AELS} denoted by the color scale) for the 21 GCMs (names given in the center) for all eight cities. Figure 3.3 a) shows that for most of the cities, the MIROC_ESM_CHEM model had the least E_{RMSE} values (best short-term

performance) while the IPSL_CM5A_MR model had the highest E_{RMSE} values (worst short-term performance).

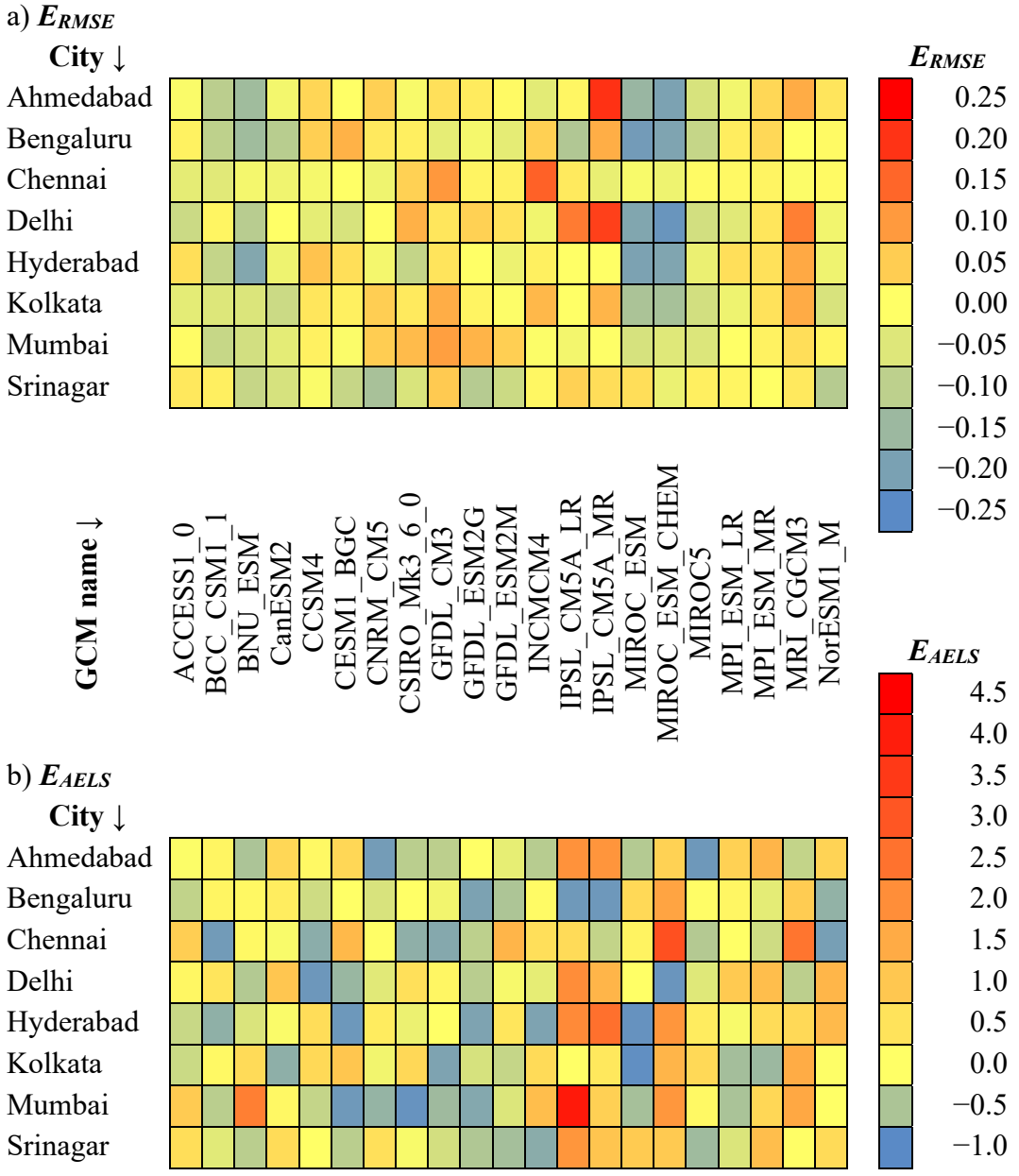

Figure 3.3: Performance of different general circulation models (GCMs) in predicting the temperatures of major Indian cities from 1969−2005 based on a) E_{RMSE} and b) E_{AELS} metrics.

On the other hand, Figure 3.3 b) shows that the GFDL_ESM2G model generally had the least E_{AELS} values (best long-term performance) while the IPSL_CM5A_LR model had some of the highest E_{AELS} values (worst long-term performance). Thus, the models that had good short-term performance did not necessarily capture the long-term temperature trends. It is also

evident from Figure 3.3 that a single GCM could not consistently perform well for all the eight Cites and that a single GCM could not consistently perform well for all the eight cities, and different models seem suitable for different cities.

Table 3.2: Selected general circulation models (GCMs) for making future temperature predictions in major Indian cities.

City	**Selected GCM**
Ahmedabad	BNU_ESM
Bengaluru	IPSL_CM5A_LR
Chennai	BCC_CSM1_1
Delhi	MIROC_ESM_CHEM
Hyderabad, Kolkata, and Mumbai	MIROC_ESM
Srinagar	GFDL_ESM2G

Thus, to choose an appropriate model for a particular city, in this study first ranked the 21 GCMs based on their short-term and long-term performances, i.e., each GCM was ranked from 1 to 21 corresponding to E_{RMSE} and E_{AELS} metrics. Subsequently, both the ranks were summed to obtain the final model rankings for each city; thus, a lower rank was represented as a well-performing model, and vice versa. The models with the best rankings (see Table 3.2) were selected to make future temperature predictions. Note that Ahmedabad had three models (BNU-ESM, MIROC-ESM, and MIROC5) while Mumbai had two models (BCC-CSM1-1 and MIROC-ESM) with equal summed ranks. Those ties were broken based on the model performances in predicting the historical CDD slopes, as discussed in the following paragraph.

This investigation assessed the performances of the GCMs by comparing the historical CDD and HDD trends (the OLS slopes described in Section 3.6.1) with their corresponding model predictions obtained from the historical runs. Figure 3.4 shows the box plots of the CDD and HDD trends from 1969–2005 predicted by the different GCMs together with the observed trends and those predicted by the selected GCMs given in Table 3.2.

Figure 3.4 shows large differences in model predictions; however, the selected GCMs can reasonably capture the historical HDD and CDD trends with prediction errors ranging between 1–39%. Thus, those GCMs were deemed suitable for forecasting future temperatures (2018–2100) and calculating the future HDDs and CDDs. Note that since there were ties in model rankings for Ahmedabad and Mumbai, the GCMs that best captured the observed CDD trends in those cities were selected for making future projections.

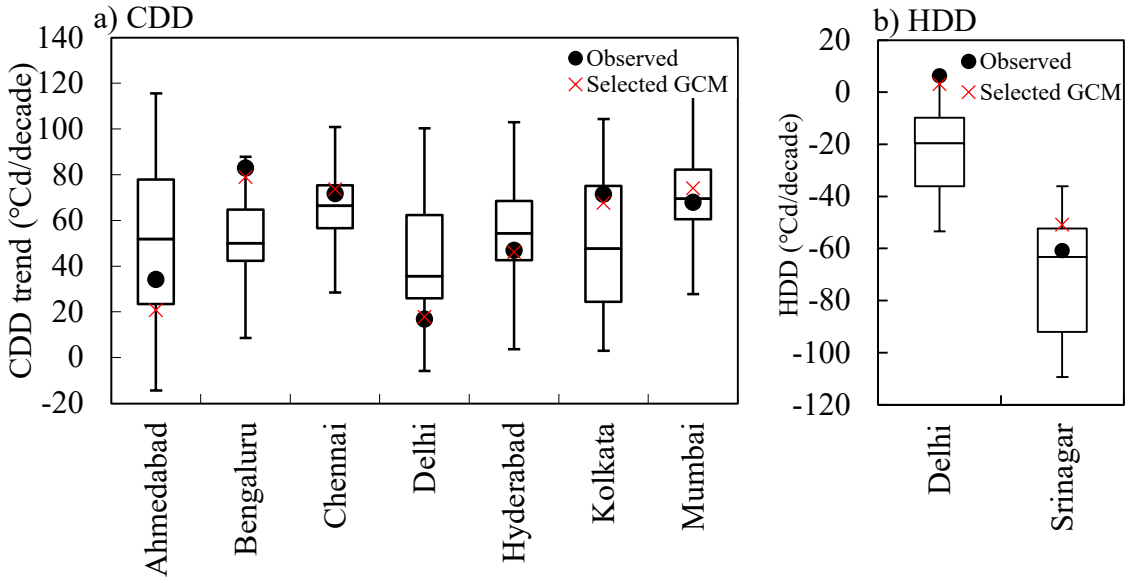

Figure 3.4: Box plots of a) CDD and b) HDD trends from 1969−2005 predicted by the different general circulation models (GCMs) in major Indian cities.

3.6 Linear Trend Analysis of Temperatures and Degree-days

This investigation quantified the trends in annual mean temperatures and degree days for the past (1969–2017) and the future (2018–2100) by using two approaches: 1) applying the ordinary least square regression to the time series (OLS analysis) and 2) prewhitening the time series followed by conducting the Mann-Kendall (MK) test and estimating the Theil-Sen (TS) slope (PWMKTS analysis).

3.6.1 Ordinary Least Square (OLS) Analysis

OLS regression is a widely used method to quantify trends in climatological time-series because of its simplicity and broad acceptance [88–93].

In this technique, a straight line is fit to the time-series modeled as:

$$x_i = a + bt + e_i, \quad i = 1, 2, \ldots n \qquad \text{(Eq. 3.7)}$$

where x_i is the ith observations in the time series, t the time, a and b are the linear intercept and slope values, respectively, and e_i is the error term. The OLS method provides an estimate of the linear trend ($\hat{b}_{OLS}$) by minimizing the sum of squared errors ($\sum_{i=1}^{n} e_i^2$). The statistical significance of the trend was tested using the Student's t-test at a significance level of 0.05.

3.6.2 Prewhitening, Mann Kendall Test, and Theil-Sen Slope (PWMKTS) Analysis

Although the OLS technique is popular for quantifying linear trends, it assumes that e_i is normally distributed and there is no autocorrelation (correlation of a variable with itself at differing time lags) among the observations, which is seldom true for climatological time-series. Thus, this study employed another model that assumes that the time-series is the sum of an AR(1) autoregressive process (current observation depends on the immediately preceding value) and a linear model [94], given by:

$$x_i = \alpha x_{i-1} + a + bt + e_i, \quad i = 1, 2, \ldots n \qquad \text{(Eq. 3.8)}$$

where α denotes the lag-1 autocorrelation between x_i and x_{i-1}.

The above equation was transformed to Eq. 3.7 by a 'prewhitening' process (substituting $y_i = x_i - \alpha x_{i-1}$ in Eq. 8 converts it into Eq. 3.7 form) that removes the lag-1 autocorrelation from the time-series without affecting the 'true' trend coefficient (b). The lag-1 autocorrelation was estimated ($\hat{\alpha}$) as the correlation coefficient between two N−1 long subsamples of the time-series lagged by one-time step using the following equation:

$$\hat{\alpha} = \frac{\frac{1}{n-1}\sum_{i=1}^{n-1}\{(x_i - \bar{x}) \times (x_{i+1} - \bar{x})\}}{\frac{1}{n}\sum_{i=1}^{n}(x_i - x)^2} \qquad \text{((Eq. 3.9)}$$

where $\bar{x}$ represents the mean value.

The lag-1 autocorrelation ($\hat{\alpha}$) was significant (significance level of 0.05) for the time-series of annual temperatures, CDDs, and HDDs and ranged between 0.3–0.9 for the different time-series, as shown in Figure AI1. Thus, the time-series were prewhitened before conducting additional statistical tests [95,96].

After prewhitening, the study applied the Mann Kendall (MK) test [97,98] on the time-series. The MK test (details in Appendix A) is a rank-based method to detect trends, which is less sensitive to outliers than the OLS method and does not require the residuals to be normally distributed. Although the MK test can detect the existence or non-existence of a trend, it cannot provide its magnitude. Thus, this study used the Theil-Sen slope [99,100] estimator ($\hat{b}_{TS}$) to calculate the magnitude of the linear trend that is given by:

$$\hat{b}_{TS} = Median\left(\frac{x_j - x_i}{j - i}\right) \text{ for all } j > i \qquad \text{(Eq. 3.10)}$$

3.7 Results

This study analyzed the annual mean temperatures, CDD, and HDD variations in eight major Indian cities for 1969–2100. In this study first discusses the historical (1969–2017) and future (2018–2100) trends in annual temperatures, followed by a similar discussion for CDDs and HDDs.

3.7.1 Temperature Trends (1969–2100)

Historical Temperature Trends (1969–2017)

Figure 3.5 shows the historical and future projections of annual mean temperature anomalies for Delhi from 1969 to 2100. The temperature anomalies were calculated as differences between the annual mean temperatures and a baseline temperature (mean temperature from 1969–2017).

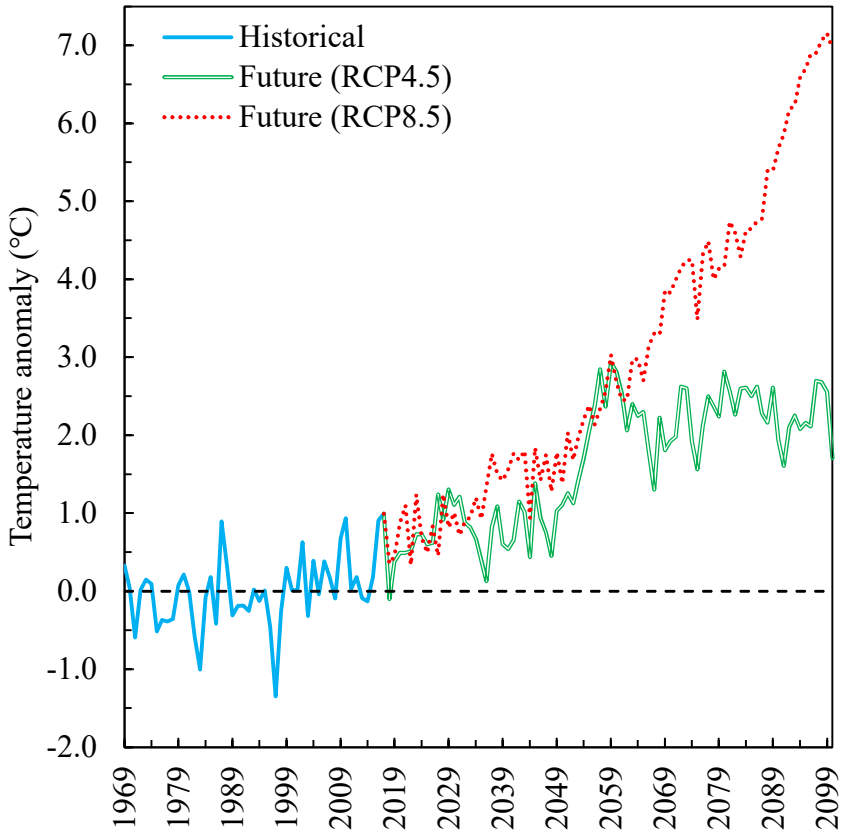

Figure 3.5: Historical and future anomalies in annual mean temperatures in Delhi.

Figure 3.5 shows that the annual mean temperatures increased (positive anomaly values) during 1969–2017 in Delhi at a rate of 0.12 °C/decade (p-value = 0.009 and 0.03–0.21 is the 95% confidence interval), as estimated from the OLS slope given in Table 3.3. It was obtained a similar conclusion from the PWMKTS analysis and the corresponding TS slope values (see Table 3.3), i.e., the observed temperature trend was significant for Delhi (p-value = 0.042), and its TS slope was 0.10 °C/decade (0.01–0.19 is the 95% confidence interval). The TS slope was slightly lower than the OLS slope since the prewhitened time-series was used for TS slope calculations, whereas the original time-series (without prewhitening) was used to calculate the OLS slope. The OLS slope possibly overestimates the annual temperature trends since there is significant positive autocorrelation in the original time-series. In contrast, the TS slope likely underestimates the trend since prewhitening could have reduced the magnitude of the trend [101].

Table 3.3: Historical and future trends in annual mean temperature.

Time period	City	OLS analysis		PWMKTS analysis	
		Slope[b] (°C/decade)	p-value	TS Slope[b] (°C/decade)	MK test p-value
Historical (1969–2017)	Ahmedabad	0.13 (0.02, 0.23)	0.019	0.09 (0.00, 0.19)	0.042
	Bengaluru	0.22 (0.15, 0.27)	< 0.001	0.13 (0.06, 0.19)	0.001
	Chennai	0.16 (0.10, 0.20)	< 0.001	0.08 (0.01, 0.14)	0.015
	Delhi	0.12 (0.03, 0.20)	0.009	0.10 (0.01, 0.19)	0.028
	Hyderabad	0.21 (0.14, 0.28)	< 0.001	0.10 (0.03, 0.18)	0.007
	Kolkata	0.23 (0.17, 0.28)	< 0.001	0.12 (0.06, 0.19)	0.001
	Mumbai	0.13 (0.06, 0.18)	< 0.001	0.01 (0.02, 0.18)	0.013
	Srinagar	0.20 (0.08, 0.32)	0.001	0.14 (0.00, 0.26)	0.044
RCP4.5 (2018–2100)	Ahmedabad	0.18 (0.14, 0.22)	< 0.001	0.05 (0.01, 0.08)	0.010
	Bengaluru	0.19 (0.16, 0.22)	< 0.001	0.03 (0.00, 0.05)	0.020
	Chennai	0.12 (0.09, 0.15)	< 0.001	0.04 (0.019, 0.08)	0.002
	Delhi	0.27 (0.22, 0.31)	< 0.001	0.03[a] (−0.01, 0.06)	0.176
	Hyderabad	0.38 (0.33, 0.43)	< 0.001	0.01[a] (−0.02, 0.03)	0.725
	Kolkata	0.21 (0.16, 0.25)	< 0.001	0.03[a] (0.00, 0.06)	0.060
	Mumbai	0.19 (0.16, 0.22)	< 0.001	0.04 (0.01, 0.07)	0.010
	Srinagar	0.10 (0.05, 0.14)	< 0.001	0.07 (0.02, 0.11)	0.006
RCP8.5 (2018–2100)	Ahmedabad	0.53 (0.49, 0.56)	< 0.001	0.06 (0.02, 0.09)	0.006
	Bengaluru	0.52 (0.50, 0.54)	< 0.001	0.03[a] (0.00, 0.05)	0.073
	Chennai	0.34 (0.31, 0.37)	< 0.001	0.04 (0.00, 0.08)	0.044
	Delhi	0.78 (0.73, 0.83)	< 0.001	0.05 (0.02, 0.09)	0.001
	Hyderabad	0.72 (0.69, 0.76)	< 0.001	0.03 (0.01, 0.06)	0.013
	Kolkata	0.65 (0.62, 0.68)	< 0.001	0.03 (0.00, 0.06)	0.023
	Mumbai	0.51 (0.49, 0.54)	< 0.001	0.04 (0.00, 0.07)	0.041
	Srinagar	0.54 (0.49, 0.58)	< 0.001	0.06 (0.01, 0.11)	0.022

[a]Not a statistically significant result (p-value > 0.05).
[b]The values in parenthesis represent the 95% confidence interval.

Similarly, for all the other seven cities, the annual temperatures increased in the past 49 years, as shown in Figures AI2 a–g, with the OLS slopes ranging from 0.13–0.23 °C/decade,

as given in Table 3.3. The PWMKTS analysis also reached a similar conclusion, i.e., the observed temperature trends were statistically significant, and the magnitudes of TS slope ranged between 0.08–0.14 °C/decade, as given in Table 3.3. Once again, the OLS slopes were higher than their corresponding TS slopes due to the reasons discussed in the preceding paragraph. This study also compared the temperature trends in the selected cities with those previously reported for India during the periods 1969–2005 [79] and 1971–2003 [80]. During 1969–2005, Basha et al. [79] reported that the country's annual temperatures increased by 0.081 °C/decade or by 0.168 °C/decade based on datasets obtained from IMD, India, or Climate Research Unit, UK, respectively. Similarly, Kothawale and Kumar [80] also reported that India's annual temperatures increased by 0.22 °C/decade during 1971–2003. Our investigation also found increasing temperature trends for the selected cities, with magnitudes ranging between 0.03–0.23 °C/decade during 1969–2005 and between 0.04–0.28 °C/decade during 1971–2003. Thus, our results are in qualitative agreement with those reported previously.

Note that the temperature rise in Indian cities may not be solely due to increasing greenhouse gas (GHG) emissions since other factors such as anthropogenic aerosols, natural forcings, and land-use/land-cover (LULC) changes also impact the surface air temperatures [79,81,82]. In India, increasing GHG emissions and LULC changes have contributed significantly towards increasing temperatures during the 20th century, while changes in anthropogenic aerosol emissions and natural forcings provided some cooling effect [79]. Thus, in this study also anticipate a similar contribution of those factors towards the estimated temperature trends in the selected cities.

Future Temperature Trends (2018–2100)

Figure 3.5 also shows that Delhi's annual temperatures will gradually increase from 2018 to 2100 under both the emission scenarios (RCP4.5 and RCP8.5). Under the RCP4.5 scenario,

the annual temperatures in Delhi are projected to be 0.6 °C higher in the 2020s (2005–2034), 1.4 °C higher in the 2050s (2035–2064), and 2.2 °C higher in the 2080s (2065–2094) when compared to the baseline (mean temperature from 1969–2017), as shown in Figure 3.5. On the other hand, under the RCP8.5 scenario, temperatures will be 0.6 °C higher in the 2020s, 2.0 °C higher in the 2050s, and 4.5 °C higher in the 2080s than the baseline temperature.

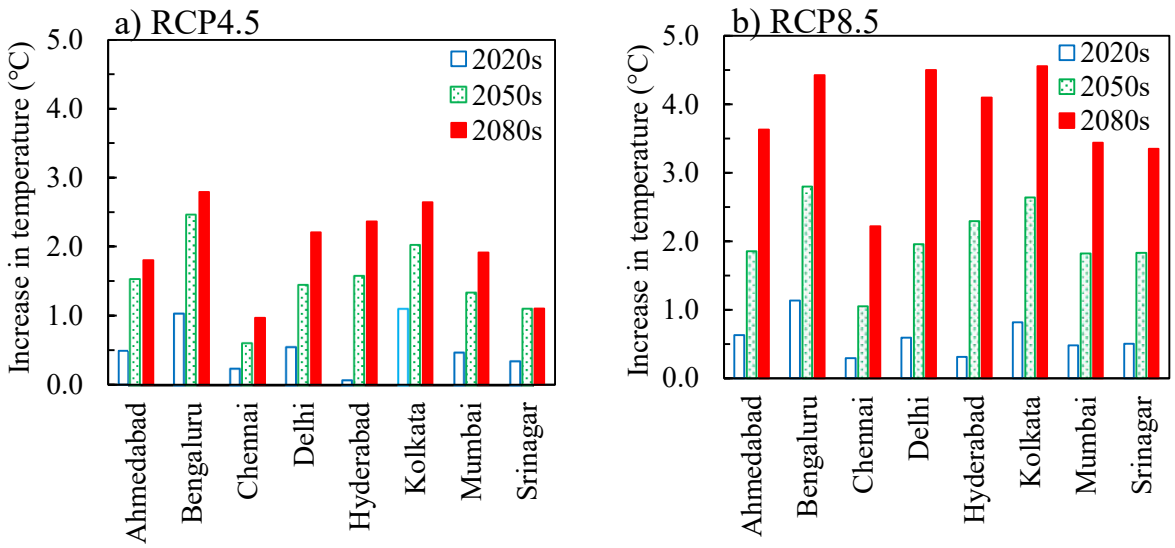

Figure 3.6: Increase in annual mean temperature in 2020s (2005–2034), 2050s (2035–2064), and 2080s (2065–2094) for eight major Indian cities under the a) RCP4.5 and b) RCP8.5 emission scenario.

Similarly, for all the other cities, the annual temperatures will increase from 2018 to 2100 under both the emission scenarios, as shown in Figure 3.6 and Figures AI2 a–g. In the 2020s, the projected increase in annual temperatures ranged between 0.1 °C–1.1 °C and was almost equal in both the scenarios for all cities. However, in the 2050s and 2080s, the annual temperature rise is projected to be significantly lower under the RCP4.5 scenario than under the RCP8.5 scenario. The OLS analysis detected statistically significant trends in the projected annual temperatures for all the eight cities (see Table 3.3), with magnitudes ranging from 0.10–0.38 °C/decade under the RCP4.5 scenario and from 0.35–0.78 °C/decade under the RCP8.5 scenario. The estimated temperature trends are in qualitative agreement with those reported by

Basha et al. [102], who found that the annual mean temperatures in India would increase by 0.52 ℃/decade in the 21st century under the RCP8.5 scenario.

The PWMKTS analysis also detected statistically significant trends for all cities in both the emission scenarios with TS slopes ranging from 0.03–0.07 °C/decade under the RCP4.5 emission scenario and from 0.03–0.06 °C/decade under the RCP8.5 scenario. The exceptions were Delhi, Hyderabad, and Kolkata under the RCP4.5 scenario, and Bengaluru under the RCP8.5 scenario, for which the PWMKTS analysis did not detect statistically significant trends (p-value > 0.05). The discrepancies between the OLS and the PWMKTS analysis arise because this study used the original time-series for the former, while the latter used the prewhitened time-series. This likely led to an overestimation of the trend by the OLS analysis and an under-estimation of the trend by the PWMKTS analysis, as discussed previously.

3.7.2 CDD Trends (1696–2100)

This section discusses the historical and future trends in CDDs for all cities, except Srinagar, which has a cold climate and therefore no cooling requirements.

Historical CDD Trends (1969–2017)

Figure 3.7 shows the historical (1969–2017) and future projections (2018–2100) of CDDs for Delhi, as well as the baseline value (2809 °Cd), which is the average CDD value from 1969 to 2017. The CDDs in Delhi increased significantly during 1969–2017, i.e., by 40.8 °Cd/decade (14.7–67.3 °Cd/decade at 95% confidence level), as quantified by the OLS slope given in Table 3.4, which corresponds to a 1.5% CDD increase per decade. The PWMKTS analysis also detected a statistically significant trend in CDDs during 1969–2017 of magnitude 34.2 °Cd/decade (6.6–60.5 at 95% confidence level), as shown in Table 4, i.e., a 1.2% CDD increase per decade.

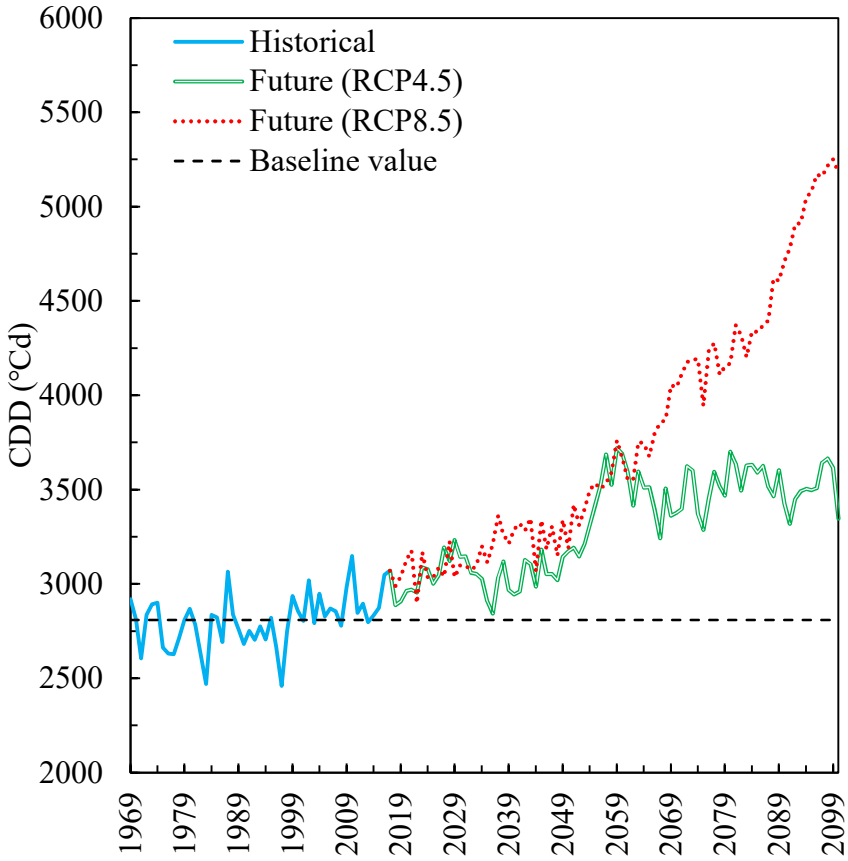

Figure 3.7: Historical and future cooling degree days (CDDs) in Delhi.

Similarly, for the other six cities with cooling requirements, CDDs increased from 1969 to 2017 (see Figures AI3 a–f). The OLS slopes for CDDs were statistically significant and ranged between 40.8–86.7 °Cd/decade (1.3–3.8 % CDD increase per decade), as given in Table 3.4. The PWMKTS analysis also detected statistically significant trends in CDDs for all cities except Ahmedabad (MK test p-value = 0.056), with the corresponding TS slopes ranging between 27.9–48.4 °Cd/decade (0.7–2.3% CDD increase per decade) in Table 3.4.

Once more, OLS slopes were higher than the corresponding TS slopes since prewhitening was used before calculating the TS slopes. Overall, it is clear that the CDDs have increased for all the cities from 1969 to 2017; thus, increasing the cooling energy requirements in buildings. The CDD trends in Indian cities are generally in qualitative agreement with previous investigations conducted in other countries (CDD trends for India are unavailable in the existing literature).

Table 3.4: Historical and future trends in cooling degree days (CDDs).

Time period	City	OLS analysis		PWMKTS analysis	
		Slope[b] (°Cd/decade)	p-value	TS Slope[b] (°Cd/decade)	MK test p-value
Historical (1969–2017)	Ahmedabad	45.7 (7.6, 83.9)	0.020	31.9 (−0.1, 66.3)	0.056
	Bengaluru	78.2 (57.7, 98.7)	< 0.001	48.4 (22.0, 68.5)	< 0.001
	Chennai	56.9 (39.1, 74.6)	< 0.001	27.9 (6.0, 49.7)	0.015
	Delhi	40.8 (14.7, 67.3)	0.003	34.2 (6.6, 60.5)	0.017
	Hyderabad	77.8 (53.4, 102.3)	< 0.001	38.5 (9.5, 67.1)	0.005
	Kolkata	86.7 (67.3, 106.1)	< 0.001	45.6 (22.1, 69.6)	0.001
	Mumbai	47.1 (23.4, 70.8)	< 0.001	35.4 (7.5, 63.4)	0.016
RCP4.5 (2018–2100)	Ahmedabad	66.8 (56.4, 77.2)	< 0.001	16.5 (4.1, 29.7)	0.012
	Bengaluru	69.9 (38.8, 101.0)	< 0.001	11.5 (1.7, 19.9)	0.022
	Chennai	44.5 (33.7, 56.3)	< 0.001	16.4 (6.3, 27.8)	0.002
	Delhi	86.0 (71.4, 98.5)	< 0.001	7.7[a] (−2.9, 17.2)	0.132
	Hyderabad	140.1 (120.7, 159.4)	< 0.001	1.6[a] (−8.1, 12.2)	0.731
	Kolkata	76.8 (59.9, 93.7)	< 0.001	10.6[a] (−0.7, 21.6)	0.063
	Mumbai	71.0 (61.1, 80.8)	< 0.001	14.3 (3.8, 25.9)	0.009
RCP8.5 (2018–2100)	Ahmedabad	193.3 (196.5, 190.2)	< 0.001	20.4 (6.0, 33.3)	0.008
	Bengaluru	191.6 (260.6, 122.7)	< 0.001	8.8[a] (−0.4, 19.8)	0.058
	Chennai	126.7 (116.4, 136.9)	< 0.001	13.6 (0.2, 27.2)	0.046
	Delhi	265.1 (246.4, 283.7)	< 0.001	18.0 (7.6, 28.8)	0.001
	Hyderabad	265.5 (252.1, 278.8)	< 0.001	11.9 (2.3, 20.7)	0.017
	Kolkata	239.7 (229.4, 279.9)	< 0.001	12.0 (1.4, 23.2)	0.031
	Mumbai	189.2 (179.4, 198.9)	< 0.001	12.7 (0.4, 23.9)	0.044

[a]Not a statistically significant result (p-value > 0.05).
[b]The values in parenthesis represent the 95% confidence interval.

However, significant differences can be seen in the quantitative values due to the differences in the climatic conditions, research approach, and the base values used for calculating CDDs. For example, it was found that during 1969–2017, the CDDs increased in Indian cities by 0.7–3.8%/decade, while other investigations have reported CDDs to increase by about 3.7–

85.4%/decade in Italian cities from 1980–2013 [103] and by 0–40%/decade in Spanish cities during 1970–2005 [104].

Future CDD Trends (2018–2100)

Figure 3.7 also shows the future projections of Delhi's CDDs from 2018–2100 under the RCP4.5 and RCP8.5 scenarios. Depending on the emission scenario, CDDs in Delhi will be higher by 6.4–7.1% in the 2020s, by 15.2–20.8% in the 2050s, and by 24.3–52.7% in the 2080s, compared to the baseline (see Figure 3.7), with the largest increase happening under RCP8.5 (high emission scenario) in the 2080s. Similarly, CDDs will increase during 2018–2100 for all the other cities under both emission scenarios, as presented in Figure 3.8 (see Figures AI3 a–f). Figure 3.8 shows that in the 2020s and 2050s, the CDD increase will be roughly equal under both the emission scenarios, with CDD increasing by 2.9–22.9% in the 2020s and by 8.3–54.1% in the 2050s for the selected cities. However, by the 2080s, the CDD increase under the RCP8.5 scenario will be much higher (by 12–29 percentage points depending on the city) than that under the RCP4.5

The OLS slopes of CDDs were also statistically significant for all the six cities, with magnitudes ranging from 44.5–140.1 °Cd/decade (1.1–4.5% CDD increase per decade) and 126.7–265.5 °Cd/decade (3.3–9.4% CDD increase per decade) under the RCP4.5 and RCP8.5 scenarios, respectively, as shown in Table 3.5. The PWMKTS analysis also detected statistically significant CDD trends for most cities, except Delhi, Hyderabad, and Kolkata under the RCP4.5 scenario and Bengaluru under the RCP8.5 scenario. The corresponding TS Slopes (when statistically significant) ranged between 11.5–16.5 °Cd/decade (0.1–0.6% CDD increase per decade) and 11.9–20.4 °Cd/decade (0.4–0.6% CDD increase per decade) under RCP4.5 and RCP8.5 scenarios, respectively. The discrepancies in detecting trends between the

OLS and PWMKTS analysis arise due to the prewhitening process applied in PWMKTS analysis.

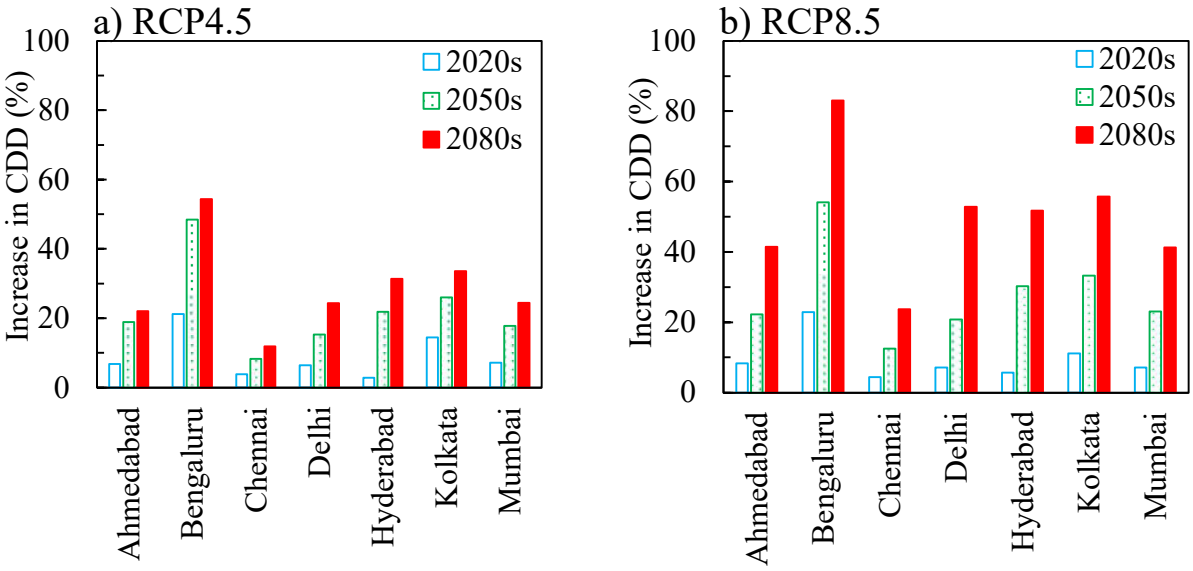

Figure 3.8: Increase in cooling degree days (CDDs) in 2020s (2005–2034), 2050s (2035–2064), and 2080s (2065–2094) for seven major Indian cities under the a) RCP4.5 and b) RCP8.5 emission scenario.

3.7.3 HDD Trends (1969–2100)

This section discusses the historical and future trends in HDDs for Delhi and Srinagar since only those cities have heating requirements.

Historical HDD Trends (1969–2017)

Figure 3.9 shows the historical (1969–2017) and future (2018–2100) projections of HDDs for Delhi, along with its baseline value (277 °Cd). The HDDs were almost constant during 1969–2017, which was also established from the OLS and PWMKTS analysis (no significant linear trend), presented in Table 3.5. In contrast, HDDs in Srinagar decreased significantly during 1969–2017 (see Figure AI4), with an OLS slope of −68.9 °Cd/decade (−100.0, −37.8 °Cd/decade at 95% confidence level), as presented in Table 5, which corresponds to a 3.1% HDD decrease per decade. The PWMKTS analysis also obtained a similar conclusion, i.e., there was a significant downward HDD trend in Srinagar (see Table 3.5). Srinagar's HDDs

decreased by 42.5 °Cd/decade (5.6–77.2 °Cd/decade is the 95% confidence level), which amounts to 1.9% HDD decrease per decade.

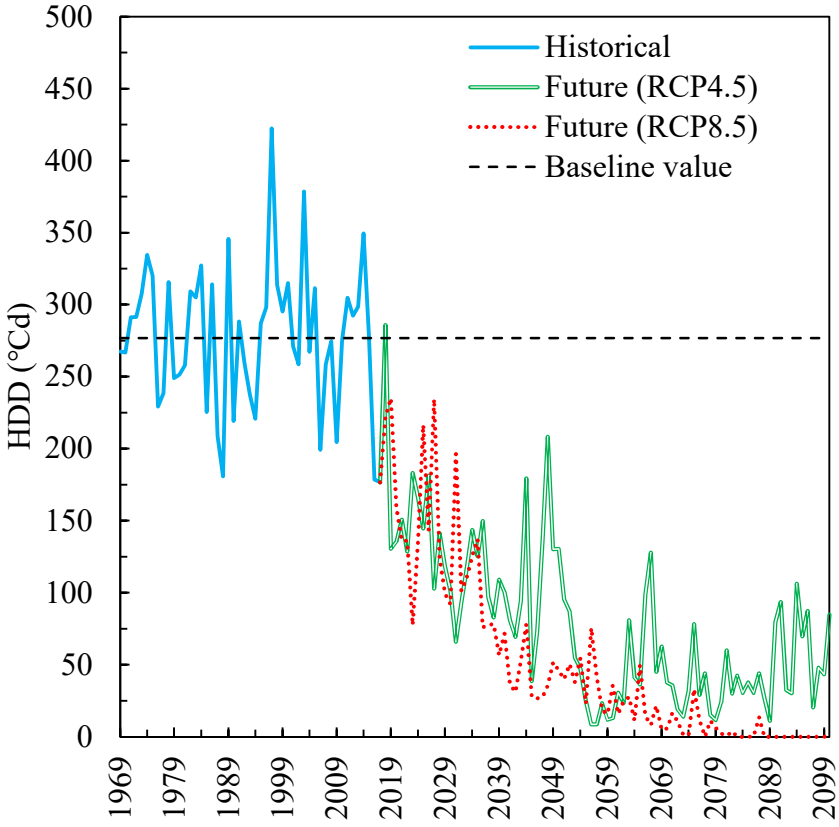

Figure 3.9: Historical and future heating degree days (HDDs) in Delhi.

Thus, building heating requirements decreased in Srinagar while they remained constant in Delhi during 1969–2017. The decrease in HDDs during 1969–2017 was less than 3.1%/decade in Indian cities, whereas HDDs decreased by 1.3–8.6%/decade during 1980–2013 and by 2.3–6.0 %/decade during 1970–2005 in Italian [25] and Spanish [23] cities, respectively. Therefore, out estimated results are also in qualitative agreement with the previous investigation.

Future HDD Trends (2018–2100)

Figure 3.10 shows that HDDs will decrease in the future in Delhi and Srinagar under both the emission scenarios when compared to their corresponding baseline values. For Delhi, HDDs decrease by 28.4–30.3% in the 2020s, by 71.6–83.3% in the 2050s, and by 83.5–97.1% in the 2080s, depending on the emission scenario. Thus, the building heating requirements will

become very small (HDDs < 80 °Cd) in Delhi by the 2050s under both emission scenarios (see Figure 3.9).

Table 3.5: Historical and future trends in heating degree days (HDDs).

Time period	City	OLS analysis		PWMKTS analysis	
		Slope[b] (°Cd/decade)	p-value	Slope[b] (°Cd/decade)	MK test p-value
Historical (1969–2017)	Delhi	−3.2[a] (−13.6, 7.2)	0.541	−3.8[a] (−13.2, 7.7)	0.472
	Srinagar	−68.9 (−100.0, −37.8)	< 0.001	−42.4 (−77.2, −5.6)	0.020
RCP4.5 (2018–2100)	Delhi	−14.8 (−18.6, −11.0)	< 0.001	−4.6 (−7.6, −1.2)	0.010
	Srinagar	−29.2 (−39.8, −18.5)	< 0.001	−19.2 (−30.7, −7.8)	0.002
RCP8.5 (2018–2100)	Delhi	−21.2 (−2.3, −18.1)	< 0.001	−1.3[a] (−3.7, 0.0)	0.065
	Srinagar	−102.4 (−15.2, −89.7)	< 0.001	−19.2 (−34.9, −4.1)	0.013

[a]Not a statistically significant result (p-value > 0.05).
[b]The values in parenthesis represent the 95% confidence interval.

Similarly, Srinagar's building heating requirements will also reduce, as HDDs decrease by 8.1–10.4% in the 2020s, by 17.6–23.9% in the 2050s, and by 19.3–38.1% in the 2080s, depending on the emission scenario. The OLS analysis found significant linear trends in future HDDs for Delhi. Delhi's HDDs decrease by –14.8 °Cd/decade (–5.5% per decade) and by –21.2 °Cd/decade (–7.9% per decade) under the RCP4.5 and RCP8.5 scenarios, respectively. On the other hand, the PWMKTS analysis detected a significant HDD trend of magnitude –4.6 °Cd/decade (–1.7% per decade) under the RCP4.5 scenario, but not under the RCP8.5 scenario. For Srinagar, both the OLS and PWMKTS analysis detected significant decreasing trends in future HDDs. The OLS slopes were –29.2 °Cd/decade (–1.3% per decade) and –102.4

°Cd/decade (–4.6% per decade) under the RCP4.5 and RCP8.5 scenarios, respectively, while the TS slope was –19.2 °Cd/decade (–0.9% per decade) under both scenarios.

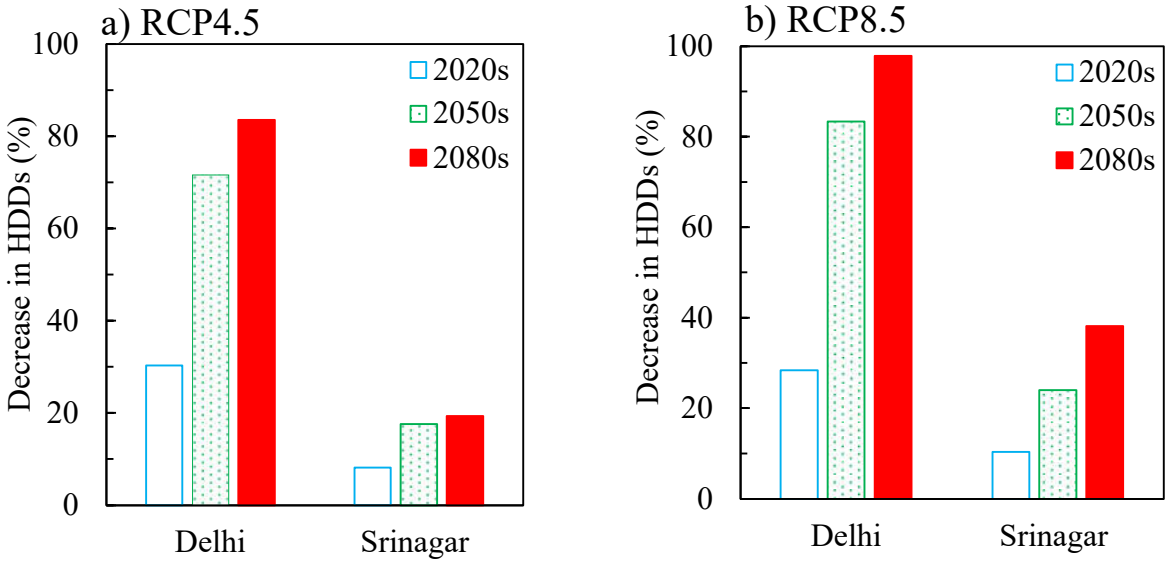

Figure 3.10: Decrease in annual heating degree days (HDDs) in 2020s (2005–2034), 2050s (2035–2064), and 2080s (2065–2094) for two major Indian cities under the a) RCP4.5 and b) RCP8.5 emission scenario.

Once more, in this study postulate that the "true" HDD trend is likely overestimated by OLS analysis as it does not account for autocorrelation in the time-series, while the PWMKTS analysis underestimates it since prewhitening can partly remove the trend.

4.1 Methodology

A review of the literature presented in Chapter 2 reveals that the indoor thermal comfort significantly depends upon the climate and building envelope. Thus, to evaluate any envelope retrofit solution, the as-built thermal comfort of the houses should be evaluated. This study conducted year-long measurements (from 1st April 2021 to 31st March 2022) of the weather and indoor environmental conditions in the bedroom of a typical stand-alone house (see Figure 4.1), located in Pilani, Rajasthan, India (latitude = 28.38° N, longitude = 75.61° E). The location experiences hot-semi arid climatic conditions (details in Section 4.5.1). The measurements were used to evaluate occupants' thermal comfort in the as-built state of the house.

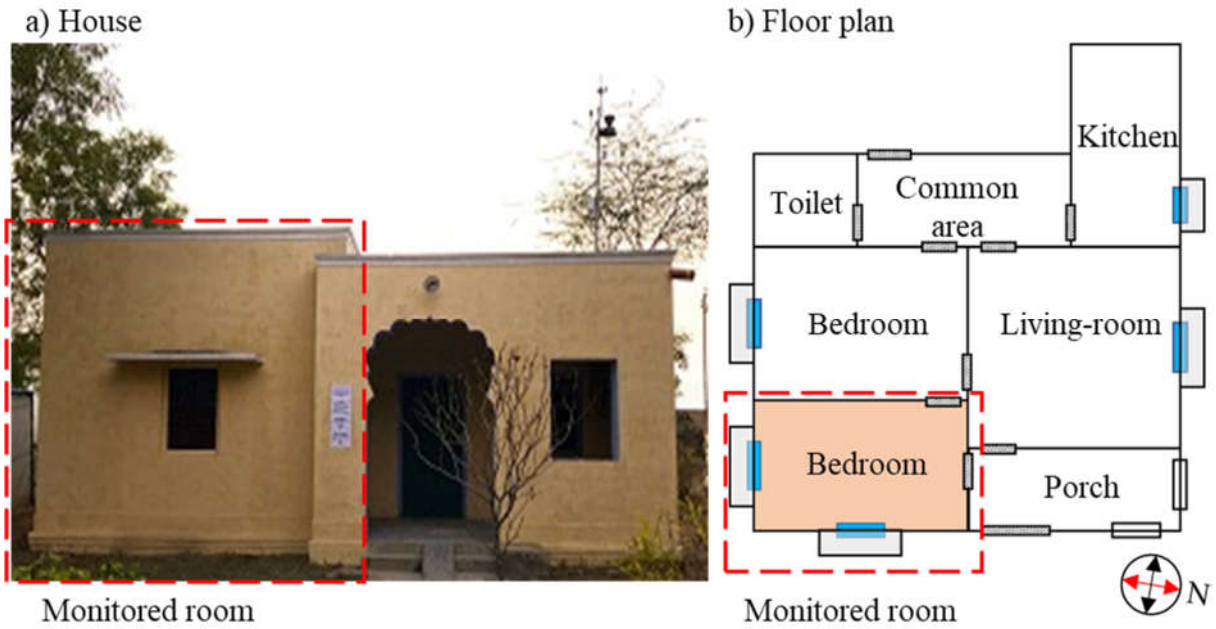

Figure 4.1: a) The monitored room in a single-story house and b) the floor plan.

4.2 Monitored Room Description

The monitored room was part of an unoccupied house (~94 m^2 built-up area) with two bedrooms, a living room, and a kitchen, as shown in Figure 4.1. The house is a slab-on-grade construction, with brick masonry walls and a reinforced brick concrete roof. The monitored room (4.5×3.6×3.7 m^3 in size) has three exterior walls (facing east, south, and north), two internal partition walls, and two wooden doors. The exterior walls (east and south facing) have casement windows with horizontal overhangs.

4.3 Monitoring Setup

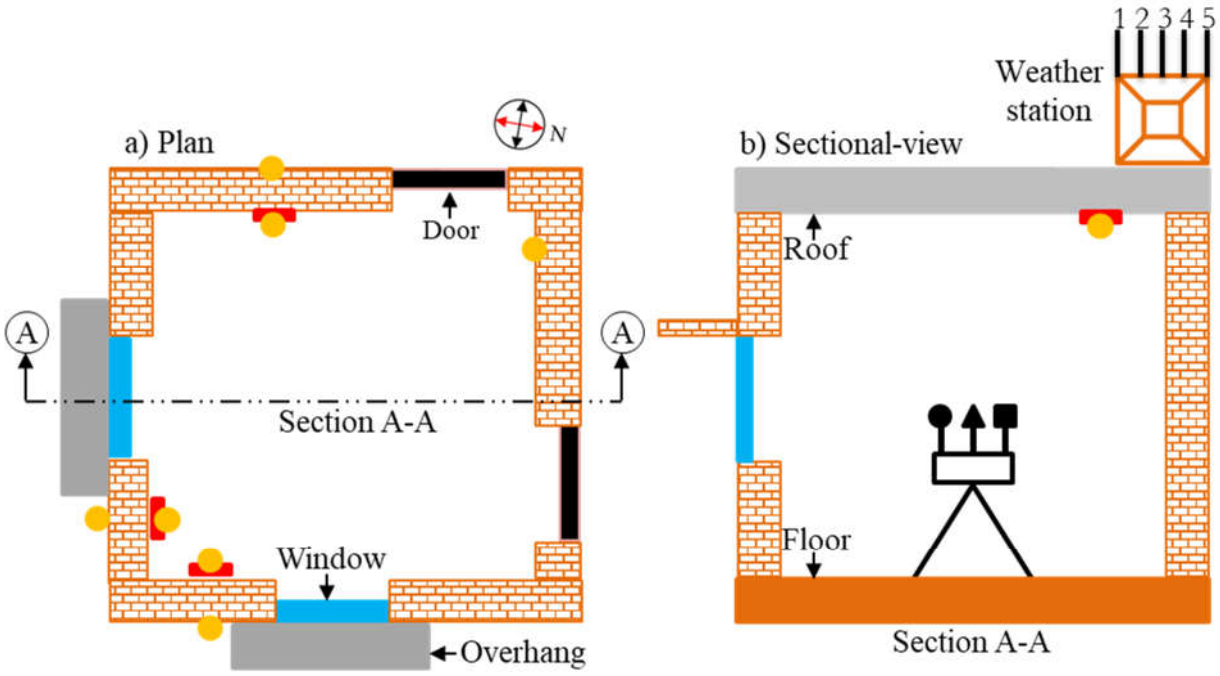

1. Temperature and RH, 2. solar radiation, 3. wind speed, 4. wind direction, 5. precipitation, 6. indoor temperature and RH (▲), 7. black globe temperature (●), 8. air speed (■), 9. surface temperature (●), and 10. heat flux (●).

Figure 4.2: The sensor positions inside and outside the room as shown in the a) plan and b) section.

The room's indoor and outdoor environmental conditions, envelope heat fluxes, and surface temperatures were monitored, as depicted in Figure 4.2. The sensor details are provided in Table 4.1. The weather parameters: outdoor air temperature, relative humidity (RH), global horizontal radiation (GHI), precipitation, and wind conditions were measured using a weather

station mounted on the roof of the monitored house (see also Figure 4.3). The heat fluxes through the roof and walls, along with their inside and outside surface temperatures, were measured (see Figure 4.2 and Figure 4.3) to analyze the thermal behavior of the room. The occupants' thermal comfort conditions in the room were also assessed by monitoring the air temperature, black globe temperature, RH, and airspeed in the center of the room at a height of ~1.1 m above the floor.

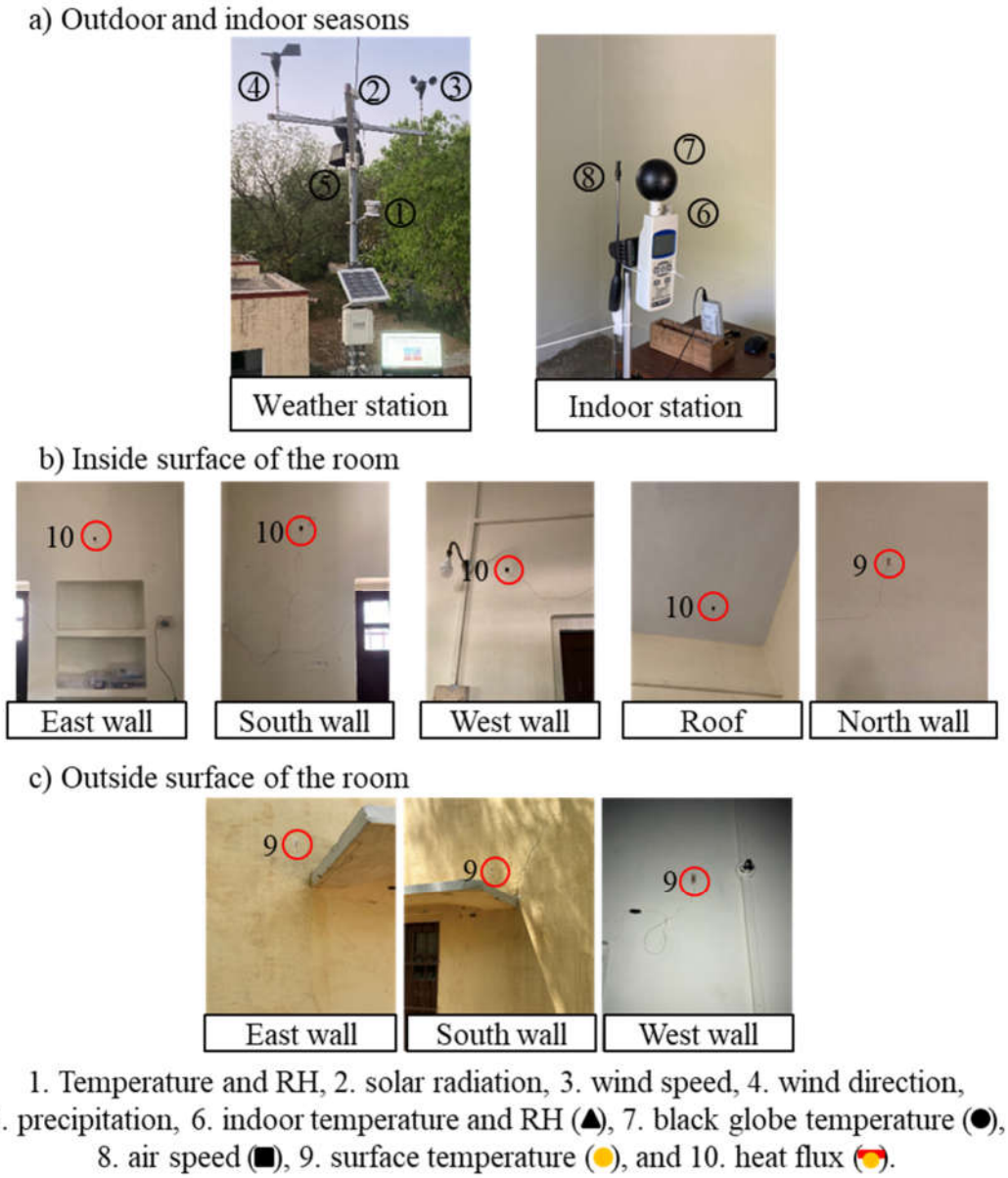

Figure 4.3: Actual sensors position a) outdoor weather station and indoor thermal comfort sensors, b) heat flux and surface temperature positions inside the surface of the room, and c) surface temperature positions outside the surface of the room.

Table 4.1: The details of the sensors.

A) Weather sensors			
Sensor [Model]	**Parameter**	**Resolution**	**Accuracy [Range]**
Silicon pyranometer [S-LIB-M003]	Global horizontal irradiance	1.25 W/m^2	± 10 W/m^2 [0 to 1280 W/m^2]
Temperature and RH sensor with radiation shield [S-THB-M002]	Air temperature	0.02 °C	± 0.21 [− 40 to 70 °C]
	RH	0.1%	± 2.5% [0 to 100%]
Cup-type anemometer [S-WSB-M003]	Wind speed	0.5 m/s	± 1.1 m/s [0 to 76 m/s]
Wind vane [S-WDA-M003]	Wind direction	1.4 °	± 5° [0 to 355 °]
Rain gauge [S-RGF-M002]	Precipitation	0.2 mm	± 5% [0 to 102 mm]
B) Heat flux and surface temperature sensors			
Heat flux [PHFS-01e]	Heat flux	1 W/m^2	± 5% [−150 to 150 kW/m^2]
	Surface temperature	1 °C	1 °C [0 to 200 °C]
Surface temperature [FTC]	Surface temperature	1 °C	1 °C [0 to 200 °C]
C) Thermal comfort sensors			
Heat index meter [WBGT-2010SD]	Air temperature	0.1 °C	± 0.8 °C [0 to 50 °C]
	RH	0.1%	± 3 % [5 to 95%]
	Black globe temperature	0.1 °C	± 0.6 °C [0 to 80 °C]
Hot-wire anemometer [Luton AM-4214SD]	Airspeed	0.1 m/s	± 0.3 m/s [0.2 to 25 m/s]
	Air temperature	0.1 °C	± 0.8 °C [0 to 50 °C]

The data collected from the outdoor weather station was validated with the Typical Meteorological Year (TMY) file developed by the Indian Society of Heating, Refrigerating,

and Air Conditioning Engineers (ISHRAE) for the nearest city (Delhi). The heat flux and surface temperature sensors were corrected every three months by comparing their performance to remove any bias in the sensor. The performance of the thermal comfort sensor (air temperature) is compared with the outdoor weather station sensor in a controlled environment before the beginning of the monitoring period.

4.4 Adaptive Thermal Comfort

To evaluate the comfort conditions in the room, this study used the adaptive thermal comfort (ATC) framework, which recognizes that humans can adapt to a wide range of thermal conditions through their ability to regulate their clothing and immediate environment (see Table 4.2). We compared two different ATC models, the Indian Model for Adaptive Comfort-Residential (IMAC-R) and the American Society of Heating, Refrigerating, and Air-Conditioning Engineers (ASHRAE) 55–2020 model, in their ability to predict the room's comfort conditions.

Table 4.2: Adaptive thermal comfort criteria for ASHRAE-55 and IMAC-R.

Thermal parameters	**ASHRAE-55**	**IMAC-R**
Participants	Globally	Indian
Ventilation	Nature	Nature and mixed mode
Opening windows	Yes	Yes
Heating/ cooling system	No	No
Cloth insulation (clo)	0.5–1.0	0.1–1.0
Metabolic rate (met)	1.0–1.3	0.7–1.7
$T_{out-30d}$ (°C)	10–33.5	5.5–33

The IMAC-R model was developed based on field surveys conducted in eight cities, covering all the climate zones of India, while the ASHRAE 55 standard is a globally recognized ATC model. Both models prescribe the operative temperature bands for thermal acceptability in correlation with the outdoor reference temperature for naturally ventilated residences. However, the neutral temperature (the indoor temperature that an average occupant finds

neutral, i.e., neither warm nor cool) prescribed by IMAC-R is 2 °C warmer than that recommended by the ASHRAE 55 standard. The details of those ATC models can be found in [105,106] and we only provide our application methodology here.

Using the ATC framework, we first computed the room's hourly operative temperatures, which is a measure of thermal comfort that accounts for the air temperature and radiation effects in the built environment, using:

$$T_{op} = \beta T_a + (1 - \beta) T_{MRT} \quad \text{(Eq. 4.1)}$$

where T_{op} is the operative temperature, T_a is the indoor air temperature, and T_{MRT} is the mean radiant temperature. β is a dimensionless constant that depends on the indoor air speed ($\beta = 0.5$ for air speeds below 0.2 m/s, $\beta = 0.6$ for air speeds between 0.2–0.6 m/s, and $\beta = 0.7$ for air speeds above 0.6 m/s). Next, we estimated the 80% comfort band, i.e., the operating temperature range in which 80% of occupants find the environment thermally acceptable, from the location's prevailing outdoor temperatures using:

$$AT_{out-30d} + B - C \leq T_{op} \leq AT_{out-30d} + B + C \quad \text{(Eq. 4.2)}$$

where $T_{out-30d}$ is the 30-day outdoor running mean temperature, and A, B, and C are the ATC model constants (A = 0.31, B = 17.8 °C, and C = 3.5 °C for ASHRAE 55; while A = 0.42, B = 17.6 °C, C = 3.6 °C for IMAC-R). Thus, if the room's operative temperature falls within the above comfort band, the thermal environment is deemed comfortable; if higher, then unacceptably hot, and if lower, then unacceptably cold.

4.5 Results

The first reports the performance of the monitoring instruments, followed by the measurements of the location's weather conditions and the room's thermal characteristics in the as-built state during the monitoring period.

4.5.1 Measurements of the Weather Conditions

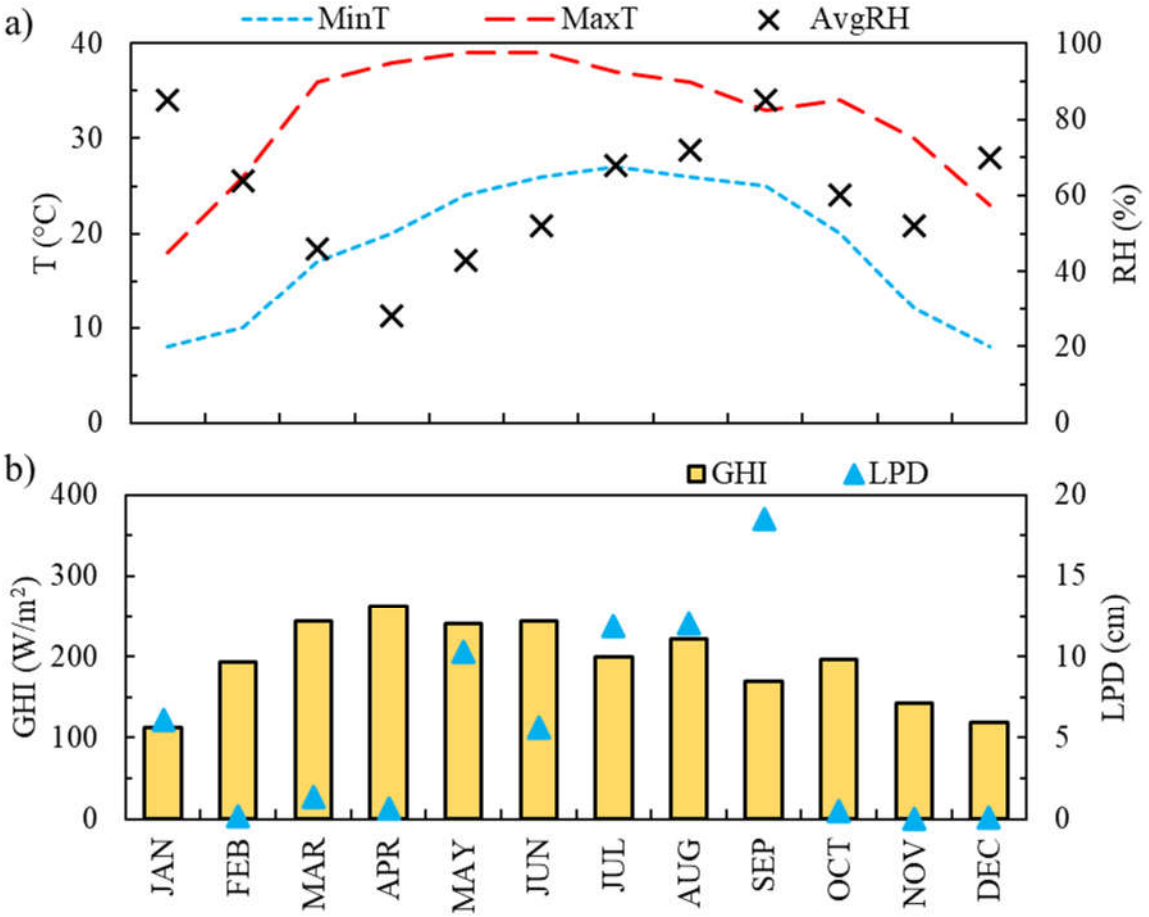

Figure 4.4: a) The monthly averages of the minimum/maximum outdoor air temperatures (T) and RH, and b) the monthly average GHI and the total LPD.

Figure 4.4 depicts the monthly averages of the minimum and maximum outdoor air temperatures (MinT and MaxT), RH, GHI, and the liquid precipitation depth (LPD) during the monitoring period. The location experiences a cold and dry winter season (November to February), with daily minimum temperatures routinely falling below 10 °C (for 71 days). Even in winter, the location receives sufficient solar radiation and experiences calm wind conditions see Figure AII1 (Appendix-II). The remaining months (March and October) had relatively moderate air temperatures, relative humidity, and negligible rainfall. Overall, the location exhibited scorching hot summers and cold winters, typical of a hot semi-arid climate (BSh according to the Köppen-Geiger climate classification system).

4.5.2 Measurements of the Room's Indoor Environment and Thermal Comfort

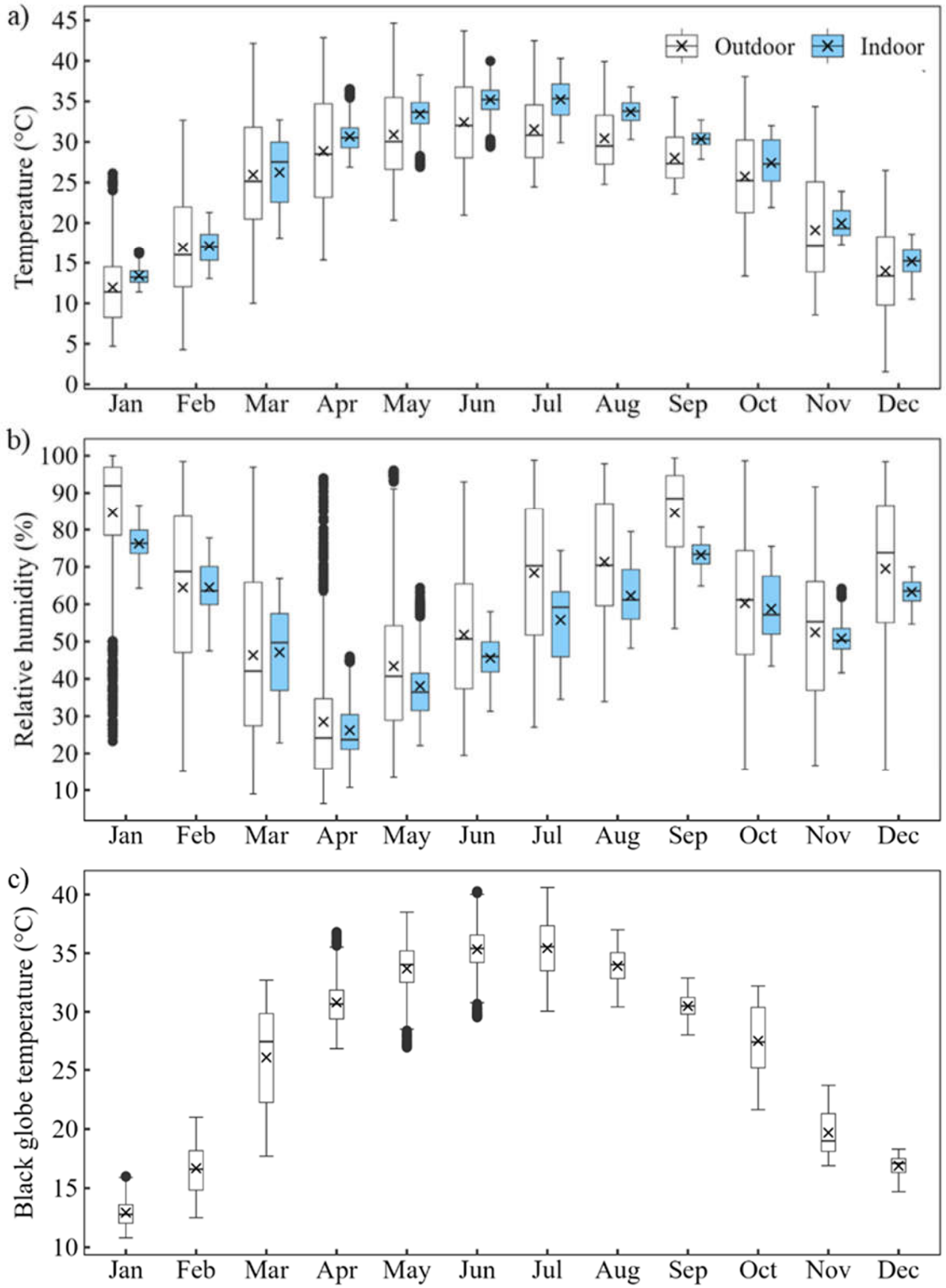

Figure 4.5: Boxplots of the monthly variations of the outdoor and indoor a) air temperatures, b) relative humidity, and c) indoor black globe temperature. The mean temperature values are also shown using the cross (×) symbol.

In addition to the outdoor weather conditions, the room's indoor air conditions were monitored for one year (Table 4.1 provides the measured parameters). Figure 4.6 a compares the outdoor and indoor temperatures for the study period. Expectedly, the indoor air temperature swing was much lower than the outdoor air temperature due to the envelope's thermal mass and resistance. During winter (November to January), the indoor temperatures range between 10–24 °C, thus usually causing cold discomfort. Conversely, in summer (April to September), indoor temperatures always exceed 27 °C (the approximate upper limit for thermal comfort in air-conditioned buildings) and can even reach 40 °C, leading to extreme hot discomfort for occupants. During the moderate season (March and October), the indoor temperatures range between 18–33 °C, making it relatively comfortable for occupancy.

The room's RH conditions are shown in Figure 4.6 b. The indoor RH showed a similar pattern as the outdoor RH but with lower diurnal variations. We also measured the black globe temperature in the room, as shown in Figure 4.6 c, which was nearly equal to the indoor air temperature due to the absence of any strong radiation sources. The indoor air speed was around 0.4 m/s when the ceiling fan was running (from 4th April 2021 to 27th October 2022), while it was below 0.2 m/s for the remaining period when the ceiling fan was turned off.

Based on the measurements of the room's indoor conditions, we also estimated occupants' thermal comfort using the IMAC-R model and ASHRAE 55 standard (see Section 4.4 for details), as shown in Figure 4.7. Remarkably, the two models showed significant differences in their comfort predictions. On the one hand, the IMAC-R model classified 1658 h as unacceptably hot, 3165 h as unacceptably cold, and 3762 h as comfortable. On the other hand, the ASHRAE standard classified 4006 h as unacceptably hot, 2626 h as unacceptably cold, and 1953 h as comfortable. This was because the IMAC-R prescribes a 2 °C warmer neutral temperature than the ASHRAE standard, which led to the IMAC-R predicting much higher comfort hours in summers and lower in winters.

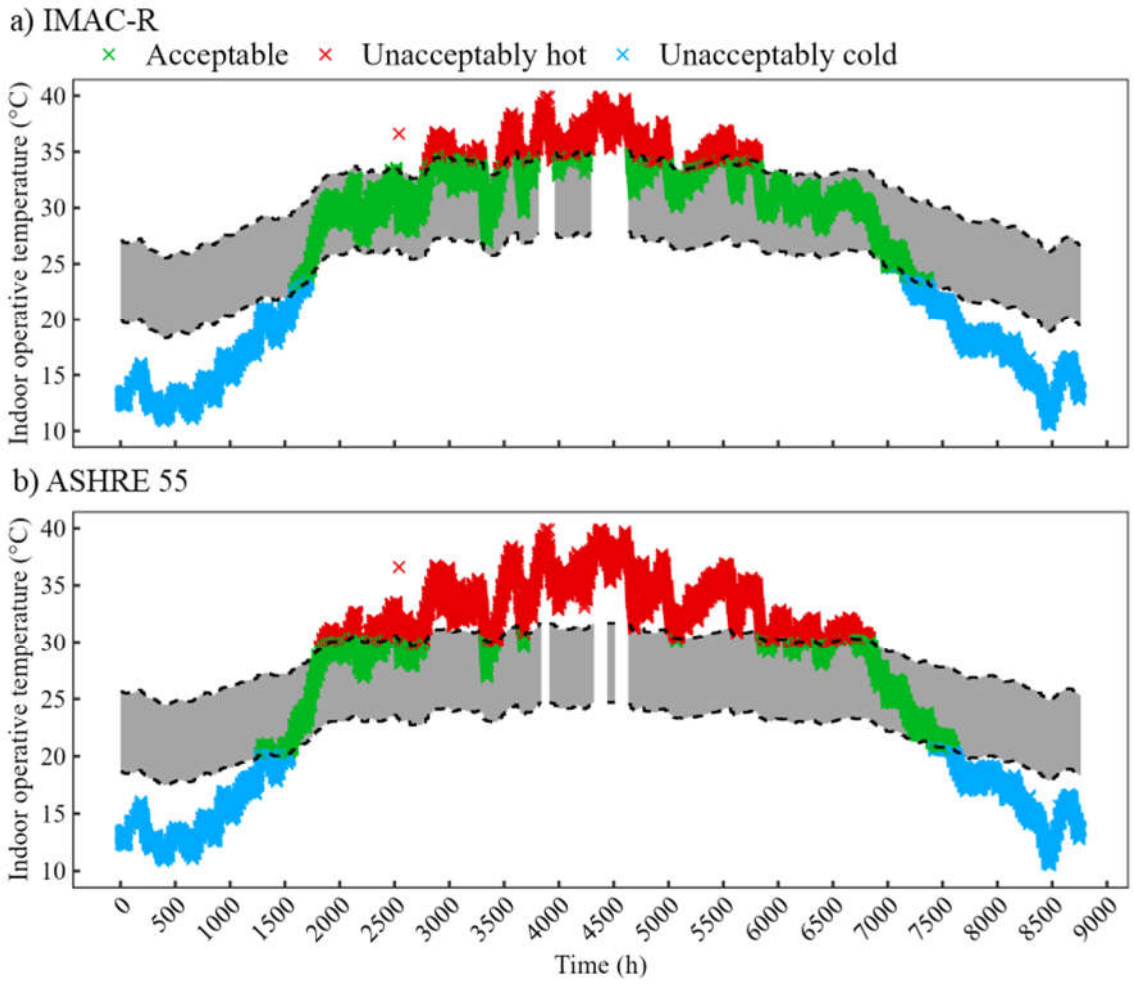

Figure 4.6: The measured indoor operative temperatures and the 80% acceptability (gray) band as per a) IMAC-R and b) ASHRAE 55 adaptive thermal comfort models.

Note that the IMAC-R model predicted significantly more thermal discomfort in winter (3165 h) than in summer (1658 h), while the ASHRAE model predicted it the other way around. We considered the ASHRAE model to be more in line with the actual thermal comfort situation in the room based on our experience of living in that location, according to which thermal discomfort in summer dwarfs winter discomfort. Thus, this investigation selected the ASHRAE model for assessing thermal comfort. Note that we could not evaluate thermal comfort for 175 hours during the year (~2% of the year) due to equipment malfunction.

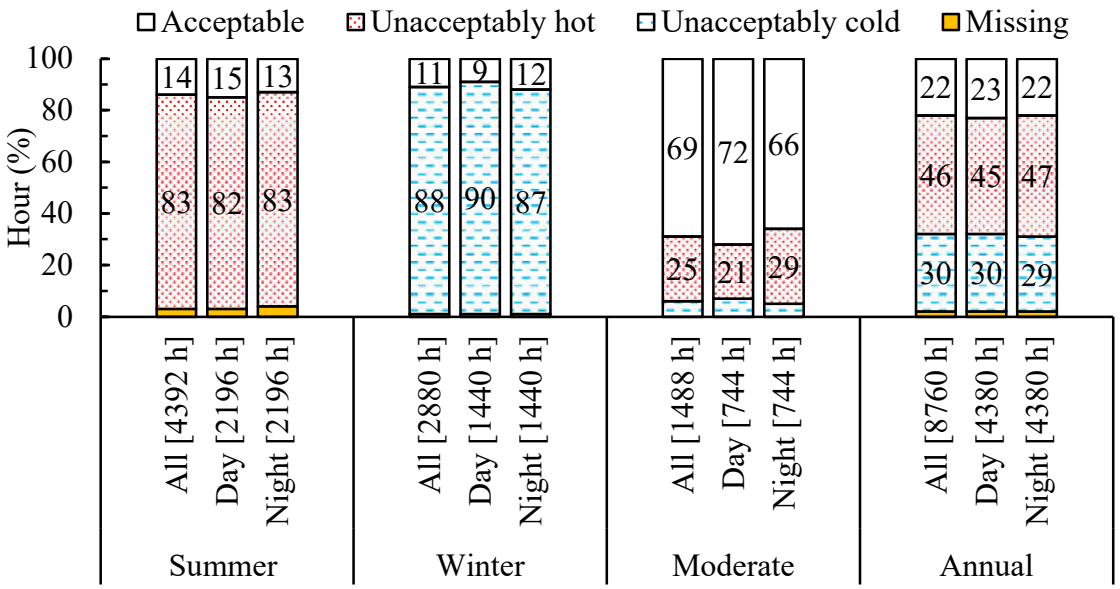

Figure 4.7: Percentages of comfort and discomfort hours during the monitoring period.

Figure 4.7 shows the seasonal and diurnal variations of thermal comfort in the room as per the ASHRAE 55 standard. The Figure shows that during the summer season, a significant portion (83%) of the hours were uncomfortably hot, while in the winter, most hours (88%) were uncomfortably cold. The most comfortable hours (69%) were during the moderate season. The comfortable/uncomfortable hours were evenly distributed between day (7 am to 7 pm) and night (7 pm to 7 am) throughout the year. Overall, only 22% of hours in the year were comfortable, making the room an ideal candidate for envelope retrofits, as discussed in Chapter 5.

5.1 Methodology

A thermal model of the monitoring room in EnergyPlus was developed to assess different envelope retrofit solutions. The model was constructed using the building geometry, thermal properties, occupancy schedules, and weather data (see Figure 5.1). Subsequently, the thermal model was calibrated and validated based on the monitored data (see Chapter 4). Furthermore, using the validated thermal model, various envelope retrofit options for improving thermal comfort conditions in a detached single-story house in India's hot-semi-arid climate zone were compared.

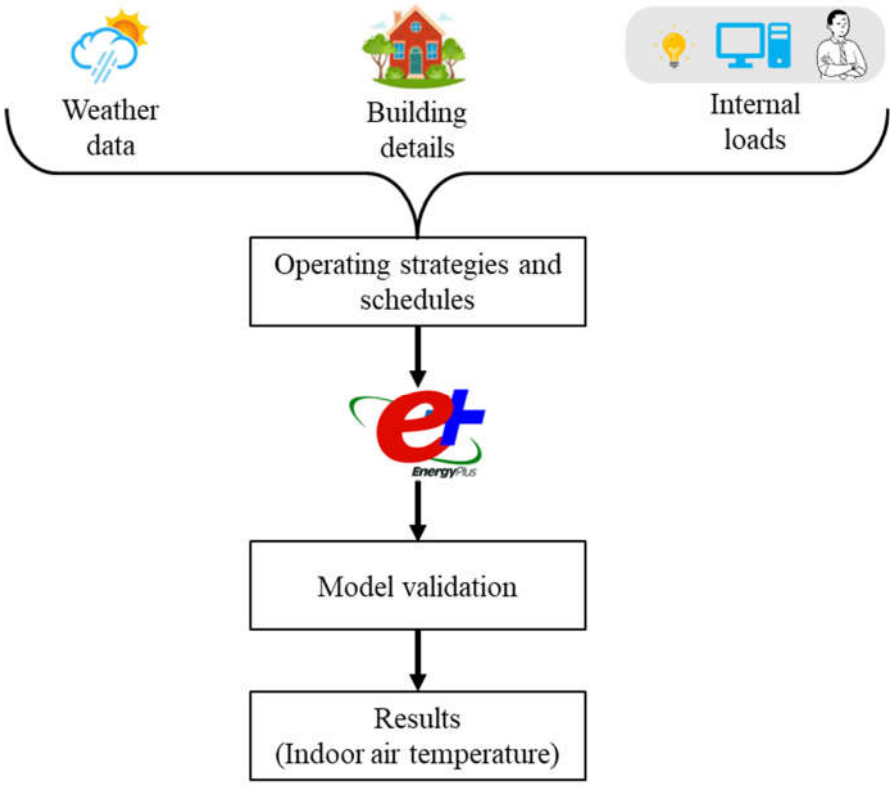

Figure 5.1: Modeling flow chart of EnergyPlus.

5.2 Thermal Physical Properties of Building Materials

The construction details of the room's envelope were obtained from the building records and physical observations, as given in Table 5.1, along with the thermo-physical properties of

the building material used in the EnergyPlus model. The thermo-physical properties were taken from their typical values found in the literature [107,108], except for the brick's thermal conductivity. The brick's thermal conductivity was obtained from in-situ measurements of thermal resistances of the external walls using Anderlind's Pentaur method [109], which was also found to agree with its typically reported value [107].

Table 5.1: Building envelope details and material properties.

A) Envelope details				
Roof	0.15 m thick reinforced brick concrete (RCB) with 0.02 m cement plaster on both sides.			
External walls	0.36 m thick fired clay brick with 0.015 m cement plaster on both sides.			
Internal walls	0.24 m thick fired clay brick with 0.01 m cement plaster on both sides.			
Floor	0.25 m cement mortar with 0.02 m Kota stone tiles.			
Windows	Size: 0.6 m × 0.9 m. Material: half of the window pane is made of 0.006 mm clear glass, and the rest is 0.006 m wooden. External shading: 0.6 m horizontal static overhang at lintel level.			
Doors	External door size: 1.8 m × 1.2 m, Internal door size: 1.8 m × 0.9 m. Material: 0.035 m thick wooden door with wooden frame.			
B) Material properties				
Material	Thermal conductivity (W/m-K)	Density (kg/m^3)	Specific heat capacity (J/kg-K)	Emittance (-)
Fired clay bricks	1.15	2028	928	0.9
Cement plaster	0.72	1860	835	0.9
RCB	1.4	1920	900	0.9
Mortar	0.88	2880	896	0.9
Kota stone tiles	1.47	2750	1200	0.9
Wood	0.17	704	2000	0.9
Clear glass	0.9	-	-	0.8
EPS insulation*	0.15	24	1340	-

*Expanded polystyrene (EPS) insulation was not part of the original construction but was used as one of the retrofit options.

5.3 Simulation Parameters and Boundary Conditions

The EnergyPlus model was developed to simulate the indoor environmental conditions of the monitored room from the room's construction details and the measured weather conditions as shown in Figure 5.2. Note that the weather station deployed could only measure the GHI and did not give the values of direct normal irradiance (DNI) and diffuse horizontal irradiance (DHI) components, which are essential for conducting energy simulation. Thus, the Boland–Ridley–Laurent (BRL) model [110] to estimate those components from the measured GHI values.

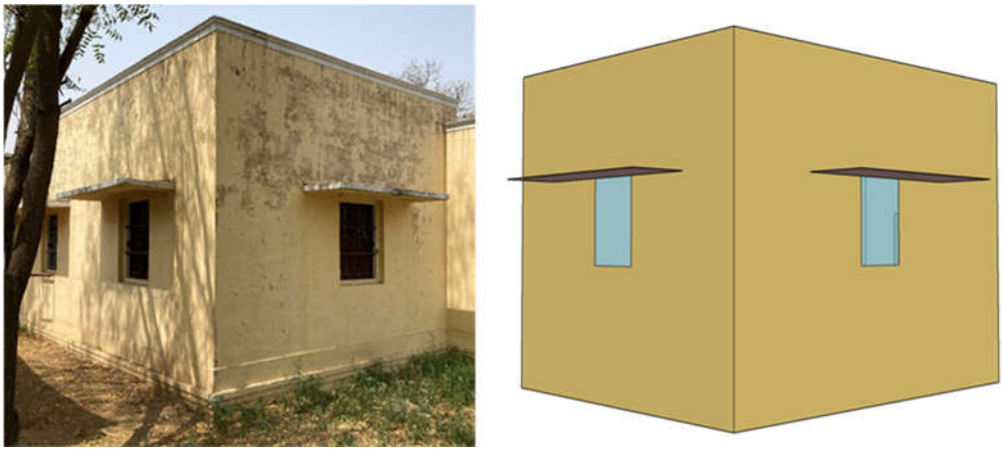

Figure 5.2: The monitored room and its EnergyPlus model.

In our simulation, the room's exterior walls and ceiling were exposed to outdoor conditions, while the interior walls were assumed to be adiabatic as the heat transfer through these surfaces would be pretty small. The heat transfer through the floor was calculated using the F-factor method [111]. A constant infiltration rate of 0.5 h^{-1} throughout the year was assumed, which was estimated by conducting a carbon dioxide decay test in the room [112]. No occupants were present in the room, and the internal loads were estimated from the equipment usage in the room (a laptop for data collection and a fan operating from April 2021 to October 2021). No heating or cooling systems were present in the room, and the windows were closed throughout the year.

5.4 Thermal Model Calibration and Validation

The room had an uninsulated slab-on-grade foundation, with the floor constituting about one-fourth of the room's total area exposed to the outdoors (outdoor air and ground). Thus, characterizing the floor-ground heat transfer became crucial to obtain a well-calibrated model [113]. The F-factor method was used to model the floor-ground heat transfer, and the monthly ground temperature between 12–32.4 °C (see Table AII1) was adjusted to minimize the difference between the measured and simulated indoor air temperatures.

The EnergyPlus model was validated using the measured values of indoor air temperatures, envelope heat fluxes, and surface temperatures. Figure 5.3 compares the measured and simulated values of the hourly indoor air temperatures for July and February, i.e., when the model performed best and worst, respectively. It is clear from the figure that the model well captured the qualitative trends in the indoor air temperature, even in its worst-performing month (February).

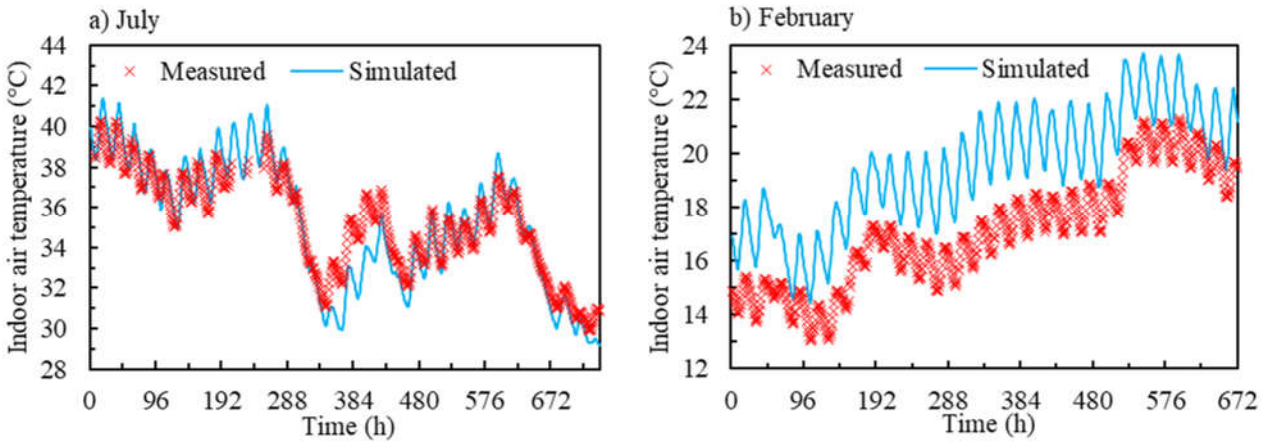

Figure 5.3: Comparison between the measured and simulated indoor air temperatures for a) July and b) February.

For a qualitative assessment of the model's performance, we calculated the normalized mean bias error (NMBE) and the coefficient of variation of the root mean square error (CVRMSE) for the hourly indoor air temperature by using

$$\mathrm{NMBE}(\%) = \frac{\sum_{i=1}^{N_i} S_i - M_i}{\sum_{i=1}^{N_i} M_i} \times 100 \quad \text{(Eq. 5.1)}$$

$$\mathrm{CVRMSE} = \frac{\sqrt{\sum_{i=1}^{N_i} \frac{(S_i - M_i)^2}{N_i}}}{\frac{1}{N_i}\sum_{i=1}^{N_i} M_i} \times 100 \quad \text{(Eq. 5.2)}$$

where S_i is the simulated value, M_i is the measured value, and N_i is the number of data points.

The monthly and overall values of those metrics are shown in Figure 5.4. Figure 5.4 shows that the monthly NMBE ranged from −1.9% to 14% (overall = 4.6%), meaning that the model generally overpredicted indoor air temperatures, especially in winter and moderate months. Similarly, the CVRMSE values were also relatively higher in those months, as shown in Figure 5.4. The NMBE and CVRMSE values were well within those reported in the literature, i.e., NMBE ranging between −4% to 9% [37,114] and CVRMSE ranging between 3% to 23% [114–116]. Thus, the model was deemed suitable for predicting the room's indoor air temperatures.

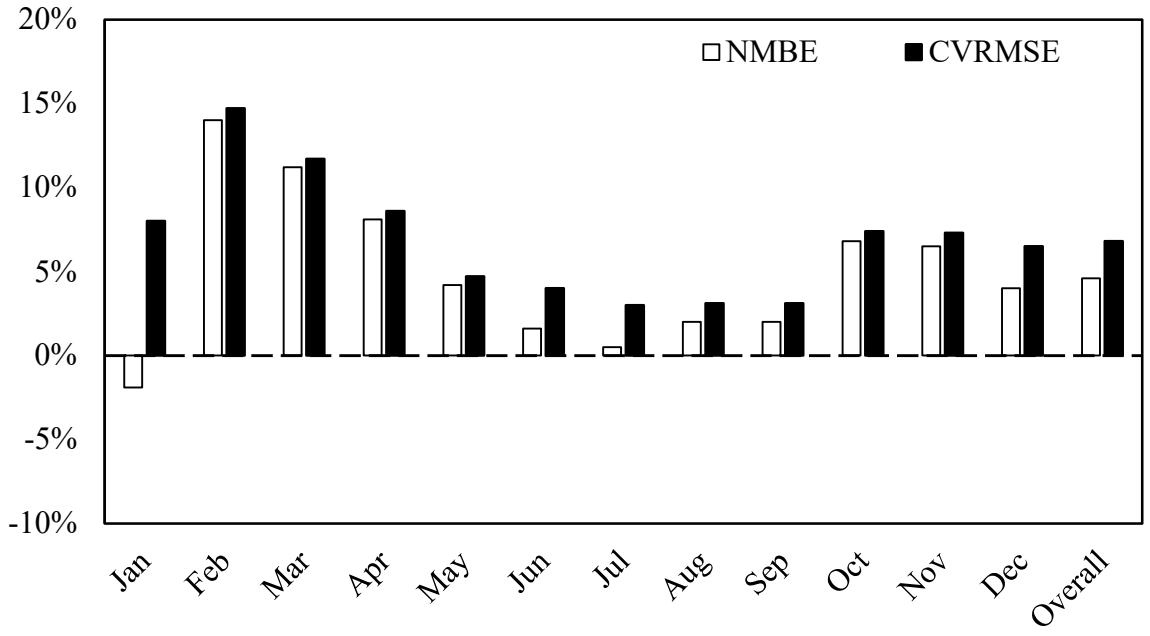

Figure 5.4: The modeling errors (NMBE and CVRMSE) estimated for the indoor air temperatures.

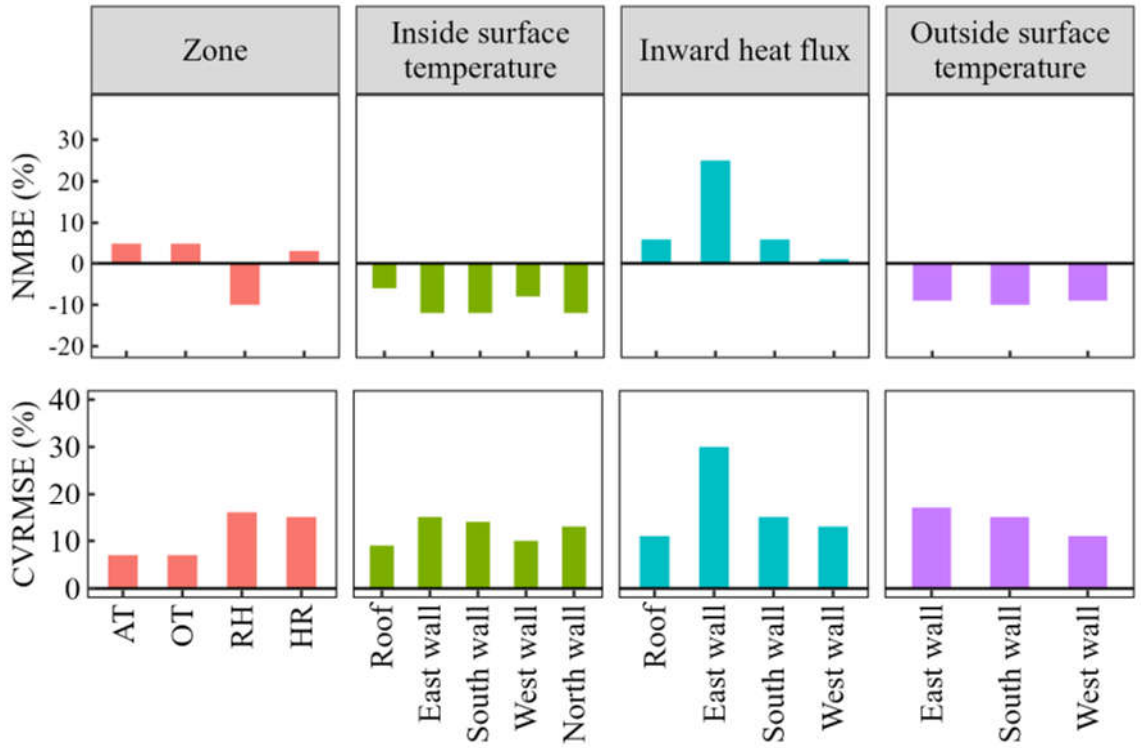

Figure 5.5: The modeling errors (NMBE and CVRMSE) were estimated for the different measured parameters.

NMBE and CVRMSE were also calculated for the other measured parameters, including indoor RH, wall surface temperatures, and envelope heat fluxes, to further assess the model's performance. As shown in Figure 5.5, the NMBE was generally within ±10%, while the CVRMSE was generally below 30%, which further confirms that the model is suitable for conducting thermal simulations of the room.

5.5 Simulation of the Room's Indoor Environment and Thermal Comfort

Although the measurements discussed in Chapter 4 provide valuable insights about the room's thermal environment and comfort conditions in the "as-built" state, they cannot be directly used to evaluate the impact of different envelope retrofit solutions. Thus, this investigation used an EnergyPlus model (details given in above section) of the room to study the effect of envelope retrofit solutions on comfort conditions. Figure 5.6 compares the measured and simulated values of the room's operative temperature for the monitoring duration

and also shows the comfort band (with 80% acceptability) obtained using the ASHRAE 55 model.

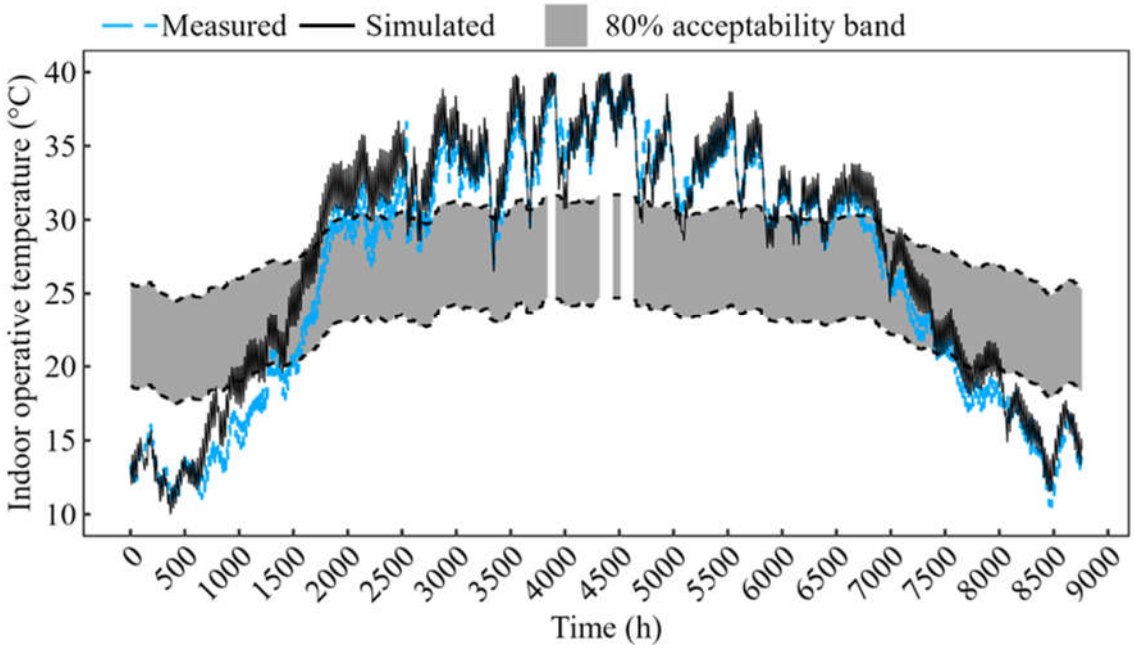

Figure 5.6: Comparison between the measured and simulated operative temperatures.

The Figure shows reasonable agreement between the measured and simulated values of operative temperature (NMBE = 5% and RMSE = 7%). The measured and simulated values of comfort hours were also quite similar (1953 h versus 2022 h), as shown in the Figure. However, the model overpredicted unacceptably hot hours (4006 h versus 4603 h) and underpredicted unacceptably cold hours (2626 h versus 1960 h) since the model overpredicts the room's operative temperature.

The energy simulations of the room also provided valuable insights into the thermal interaction between the room and the outdoors. Figure 5.7 shows the contributions of different room elements to its monthly heat gains (monthly gains were obtained by summing over the hourly values). A negative value means an overall heat loss from the room due to that element (e.g., infiltration). The figure shows that the roof and internal loads (computer and fan) were

the dominant sources of heat gain in the room throughout the year. On the other hand, the external walls, floor, door, and infiltration largely contributed to the heat loss from the room.

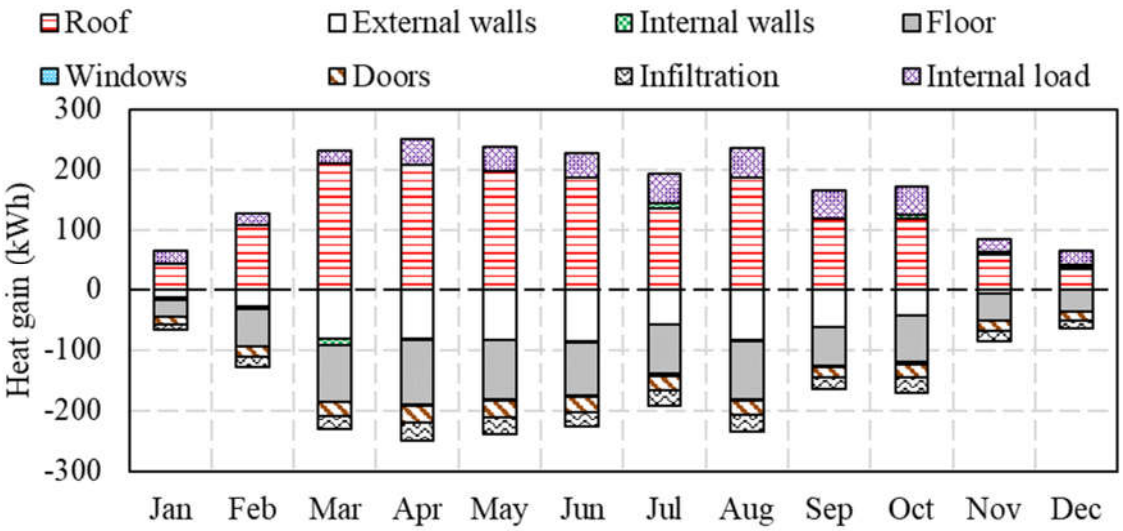

Figure 5.7: Contributions of different building elements to the rooms's monthly heat gains and losses.

5.6 Results

The above results show that the room's EnergyPlus model could reasonably mimic the thermal environment and comfort conditions prevailing in the monitored room, as well as provide valuable insights into its thermal behavior. Thus, it was used to assess the impact of different envelope retrofit solutions, such as i) cool roof, ii) roof insulation, iii) envelope insulation, and iv) wall insulation, on the room's thermal environment, as discussed in the following sub-sections.

5.6.1 Cool and Super-cool Roofs

To assess the impact of applying cool/super-cool roof paints on the room's thermal environment, the room was simulated with different values of α and ϵ for the roof. The model for the as-built construction assumed a gray roof with $\alpha = 0.7$ and $\epsilon = 0.9$ [12]. Three retrofit cases were simulated with a cool roof (α between 0.1–0.3 and $\varepsilon = 0.9$), and one retrofit case was simulated with a super-cool roof ($\alpha = 0.05$ and $\varepsilon = 0.95$).

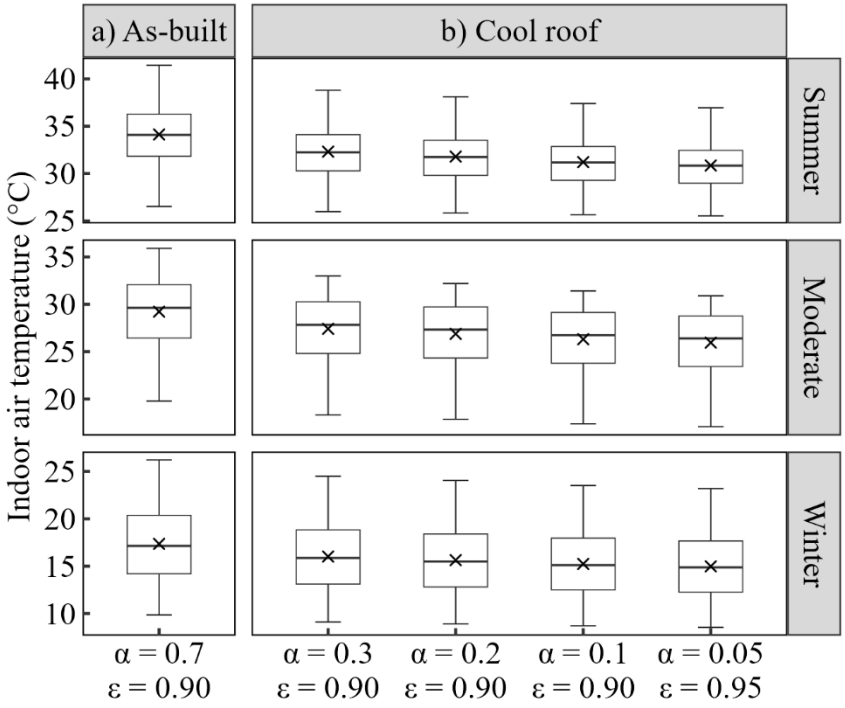

Figure 5.8: Boxplots of the hourly variations of the indoor air temperatures for different seasons for the as-built construction and those with cool/super-cool roofs. Cross (×) symbol denotes the mean.

Figure 5.8 a–b shows the boxplots of hourly indoor air temperature distributions for the as-built construction and those with cool and super-cool roofs for the three seasons. For the as-built construction, the average indoor air temperatures were 34 ℃, 29 ℃, and 17 ℃, and the maximum temperatures were 41 ℃, 36 ℃, and 26 ℃ in the summer, moderate, and winter seasons, respectively. Compared to the as-built condition, in which the roof was responsible for most of the heat gain into the room, the cases with cool and super-cool roofs had significantly lower roof heat gains or even heat losses through the roof (see Figure AII2). This led to a 1.4–3.3 ℃ reduction in the room's average temperature and a 1.7–5.0 ℃ reduction in its maximum temperature, depending on the season and the roof's α and ε values.

Since the indoor temperatures decreased, the cool roof improved thermal comfort in summer and moderate months while deteriorating it in winter. With a cool roof, unacceptably hot hours were reduced by 13–29 percentage points, while unacceptably cold hours increased by 7–10 percentage points compared to the baseline construction, thus improving the overall thermal

comfort in the room by 6–19 percentage points, as shown in Figure 5.9. The comfortable/uncomfortable hours were equally distributed between day and night for the baseline construction and those with cool roofs, meaning that cool roofs will improve comfort conditions for most occupancy conditions (daytime, nighttime, or round-the-clock). It was also found that reducing α from 0.3 to 0.05 significantly enhanced the room's acceptable thermal comfort hours, i.e., by ~5 percentage points for every 0.1 reduction in α.

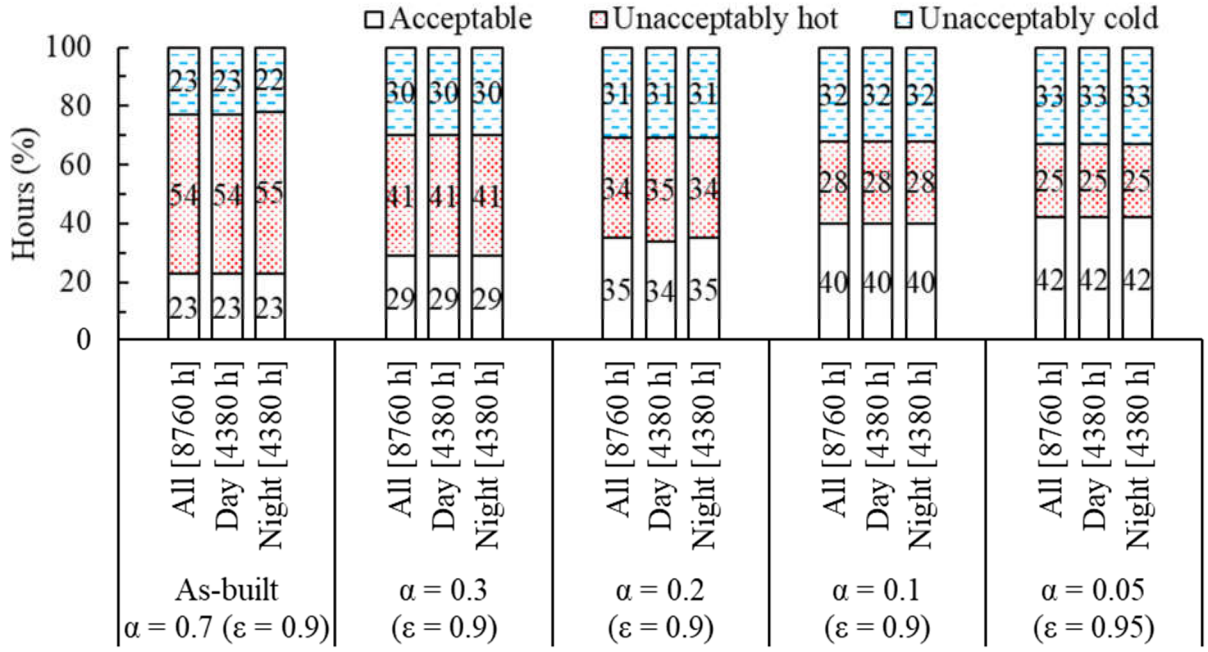

Figure 5.9: Year-round, daytime, and nighttime thermal comfort hours for the as-built construction and those with cool/super-cool roofs.

5.6.2 Roof Insulation

To evaluate the impact of roof insulation on the thermal conditions of the room, The room was simulated with varying thicknesses (30, 100, and 170 mm) of EPS insulation applied on the roof's exterior. The insulation thickness was chosen based on building energy-efficiency standards in use in India. With 30 mm thick EPS insulation, the room will comply with the IGBC's (Indian Green Building Council) energy standards [117]. In comparison, 170 mm thick EPS insulation will make the room super ECBC (Energy Conservation Building Code)

compliant [118]. The 100 mm insulation case was taken as an intermediate value between the two energy-efficiency standards.

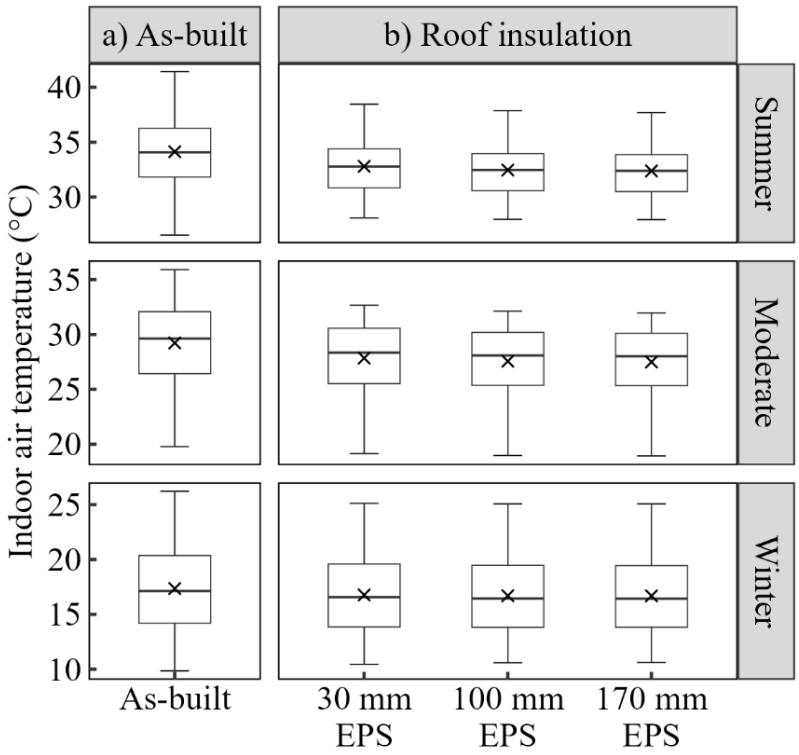

Figure 5.10: Boxplots of the hourly variations of the indoor air temperatures for different seasons for the as-built construction and those with different roof insulation levels. Cross (×) symbol denotes the mean.

Using roof insulation reduced the average indoor air temperatures by 0.6–1.7 ℃ depending on the season and insulation thicknesses (see Figure 5.10) due to significant reductions in the roof heat gain, as shown in Figure AII3. Due to reduced roof heat gains, the unacceptably hot hours reduced while the unacceptably cold hours increased, as shown in Figure 5.11. This led to an overall improvement in the room's comfort conditions both during the day and at night, with thermally comfortable hours increasing by 2–7 percentage points annually, depending on the thickness of the insulation.

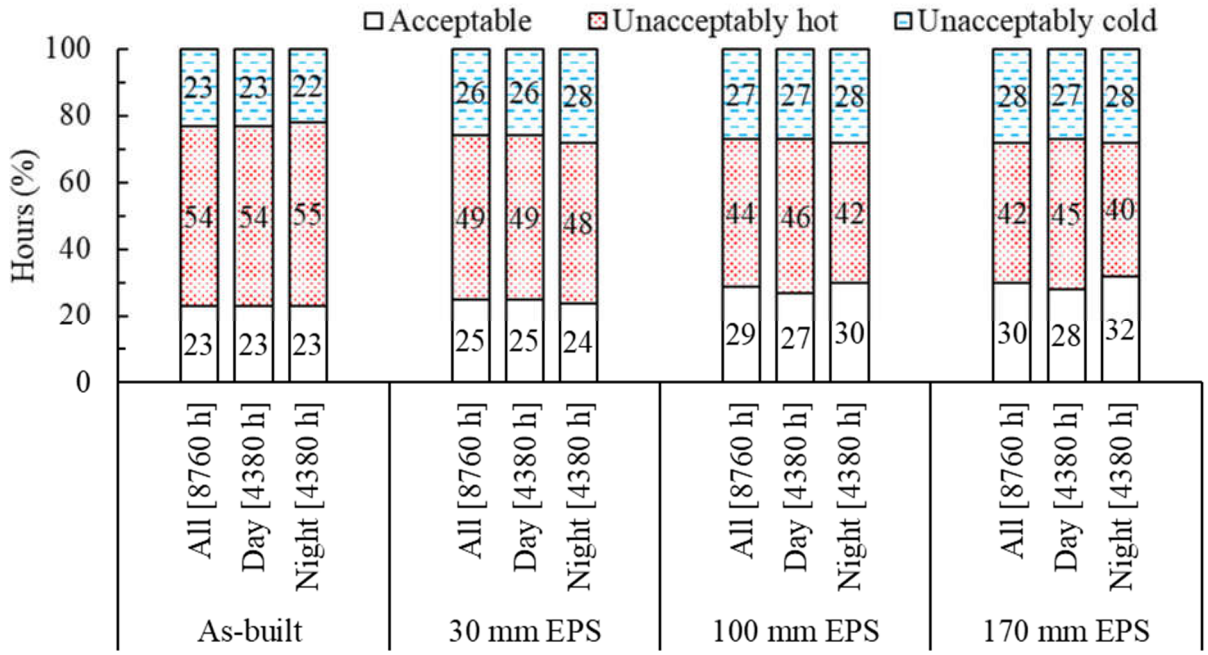

Figure 5.11: Year-round, daytime, and nighttime thermal comfort hours for the as-built construction and those with different roof insulation levels.

5.6.3 Envelope Insulation

In this method, the room's exterior walls and the roof were insulated with EPS insulation (30–170 mm thick). Figure 5.12 shows that the average indoor air temperatures decreased by 0.8–2.6 ℃ by insulating the envelope, depending on the insulation thickness and season. Similar to the previous case, the indoor temperatures decreased primarily due to reductions in the roof's heat gain (see Figure AII4). This led to a slight improvement in the room's comfort conditions, and the annual comfort hours increased by 0–8 percentage points, as shown in Figure 5.13. As before, the comfort/discomfort hours were evenly distributed between day and night. (see Figure 5.13). Once again, the comfort/discomfort hours were evenly distributed between day and night.

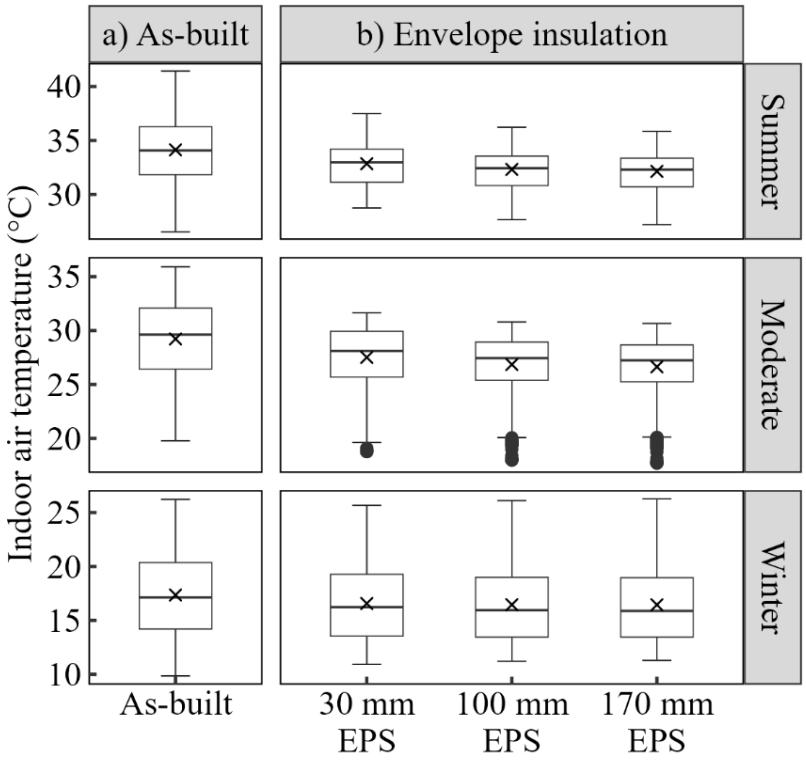

Figure 5.12: Boxplots of the hourly variations of the indoor air temperatures for different seasons for the as-built construction and those with different envelope insulation levels. Cross (×) symbol denotes the mean.

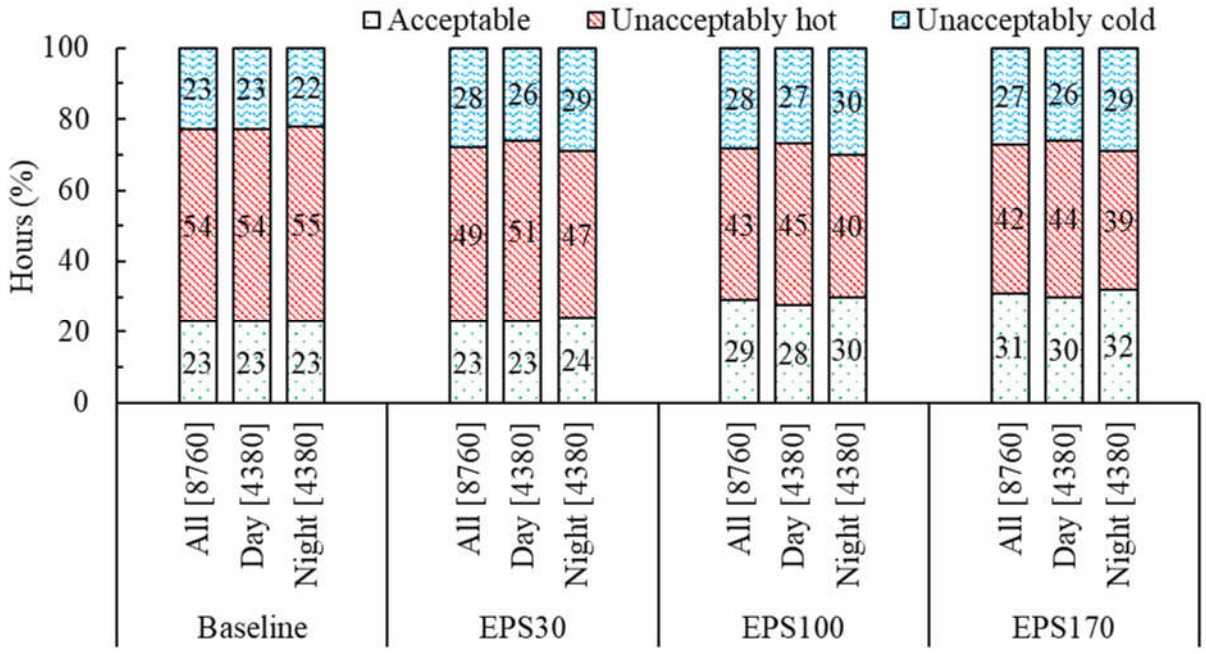

Figure 5.13: Year-round, daytime, and nighttime thermal comfort hours for the as-built construction and those with different envelope insulation levels.

5.6.4 Wall Insulation

In this method, different levels of insulation (30–170 mm thick) were implemented on the room's exterior walls only. It was found that insulating the exterior walls increased the average indoor air temperatures by up to 0.0–0.9 °C, depending on the insulation thickness and season, as shown in Figure 5.14. This temperature increase was because the external walls were primarily responsible for heat loss in the room's as-built state, and insulating them meant that the heat could not escape the room (see Figure AII5). Thus, wall insulation deteriorated comfort in summer and moderate months but slightly improved it in winter months, with an overall effect being a decrease in comfort hours by 4–5 percentage points (see Figure 5.15). Once again, the comfort/discomfort hours were evenly distributed between day and night.

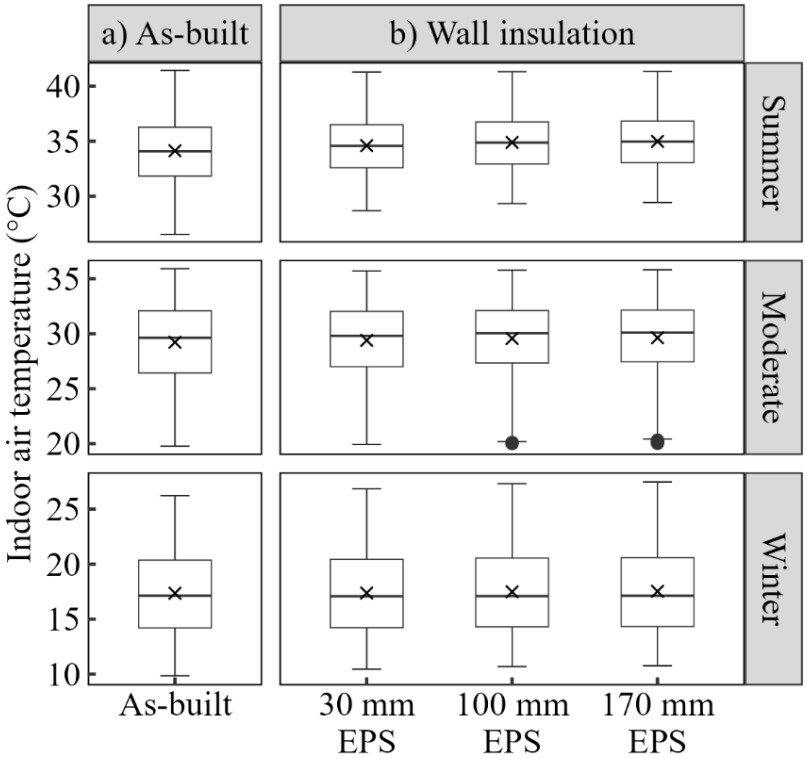

Figure 5.14: Boxplots of the hourly variations of the indoor air temperatures for different seasons for the as-built construction and those with different wall insulation levels. Cross (×) symbol denotes the mean.

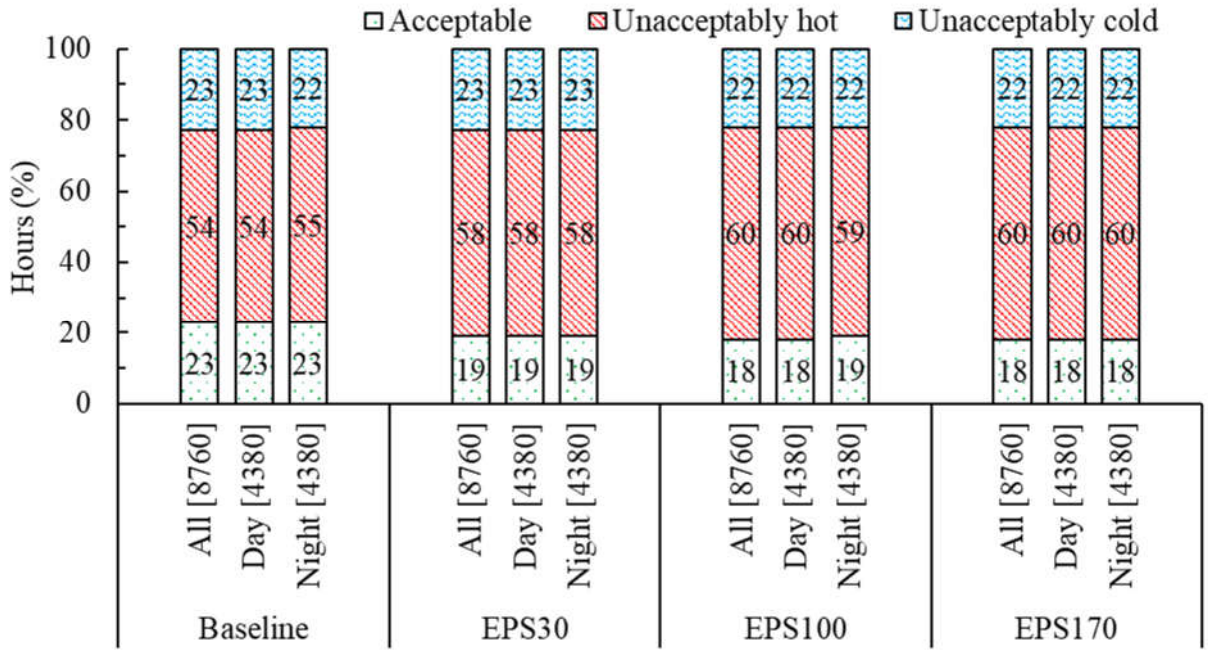

Figure 5.15: Year-round, daytime, and nighttime thermal comfort hours for the as-built construction and with different wall insulation levels.

5.6.5 Intercomparison between different Envelope Retrofits

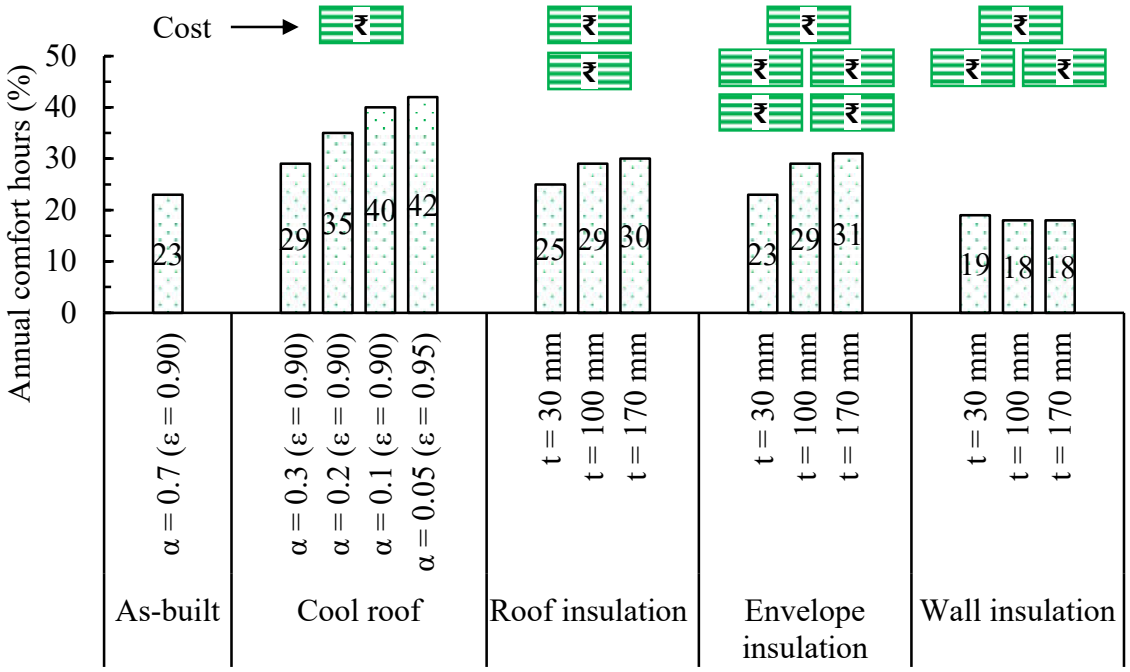

Figure 5.16: Annual comfort hours for the as-built construction and those with different envelope retrofits.

Figure 5.16 summarises the room's comfort conditions under the as-built state and with the different envelope retrofit options and also provides a qualitative estimate of the retrofit costs. Clearly, the cool and super-cool roof strategies performed best, while wall insulation performed

the worst and even deteriorated the indoor comfort conditions. Nevertheless, the material and labor cost of required to implement cool and super-cool roof retrofits is significantly lower than the other retrofit options (shown qualitatively in Figure 5.16). For example, cool roof paints cost about Rs. 100–300 per m2 ($1–4 per m2) of application area, 30 mm thick EPS insulation costs about Rs. 300–500 per m2 ($4–6 per m2), and 170 mm thick EPS insulation costs about Rs. 1500–2000 per m2 ($18–24 per m2) in the Indian market. Thus, considering the low material cost and labor required to implement cool and super-cool roof retrofits and their positive impact on the room's comfort conditions, we recommend it for such dwellings (detached non-air-conditioned single-story houses) and climatic conditions over the other studied solutions. Note that the results are also helpful for residences with similar constructions located in the BSh climate or India's composite climate zone, which includes major Indian cities such as Allahabad, Amritsar, Lucknow, etc., and a total population of about 0.4 billion people.

Chapter 6:

Conclusion

This study was motivated primarily by assessing the impact of climate change on H/C energy consumption and exploring different envelope retrofit options for improving thermal comfort conditions. In the former, historical, and future trends in temperature, CDDs, and HHDs were investigated (Section 6.1) using both parametrical and non-parametrical methods for major cities of India. In the latter, envelope retrofit solutions for detached single-story houses were investigated (Section 6.2) to enhance thermal comfort in Indian hot semi-arid climatic conditions.

6.1 Temperature, CDDs, and HDDs Trends

This investigation, first to quantify the impact of global warming on the historical (1969–2017) and future (2018–2100) annual temperatures, HDDs, and CDDs in India's eight major cities, covering all the climate zones (presented in Chapter 3). This study estimated the linear trends in the temperature, HDD, and CDD time-series by using two different techniques: i) applying ordinary least square regression on the time-series (OLS analysis) and ii) prewhitening the time-series followed by applying the Mann-Kendall Test and computing the Theil-Sen slope (PWMKTS analysis).

Both techniques showed that all cities witnessed a significant increase in temperature during 1969–2017. Depending on the city, the temperature trends were between 0.13–0.23 °C/decade or 0.08–0.13 °C/decade, obtained from the OLS or PWMKTS analysis, respectively. Due to rising temperatures, the historical CDD trends were statistically significant and positive in all seven cities with cooling requirements (Ahmedabad was a slight exception). The historical CDD trends ranged between 1.3–3.8%/decade obtained from the OLS analysis, whereas the PWMKTS analysis estimated CDD trends between 0.7–2.3%/decade. In the two cities with

heating requirements, the historical HDD trends were either insignificant (in Delhi) or decreasing (by 1.9% or 3.1% per decade in Srinagar, depending on the analysis). This study also detected statistically significant trends in most cities' future temperatures, with magnitudes ranging between 0.10–0.78 °C/decade (OLS) or 0.03–0.07 °C/decade (PWMKTS), depending upon the city and the emission scenario. Future CDDs also had an increasing trend in cities with cooling requirements, with magnitudes equal to 1.1–9.4%/decade (OLS) or 0.1–0.6%/decade (PWMKTS). In contrast, cities with heating requirements generally displayed a decreasing trend in future HDDs with magnitudes of 1.3–7.9%/decade (OLS) or 0.9–1.7% (PWMKTS).

It was also estimated that annual temperatures would be 0.1–1.1 ℃ higher in the 2020s, 0.6–2.8 ℃ higher in the 2050s, and 1.0–4.6 ℃ higher in the 2080s in the studied cities. Due to increasing temperatures, CDDs will also increase by 2.9–22.9% in the 2020s, by 8.3–54.1% in the 2050s, and by 11.89–83.0% in the 2080s, depending on the city and the emission scenario. Thus, increasing the space cooling energy requirements in buildings by a similar amount. In contrast, HDDs will decrease by 8.1–30.3% in the 2020s, by 17.6–83.3% in the 2050s, and by 19.3–97.1% in the 2080s, thereby reducing the space heating requirements.

6.2 Envelope Retrofits Solutions for a single-story house

This investigation compared different envelope retrofit options for improving the thermal comfort conditions in a detached single-story house in India's hot-semi arid climate zone (presented in Chapter 5). A year-long measurement of the weather and indoor conditions in the bedroom of the house was conducted to assess its thermal comfort conditions and heat transfer characteristics in the as-built state (presented in Chapter 4). Those measurements were also used to develop and calibrate a thermal model of the room, which helped to evaluate the impact

of different retrofit solutions (e.g., the application of cool roof paints and the insulation of walls and roof) on the room's thermal comfort conditions.

In this study, results showed that in the room's as-built state, the indoor environment was comfortable for 23%, hot for 54%, and cold for 23% of the year, with the roof being the major contributor to the heat gains and the floor and external walls largely contributing to heat losses. The applications of cool/super-cool paints on the roof significantly reduced its heat gains, led to a 1.4–3.3 °C reduction in the room's average temperature, and increased the comfort duration to between 29–42% of the year (an increase of 6–19 percentage points over the as-built state). Insulating the roof or the envelope (roof and walls) also led to slight improvements in the room's comfort conditions (comfort hours increased by 0–8 percentage points), primarily due to reduced roof heat gains. However, insulating the walls alone showed a deterioration in the room's comfort conditions (comfort hours decreased by 4–5 percentage points) since it became difficult for the heat to escape the room.

Overall, the study found that applying cool/super-cool roof paints is the most suitable envelope retrofit solution for detached single-storeyed houses in hot semi-arid climates since they lead to the most thermal comfort improvement and are low-cost and easy to implement.

6.3 Major Contributions of Thesis

The major outcomes of the current thesis are as follows:

- The study assessed the performance of various GCMs in eight selected cities and validated their accuracy for each location.
- This study analyzed historical (1969–2017) and future (2018–2100) trends in annual mean temperatures, as well as heating and cooling degree days
- The study conducted year-long measurements of the indoor and outdoor environmental conditions of a detached single-story house located in India's hot semi-arid climate zone.

- The study evaluated different envelope retrofit options for improving the thermal comfort conditions in such residences and identified a suitable solution by using a well-calibrated energy model.
- The results also provided valuable physical insights into the heat transfer characteristics of such buildings in the as-built state and with different envelope retrofits.

6.4 Limitation and Future Scope

This investigation is the first to quantify the historical trends in annual temperatures, HDDs, and CDDs in major Indian cities, together with their future projections under two different greenhouse gas emission scenarios. The study found that rising temperatures have and would significantly increase the space cooling requirements in major Indian cities, which becomes especially problematic since India is one of the world's most populous and hottest regions. A warming climate coupled with rising household incomes and built-up areas could lead to a staggering increase in air-conditioning demand in India, which has about four times the population and more than three times as many CDDs per person as the United States [10]. Thus, the study highlights the urgent need to adopt energy-efficient building practices in India and global action on climate change.

However, other factors, such as the buildings' thermal characteristics, relative humidity, and solar radiation, substantially impact the H/C energy requirements, which should be included in future investigations. Further uncertainties in results can arise due to missing values present in the historical weather data and the imputation algorithm employed for filling them, as well as the inherent limitations of the GCMs in making reliable temperature predictions. This research also did not characterize the inter-model variabilities in future climate predictions since a single GCM, selected based on its historical performance, was used for each city. Further research can provide multi-model projections of the future HDDs and CDDs in India to characterizing the inter-model variabilities. It is also recommended to explore the effects of increasing

population and incomes in India on the building energy demand and the associated CO_2 emissions.

Finally, the study focused on finding retrofit solutions for improving the thermal comfort in detached single-story houses, where occupants routinely experience thermal discomfort for a large portion of the year due to extreme climatic conditions and their inability to afford air-conditioners or room heaters. Thus, the study did not evaluate the effectiveness of different retrofit options from the point of energy savings. Future studies could focus on assessing residential retrofit options with the twin objectives of enhancing thermal comfort and reducing H/C energy consumption. In addition to that using the present thermal model future studies could conduct an assessment of climate change on H/C energy consumption in Indian residences to incorporate the future H/C energy saving and enhancing thermal comfort under different emission scenarios. This investigation only evaluated two retrofit options (cool/super-cool roof paints and envelope insulation) due to their low cost and expected high performance. Other retrofit options, passive H/C strategies, and their suitable combinations should be considered in future research. It would also be worthwhile to conduct a life-cycle cost and carbon analysis for different retrofit options to assess their financial typologies and climate conditions.

Another study limitation was that the windows were permanently closed during the experiments and in the simulation; thus, we did not consider the impact of occupants' willingness to open or close the windows on the performance of the retrofit options. However, in summer, the occupants' willingness to open the windows at night could be an effective passive cooling strategy for the studied location, where nights are significantly cooler than the days. Thus, the study reports the worst-case scenario of thermal comfort in summer, and future studies should address this issue.

[1] IEA (International Energy Agency), Global status report for buildings and construction: towards a zero-emissions, efficient and resilient buildings and construction sector, Paris, 2019.

[2] IEA (International Energy Agency), Data and statistics for India, (2018).

[3] S. Kumar, S. Kachhawa, A. Goenka, S. Kasamsetty, G. George, Demand analysis for cooling by sector in India in 2027, Alliance for an Energy Efficient Economy, New Delhi, 2018.

[4] A. Chunekar, S. Varshney, D. Shantanu, Residential electricity consumption in India: What do we know?, 2016.

[5] International Energy Agency, Energy Statistics Data Browser, (2022). https://www.iea.org/data-and-statistics/data-tools/energy-statistics-data-browser?country=INDIA&fuel=CO2 (accessed August 1, 2023).

[6] IPCC (Intergovernmental Panel on Climate Change), Climate change 2013: the physical science basis: working group I contribution to the fifth assessment report of the Intergovernmental Panel on Climate Change, Cambridge University Press, 2014.

[7] M. Santamouris, Cooling the buildings – past, present and future, Energy Build 128 (2016) 617–638. https://doi.org/10.1016/j.enbuild.2016.07.034.

[8] Ministry for Environment, Forest and Climate Change, (MoFF), India cooling action plan, Ministry of Enironment and Forests, Government of India, New Delhi, 2018.

[9] R. Ukey, A.C. Rai, Impact of global warming on heating and cooling degree days in major Indian cities, Energy Build 244 (2021) 111050. https://doi.org/10.1016/j.enbuild.2021.111050.

[10] M. Sivak, Will AC put a chill on the global energy supply?, Am Sci 101 (2013) 330–333. https://doi.org/10.1511/2013.104.330.

[11] Global Buildings Performance Network (GBPN), Achieving scale in energy-efficient building in India, 2013.

[12] V. Sharma, A.C. Rai, Performance assessment of residential building envelopes enhanced with phase change materials, Energy Build 208 (2020) 109664. https://doi.org/10.1016/j.enbuild.2019.109664.

[13] A. Mastrucci, N.D. Rao, Bridging India's housing gap: lowering costs and CO_2 emissions, Building Research and Information 47 (2019) 8–23. https://doi.org/10.1080/09613218.2018.1483634.

[14] M. Abdul Mujeebu, F. Bano, Integration of passive energy conservation measures in a detached residential building design in warm humid climate, Energy 255 (2022) 124587. https://doi.org/10.1016/j.energy.2022.124587.

[15] V. Gupta, C. Deb, Envelope design for low-energy buildings in the tropics : A review, Renewable and Sustainable Energy Reviews 186 (2023) 113650. https://doi.org/10.1016/j.rser.2023.113650.

[16] P. Shen, Impacts of climate change on U.S. building energy use by using downscaled hourly future weather data, Energy Build 134 (2017) 61–70. https://doi.org/10.1016/j.enbuild.2016.09.028.

[17] H. Wang, Q. Chen, Impact of climate change heating and cooling energy use in buildings in the United States, Energy Build 82 (2014) 428–436. https://doi.org/10.1016/j.enbuild.2014.07.034.

[18] X. Wang, D. Chen, Z. Ren, Assessment of climate change impact on residential building heating and cooling energy requirement in Australia, Build Environ 45 (2010) 1663–1682. https://doi.org/10.1016/j.buildenv.2010.01.022.

[19] M. Sivak, Potential energy demand for cooling in the 50 largest metropolitan areas of the world: implications for developing countries, Energy Policy 37 (2009) 1382–1384. https://doi.org/10.1016/j.enpol.2008.11.031.

[20] CIBSE (Chartered Institutiion of Building Services Engineers), Degree-days: theory and application (TM41: 2006), London, 2006.

[21] M. Christenson, H. Manz, D. Gyalistras, Climate warming impact on degree-days and building energy demand in Switzerland, Energy Convers Manag 47 (2006) 671–686. https://doi.org/10.1016/j.enconman.2005.06.009.

[22] F. Jiang, X. Li, B. Wei, R. Hu, Z. Li, Observed trends of heating and cooling degree-days in Xinjiang province, China, Theor Appl Climatol 97 (2009) 349–360. https://doi.org/10.1007/s00704-008-0078-5.

[23] M.J. OrtizBeviá, G. Sánchez-López, F.J. Alvarez-Garcìa, A. RuizdeElvira, Evolution of heating and cooling degree-days in Spain: trends and interannual variability, Glob Planet Change 92–93 (2012) 236–247. https://doi.org/10.1016/j.gloplacha.2012.05.023.

[24] A.R.M.T. Islam, I. Ahmed, M.S. Rahman, Trends in cooling and heating degree-days overtimes in Bangladesh? An investigation of the possible causes of changes, Natural Hazards 101 (2020) 879–909. https://doi.org/10.1007/s11069-020-03900-5.

[25] M. De Rosa, V. Bianco, F. Scarpa, L.A. Tagliafico, Historical trends and current state of heating and cooling degree days in Italy, Energy Convers Manag 90 (2015) 323–335. https://doi.org/10.1016/j.enconman.2014.11.022.

[26] I. Livada, A. Synnefa, S. Haddad, R. Paolini, S. Garshasbi, G. Ulpiani, F. Fiorito, K. Vassilakopoulou, P. Osmond, M. Santamouris, Time series analysis of ambient air-temperature during the period 1970–2016 over Sydney, Australia, Science of the Total Environment 648 (2019) 1627–1638. https://doi.org/10.1016/j.scitotenv.2018.08.144.

[27] J. Spinoni, J. V Vogt, P. Barbosa, A. Dosio, N. McCormick, A. Bigano, H.M. Füssel, Changes of heating and cooling degree-days in Europe from 1981 to 2100, International Journal of Climatology 38 (2018) e191–e208. https://doi.org/10.1002/joc.5362.

[28] Y. Petri, K. Caldeira, Impacts of global warming on residential heating and cooling degree-days in the United States, Nature Publishing Group (2010) 1–14. https://doi.org/10.1038/srep12427.

[29] D. Ramon, K. Allacker, F. De Troyer, H. Wouters, N.P.M. van Lipzig, Future heating and cooling degree days for Belgium under a high-end climate change scenario, Energy Build 216 (2020) 109935. https://doi.org/10.1016/j.enbuild.2020.109935.

[30] M. Isaac, D.P. Van Vuuren, Modeling global residential sector energy demand for heating and air conditioning in the context of climate change, 37 (2009) 507–521. https://doi.org/10.1016/j.enpol.2008.09.051.

[31] R. Warren, N. Arnell, R. Nicholls, L. Peter, J. Price, Understanding the regional impacts of climate change, Tyndall Centre for Climate Change Research Working Paper 90, 2006.

[32] D. Tian, J. Zhang, Z. Gao, The advancement of research in cool roof: super cool roof, temperature-adaptive roof and crucial issues of application in cities, Energy Build 291 (2023) 113131. https://doi.org/10.1016/j.enbuild.2023.113131.

[33] S. Mousavi, M. Gijón-Rivera, C.I. Rivera-Solorio, C. Godoy Rangel, Energy, comfort, and environmental assessment of passive techniques integrated into low-energy residential buildings in semi-arid climate, Energy Build 263 (2022) 112053. https://doi.org/10.1016/j.enbuild.2022.112053.

[34] H. Akbari, R. Levinson, Evolution of cool-roof standards in the US, Advances in Building Energy Research: Volume 3 (2012) 1–32. https://doi.org/10.3763/aber.2008.0201.

[35] T. Sinsel, H. Simon, A.M. Broadbent, M. Bruse, J. Heusinger, Modeling the outdoor cooling impact of highly radiative “super cool” materials applied on roofs, Urban Clim 38 (2021) 100898. https://doi.org/10.1016/j.uclim.2021.100898.

[36] W. Athmani, L. Sriti, M. Dabaieh, Z. Younsi, The potential of using passive cooling roof techniques to improve thermal performance and energy efficiency of residential buildings in hot arid regions, Buildings 13 (2023). https://doi.org/10.3390/buildings13010021.

[37] M. Kolokotroni, E. Shittu, T. Santos, L. Ramowski, A. Mollard, K. Rowe, E. Wilson, J.P. de B. Filho, D. Novieto, Cool roofs: High tech low cost solution for energy efficiency and thermal comfort in low rise low income houses in high solar radiation countries, Energy Build 176 (2018) 58–70. https://doi.org/10.1016/j.enbuild.2018.07.005.

[38] A.L. Pisello, V.L. Castaldo, C. Piselli, C. Fabiani, F. Cotana, Thermal performance of coupled cool roof and cool façade: experimental monitoring and analytical optimization procedure, Energy Build 157 (2017) 35–52. https://doi.org/10.1016/j.enbuild.2017.04.054.

[39] M. Zinzi, S. Agnoli, Cool and green roofs. An energy and comfort comparison between passive cooling and mitigation urban heat island techniques for residential buildings in the Mediterranean region, Energy Build 55 (2012) 66–76. https://doi.org/10.1016/j.enbuild.2011.09.024.

[40] A. Ismail, M.H.A. Samad, A.M.A. Rahman, The investigation of green roof and white roof cooling potential on single storey residential building in the Malaysian climate, World Acad Sci Eng Technol 76 (2011) 129–137.

[41] J. Feng, M. Saliari, K. Gao, M. Santamouris, On the cooling energy conservation potential of super cool roofs, Energy Build 264 (2022) 112076. https://doi.org/10.1016/j.enbuild.2022.112076.

[42] V. Garg, S. Somal, R. Arumugam, A. Bhatia, Development for cool roof calculator for India, Energy Build 114 (2016) 136–142. https://doi.org/10.1016/j.enbuild.2015.06.022.

[43] S. Mousavi, M. Gijón-Rivera, C.I. Rivera-Solorio, C. Godoy Rangel, Energy, comfort, and environmental assessment of passive techniques integrated into low-energy residential buildings in semi-arid climate, Energy Build 263 (2022) 112053. https://doi.org/10.1016/j.enbuild.2022.112053.

[44] W. Athmani, L. Sriti, M. Dabaieh, Z. Younsi, The Potential of Using Passive Cooling Roof Techniques to Improve Thermal Performance and Energy Efficiency of

Residential Buildings in Hot Arid Regions, Buildings 13 (2023). https://doi.org/10.3390/buildings13010021.

[45] F. Xu, H. Wang, D. Tian, Z. Gao, J. Zhang, Factors affecting the daytime cooling effect of cool materials: A case study combining experiment and simulation, Build Environ 250 (2024) 111213. https://doi.org/10.1016/j.buildenv.2024.111213.

[46] M. Kolokotroni, E. Shittu, T. Santos, L. Ramowski, A. Mollard, K. Rowe, E. Wilson, J.P. de B. Filho, D. Novieto, Cool roofs: High tech low cost solution for energy efficiency and thermal comfort in low rise low income houses in high solar radiation countries, Energy Build 176 (2018) 58–70. https://doi.org/10.1016/j.enbuild.2018.07.005.

[47] A. Nutkiewicz, A. Mastrucci, N.D. Rao, R.K. Jain, Cool roofs can mitigate cooling energy demand for informal settlement dwellers, Renewable and Sustainable Energy Reviews 159 (2022) 112183. https://doi.org/10.1016/j.rser.2022.112183.

[48] E. Bozonnet, M. Doya, F. Allard, Cool roofs impact on building thermal response: A French case study, Energy Build 43 (2011) 3006–3012. https://doi.org/10.1016/j.enbuild.2011.07.017.

[49] A. Synnefa, M. Santamouris, H. Akbari, Estimating the effect of using cool coatings on energy loads and thermal comfort in residential buildings in various climatic conditions, Energy Build 39 (2007) 1167–1174. https://doi.org/10.1016/j.enbuild.2007.01.004.

[50] M. Dabaieh, O. Wanas, M.A. Hegazy, E. Johansson, Reducing cooling demands in a hot dry climate: A simulation study for non-insulated passive cool roof thermal performance in residential buildings, Energy Build 89 (2015) 142–152. https://doi.org/10.1016/j.enbuild.2014.12.034.

[51] R. Levinson, H. Akbari, J.C. Reilly, Cooler tile-roofed buildings with near-infrared-reflective non-white coatings, Build Environ 42 (2007) 2591–2605. https://doi.org/10.1016/j.buildenv.2006.06.005.

[52] A.L. Pisello, F. Cotana, The thermal effect of an innovative cool roof on residential buildings in Italy: Results from two years of continuous monitoring, Energy Build 69 (2014) 154–164. https://doi.org/10.1016/j.enbuild.2013.10.031.

[53] K. Bamdad, Cool roofs: A climate change mitigation and adaptation strategy for residential buildings, Build Environ 236 (2023) 110271. https://doi.org/10.1016/j.buildenv.2023.110271.

[54] S. Garshasbi, J. Feng, R. Paolini, J. Jonathan Duverge, C. Bartesaghi-Koc, S. Arasteh, A. Khan, M. Santamouris, On the energy impact of cool roofs in Australia, Energy Build 278 (2023) 112577. https://doi.org/10.1016/j.enbuild.2022.112577.

[55] A.M. Papadopoulos, Forty years of regulations on the thermal performance of the building envelope in Europe: Achievements, perspectives and challenges, Energy Build 127 (2016) 942–952. https://doi.org/10.1016/j.enbuild.2016.06.051.

[56] S.S. Chandel, A. Sharma, B.M. Marwaha, Review of energy efficiency initiatives and regulations for residential buildings in India, Renewable and Sustainable Energy Reviews 54 (2016) 1443–1458. https://doi.org/10.1016/j.rser.2015.10.060.

[57] A. Sarkar, S. Bose, Exploring impact of opaque building envelope components on thermal and energy performance of houses in lower western Himalayans for optimal selection, Journal of Building Engineering 7 (2016) 170–182. https://doi.org/10.1016/j.jobe.2016.06.009.

[58] A. Hashemi, Effects of thermal insulation on thermal comfort in low-income tropical housing, Energy Procedia 134 (2017) 815–824. https://doi.org/10.1016/j.egypro.2017.09.535.

[59] L.F. Cabeza, A. Castell, M. Medrano, I. Martorell, G. Pérez, I. Fernández, Experimental study on the performance of insulation materials in Mediterranean construction, Energy Build 42 (2010) 630–636. https://doi.org/10.1016/j.enbuild.2009.10.033.

[60] D. D'Agostino, D. Parker, P. Melià, G. Dotelli, Optimizing photovoltaic electric generation and roof insulation in existing residential buildings, Energy Build 255 (2022) 111652. https://doi.org/10.1016/j.enbuild.2021.111652.

[61] International Energy Agency, Energy Statistics Data Browser, (2022). https://www.iea.org/data-and-statistics/data-tools/energy-statistics-data-browser?country=INDIA&fuel=CO2 (accessed August 1, 2023).

[62] W.A. Friess, K. Rakhshan, T.A. Hendawi, S. Tajerzadeh, Wall insulation measures for residential villas in Dubai: A case study in energy efficiency, Energy Build 44 (2012) 26–32. https://doi.org/10.1016/j.enbuild.2011.10.005.

[63] S. Attia, C. Benzidane, R. Rahif, D. Amaripadath, M. Hamdy, P. Holzer, A. Koch, A. Maas, S. Moosberger, S. Petersen, A. Mavrogianni, J. Maria Hidalgo-Betanzos, M. Almeida, J. Akander, H. Khosravi Bakhtiari, O. Kinnane, R. Kosonen, S. Carlucci, Overheating calculation methods, criteria, and indicators in European regulation for residential buildings, Energy Build 292 (2023) 113170. https://doi.org/10.1016/j.enbuild.2023.113170.

[64] J. Taylor, R. McLeod, G. Petrou, C. Hopfe, A. Mavrogianni, R. Castaño-Rosa, S. Pelsmakers, K. Lomas, Ten questions concerning residential overheating in Central and

Northern Europe, Build Environ 234 (2023). https://doi.org/10.1016/j.buildenv.2023.110154.

[65] J. Taylor, M. Davies, A. Mavrogianni, Z. Chalabi, P. Biddulph, E. Oikonomou, P. Das, B. Jones, The relative importance of input weather data for indoor overheating risk assessment in dwellings, Build Environ 76 (2014) 81–91. https://doi.org/10.1016/j.buildenv.2014.03.010.

[66] V. Tink, S. Porritt, D. Allinson, D. Loveday, Measuring and mitigating overheating risk in solid wall dwellings retrofitted with internal wall insulation, Build Environ 141 (2018) 247–261. https://doi.org/10.1016/j.buildenv.2018.05.062.

[67] D. Fosas, D.A. Coley, S. Natarajan, M. Herrera, M. Fosas de Pando, A. Ramallo-Gonzalez, Mitigation versus adaptation: does insulating dwellings increase overheating risk?, Build Environ 143 (2018) 740–759. https://doi.org/10.1016/j.buildenv.2018.07.033.

[68] L. Aditya, T.M.I. Mahlia, B. Rismanchi, H.M. Ng, M.H. Hasan, H.S.C. Metselaar, O. Muraza, H.B. Aditiya, A review on insulation materials for energy conservation in buildings, Renewable and Sustainable Energy Reviews 73 (2017) 1352–1365. https://doi.org/10.1016/j.rser.2017.02.034.

[69] O. Kaynakli, A review of the economical and optimum thermal insulation thickness for building applications, Renewable and Sustainable Energy Reviews 16 (2012) 415–425. https://doi.org/10.1016/j.rser.2011.08.006.

[70] P. Arumugam, V. Ramalingam, P. Vellaichamy, Effective PCM, insulation, natural and/or night ventilation techniques to enhance the thermal performance of buildings

located in various climates – A review, Energy and Buildings 258 (2022) 111840. https://doi.org/10.1016/j.enbuild.2022.111840.

[71] V. Chaturvedi, J. Eom, L.E. Clarke, P.R. Shukla, Long term building energy demand for India: Disaggregating end use energy services in an integrated assessment modeling framework, Energy Policy 64 (2014) 226–242. https://doi.org/10.1016/j.enpol.2012.11.021.

[72] M.S. Al-Homoud, Performance characteristics and practical applications of common building thermal insulation materials, Building and Environment 40 (2005) 353–366. https://doi.org/10.1016/j.buildenv.2004.05.013.

[73] E. Rodrigues, M.S. Fernandes, N. Soares, Á. Gomes, A.R. Gaspar, J.J. Costa, The potential impact of low thermal transmittance construction on the European design guidelines of residential buildings, Energy and Buildings 178 (2018) 379–390. https://doi.org/10.1016/j.enbuild.2018.08.009.

[74] Arul Babu, A. De Chinnu, R.S. Srivastava, A.C. Rai, Impact of climate change on the heating and cooling load components of an archetypical residential room in major Indian cities, Build Environ 250 (2024) 111181. https://doi.org/10.1016/j.buildenv.2024.111181.

[75] N. Kishore, Impact of climate change on future bioclimatic potential and residential building thermal and energy performance in India, Indoor and Built Environment 31 (2022) 329–354. https://doi.org/10.1177/1420326X21993919.

[76] N. Kishore, Impact of climate change on future bioclimatic potential and residential building thermal and energy performance in India, Indoor and Built Environment 31 (2022) 329–354. https://doi.org/10.1177/1420326X21993919.

[77] S. Thapa, Risk of overheating in low-rise naturally ventilated residential buildings of northeast India–an effect of climate change, Archit Sci Rev 65 (2022) 14–41. https://doi.org/10.1080/00038628.2021.1941748.

[78] BIS (Bureau of Indian Standards), National building code of India 2005, Bureau of Indian standards, New Delhi, 2005.

[79] ASHRAE (American Society of Heating Refrigerating and Air-conditioning Engineers), Handbook HVAC fundamentals, 2009.

[80] M. Bhatnagar, J. Mathur, V. Garg, Determining base temperature for heating and cooling degree-days for India, Journal of Building Engineering 18 (2018) 270–280. https://doi.org/10.1016/j.jobe.2018.03.020.

[81] L.S. Rathore, S.D. Attri, A.K. Jaswal, State level climate change trends in India, Ministry of Earth Sciences, Goverment of India, New Delhi, 2013.

[82] G. Tardivo, A. Berti, A dynamic method for gap filling in daily temperature datasets, J Appl Meteorol Climatol 51 (2012) 1079–1086. https://doi.org/10.1175/JAMC-D-11-0117.1.

[83] W.P. Kemp, D.G. Burnell, D.O. Everson, A.J. Thomson, Estimating missing daily maximum and minimum temperatures, Journal of Climate & Applied Meteorology 22 (1983) 1587–1593. https://doi.org/10.1175/1520-0450(1983)022<1587:EMDMAM>2.0.CO;2.

[84] C. Dunis, V. Karalis, Weather derivatives pricing and filling analysis for missing temperature data, Derivative Use Trading Regulation (2003) 1–19.

[85] A.M. Thomson, K. V Calvin, S.J. Smith, G.P. Kyle, A. Volke, P. Patel, S. Delgado-Arias, B. Bond-Lamberty, M.A. Wise, L.E. Clarke, J.A. Edmonds, RCP4.5: a pathway for stabilization of radiative forcing by 2100, Clim Change 109 (2011) 77–94. https://doi.org/10.1007/s10584-011-0151-4.

[86] K. Riahi, S. Rao, V. Krey, C. Cho, V. Chirkov, G. Fischer, G. Kindermann, N. Nakicenovic, P. Rafaj, RCP 8.5–a scenario of comparatively high greenhouse gas emissions, Clim Change 109 (2011) 33–57. https://doi.org/10.1007/s10584-011-0149-y.

[87] P.J. Gleckler, K.E. Taylor, C. Doutriaux, Performance metrics for climate models, J Geophys Res 113 (2008) 1–20. https://doi.org/10.1029/2007JD008972.

[88] M.S. Desai, A.G. Dhorde, Trends in thermal discomfort indices over western coastal cities of India, Theor Appl Climatol 131 (2018) 1305–1321. https://doi.org/10.1007/s00704-017-2042-8.

[89] S.G. Meshram, V.P. Singh, C. Meshram, Long-term trend and variability of precipitation in Chhattisgarh State, India, Theor Appl Climatol 129 (2017) 729–744. https://doi.org/10.1007/s00704-016-1804-z.

[90] P. Singh, V. Kumar, T. Thomas, M. Arora, Basin-wide assessment of temperature trends in northwest and central India, Hydrological Sciences Journal 53 (2008) 421–433. https://doi.org/10.1623/hysj.53.2.421.

[91] P. Sonali, D. Nagesh Kumar, Review of trend detection methods and their application to detect temperature changes in India, J Hydrol (Amst) 476 (2013) 212–227. https://doi.org/10.1016/j.jhydrol.2012.10.034.

[92] H. Tabari, P.H. Talaee, Recent trends of mean maximum and minimum air temperatures in the western half of Iran, Meteorology and Atmospheric Physics 111 (2011) 121–131. https://doi.org/10.1007/s00703-011-0125-0.

[93] I. Livada, A. Synnefa, S. Haddad, R. Paolini, S. Garshasbi, G. Ulpiani, F. Fiorito, K. Vassilakopoulou, P. Osmond, M. Santamouris, Time series analysis of ambient air-temperature during the period 1970–2016 over Sydney, Australia, Science of the Total Environment 648 (2019) 1627–1638. https://doi.org/10.1016/j.scitotenv.2018.08.144.

[94] K.H. Hamed, Enhancing the effectiveness of prewhitening in trend analysis of hydrologic data, J Hydrol (Amst) 368 (2009) 143–155. https://doi.org/10.1016/j.jhydrol.2009.01.040.

[95] M. Gocic, S. Trajkovic, Analysis of changes in meteorological variables using Mann-Kendall and Sen's slope estimator statistical tests in Serbia, Glob Planet Change 100 (2013) 172–182. https://doi.org/10.1016/j.gloplacha.2012.10.014.

[96] J.D. Salas, J.W. Delleur, V.M. Yevjevich, W.L. Lane, Applied modeling of hydrologic time series, Water Resource Publications, Colorado, 1980.

[97] H.B. Mann, Nonparmetric tests against trend, Econometrica 13 (1945) 245–259.

[98] M.G. Kendall, Rank correlation methods, fourth edition, Charles Griffin, London., 1948.

[99] P.K. Sen, N. Carolina, C. Hill, Estimates of the regression coefficient based on Kendall's tau, J Am Stat Assoc 1459 (1968).

[100] H. Theil, A rank-invariant method of linear and polynomial regression analysis, Part I, Royal Netherlands Academy of Art and Scinces, 1950. https://doi.org/10.1007/978-94-011-2546-8_20.

[101] S. Yue, P. Pilon, B. Phinney, G. Cavadias, The influence of autocorrelation on the ability to detect trend in hydrological series, Hydrol Process 16 (2002) 1807–1829. https://doi.org/10.1002/hyp.1095.

[102] G. Basha, P. Kishore, M.V. Ratnam, A. Jayaraman, A.A. Kouchak, T.B.M.J. Ouarda, I. Velicogna, Historical and projected surface temperature over India during the 20th and 21st century, Sci Rep 7 (2017) 1–10. https://doi.org/10.1038/s41598-017-02130-3.

[103] M. De Rosa, V. Bianco, F. Scarpa, L.A. Tagliafico, Historical trends and current state of heating and cooling degree days in Italy, Energy Convers Manag 90 (2015) 323–335. https://doi.org/10.1016/j.enconman.2014.11.022.

[104] M.J. OrtizBeviá, G. Sánchez-López, F.J. Alvarez-Garcìa, A. RuizdeElvira, Evolution of heating and cooling degree-days in Spain: trends and interannual variability, Glob Planet Change 92–93 (2012) 236–247. https://doi.org/10.1016/j.gloplacha.2012.05.023.

[105] American Society of Heating Refrigerating and Air-Conditioning Engineers - ASHRAE, Thermal environmental conditions for human occupancy, ANSI/ASHRAE Standard - 55 7 (2020) 6.

[106] R. Rawal, Y. Shukla, V. Vardhan, S. Asrani, M. Schweiker, R. de Dear, V. Garg, J. Mathur, S. Prakash, S. Diddi, S.V. Ranjan, A.N. Siddiqui, G. Somani, Adaptive thermal comfort model based on field studies in five climate zones across India, Build Environ 219 (2022). https://doi.org/10.1016/j.buildenv.2022.109187.

[107] R. Rawal, S. Maithel, Y. Shukla, S. Rana, G. Gowri, J. Patel, S. Kumar, Thermal performance of walling material and wall technology, 2020.

[108] F.P. Incropera, D.P. Dewiti, T.L. Bergman, A. s Lavine, Fundamentals of heat and mass transfer, Vol. 6, Wiley, New York, 1996.

[109] G. Anderlind, Comparison of two methods for analyzing in situ thermal measurements. The marriage between zones physics and statistics, (2017). https://doi.org/10.13140/RG.2.2.10032.87041.

[110] B. Ridley, J. Boland, P. Lauret, Modelling of diffuse solar fraction with multiple predictors, Renew Energy 35 (2010) 478–483. https://doi.org/10.1016/j.renene.2009.07.018.

[111] DoE (Department of Energy), EnergyPlus documentation, engineering reference, the reference to EnergyPlus calculations, The Encyclopedic Reference to EnergyPlus Input and Output (2018) 1996–2016. https://energyplus.net/sites/all/modules/cust%0Aom/nrel_custom/pdfs/pdfs_v9.0.1/EngineeringReference.pdf (accessed August 27, 2023).

[112] S. Cui, M. Cohen, P. Stabat, D. Marchio, CO_2 tracer gas concentration decay method for measuring air change rate, Build Environ 84 (2015) 162–169. https://doi.org/10.1016/j.buildenv.2014.11.007.

[113] V. Gutiérrez González, G. Ramos Ruiz, C. Fernández Bandera, Ground characterization of building energy models, Energy Build 254 (2022). https://doi.org/10.1016/j.enbuild.2021.111565.

[114] D. Bienvenido-Huertas, D. Sánchez-García, C. Rubio-Bellido, J. Solís-Guzmán, Using adaptive strategies of natural ventilation with tolerances applied to the upper limit to improve social dwellings' thermal comfort in current and future scenarios, Sci Technol Built Environ 28 (2022) 527–546. https://doi.org/10.1080/23744731.2022.2040884.

[115] I. Sarna, J. Ferdyn-Grygierek, K. Grygierek, Thermal model validation process for building environment simulation: a case study for single-family house, Atmosphere (Basel) 13 (2022). https://doi.org/10.3390/atmos13081295.

[116] N. Kishore, Impact of climate change on future bioclimatic potential and residential building thermal and energy performance in India, Indoor and Built Environment 31 (2022) 329–354. https://doi.org/10.1177/1420326X21993919.

[117] Indian Green Building Council (IGBC), IGBC Green Affordable Housing: IGBC rating system (pilot version), Hyderabad, India, 2017.

[118] Bureau of Energy Efficiency (BEE), Energy Conservation Building Code 2017 (with amendments 2020), New Delhi, India, 2017. https://doi.org/https://beeindia.gov.in/sites/default/files/BEE_ECBC 2017.pdf.

Table AI1: RMSE values for the different datasets.

Compared datasets	City	Common data-points*	RMSE
IMD and NOAA	Ahmedabad	16,113	1.38
	Bengaluru	6,742	0.97
	Chennai	7,566	0.79
	Delhi	11,004	0.96
	Hyderabad	8,002	0.82
	Kolkata	6,092	0.87
	Mumbai	7,296	2.10
	Srinagar	1,719	2.08
IMD and Mean model	Ahmedabad	13,513	1.90
	Bengaluru	12,116	1.27
	Chennai	13,402	1.46
	Delhi	13,311	2.25
	Hyderabad	13,341	1.70
	Kolkata	13,286	1.75
	Mumbai	13,434	1.48
	Srinagar	12,760	2.67
IMD and TuTempo.net	Ahmedabad	30	1.00
	Bengaluru	30	1.19
	Chennai	30	0.46
	Delhi	30	0.62
	Hyderabad	30	0.92
	Kolkata	30	1.02
	Mumbai	30	0.93
	Srinagar	30	1.95

*RMSE values were calculated using all common data-points available between the primary and secondary datasets, except for the TuTiempo data, for which we randomly selected 30 data points for RMSE calculation.

Table AI2: Details of the general circulation models (GCMs).

S. No.	GCM name	Modeling center name
1	BCC-CSM1.1	Beijing Climate Center, China Meteorological Administration
2	CanESM2	Canadian Centre for Climate Modelling and Analysis
3	CNRM-CM5	Centre National de Recherches Meteorologiques/Centre Europeen de Recherche et Formation Avanceesen Calcul Scientifique
4	ACCESS1.0	CSIRO (Commonwealth Scientific and Industrial Research Organization, Australia), and BOM (Bureau of Meteorology, Australia)
5	CSIRO-Mk3.6	Commonwealth Scientific and Industrial Research Organization in collaboration with the Queensland Climate Change Centre of Excellence
6	BNU-ESM	College of Global Change and Earth System Science, Beijing Normal University
7	INM-CM4	Institute for Numerical Mathematics
8	IPSL-CM5A-LR	Institute Pierre-Simon Laplace
9	IPSL-CM5A-MR	Institute Pierre-Simon Laplace
10	MIROC5	Atmosphere and Ocean Research Institute (The University of Tokyo), National Institute for Environmental Studies, and Japan Agency for Marine-Earth Science and Technology
11	MIROC-ESM	Japan Agency for Marine-Earth Science and Technology, Atmosphere and Ocean Research Institute (The University of Tokyo), and National Institute for Environmental Studies
12	MIROC-ESM-CHEM	Japan Agency for Marine-Earth Science and Technology, Atmosphere and Ocean Research Institute (The University of Tokyo), and National Institute for Environmental Studies
13	MPI-ESM-LR	Max Planck Institute for Meteorology (MPI-M)
14	MPI-ESM-MR	Max Planck Institute for Meteorology (MPI-M)
15	MRI-CGCM3	Meteorological Research Institute
16	CCSM4	National Center for Atmospheric Research (NCAR)
17	NorESM1-M	Norwegian Climate Centre
18	GFDL-CM3	Geophysical Fluid Dynamics Laboratory
19	GFDL-ESM2G	Geophysical Fluid Dynamics Laboratory
20	GFDL-ESM2M	Geophysical Fluid Dynamics Laboratory
21	CESM1-BGC	National Science Foundation, Department of Energy, (NCAR)

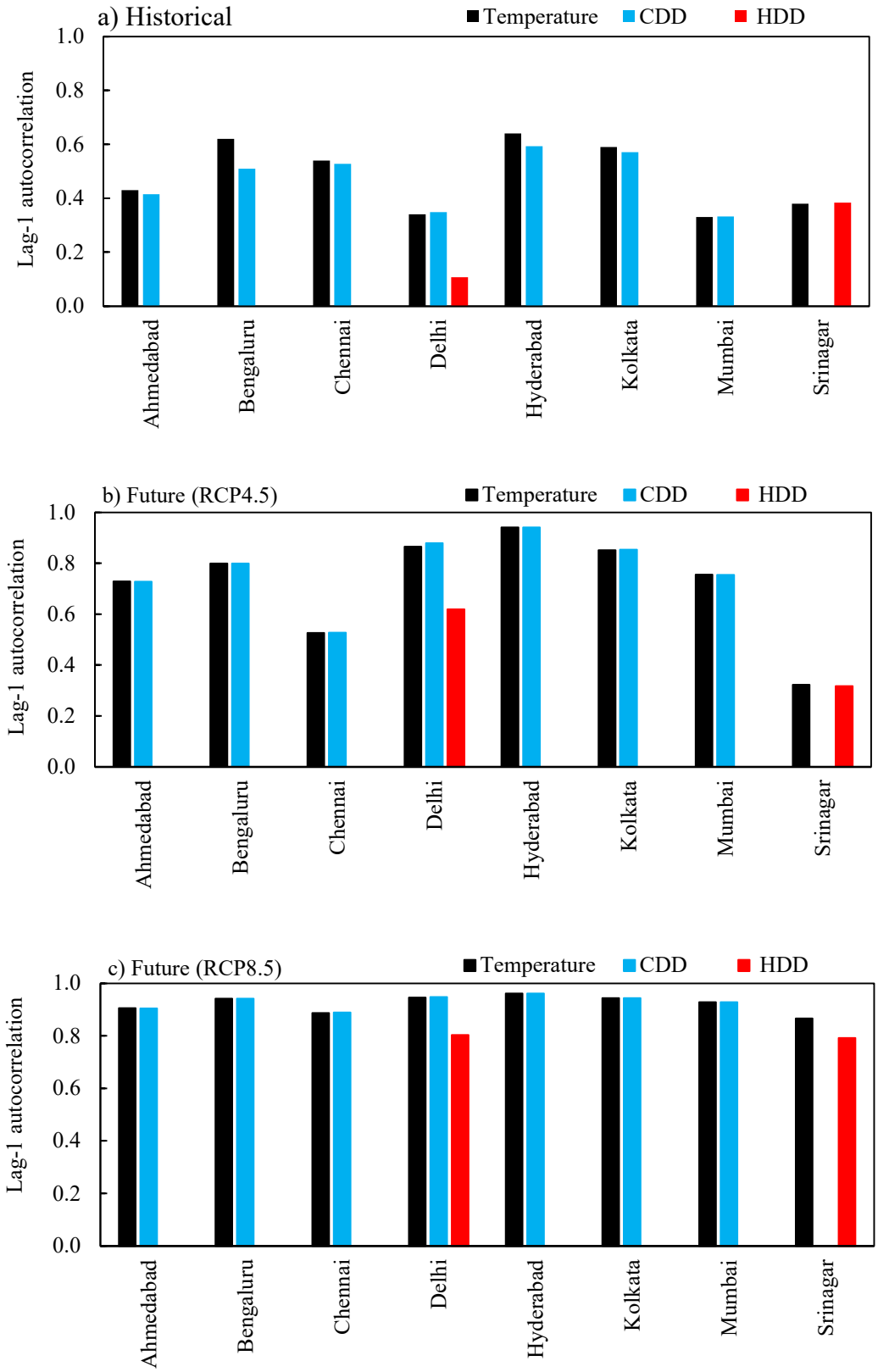

Figure AI1: Lag-1 autocorrelation for the temperature, cooling degree days (CDDs), and heating degree days (HDDs) for the a) historical, b) RCP4.5, and c) RCP8.5 conditions.

Mann Kendall (MK) Test Details

For a time-series represented by $x_1, x_2, \ldots\ x_n$, the MK test statistic is given by:

$$S = \sum_{i=1}^{n-1} \sum_{j=i+1}^{n} signum(x_j - x_i) \qquad \text{(Eq. 1)}$$

where S is the test statistic, n the number of observations in the time-series, x_i and x_j are the data values in the time-series at time i and j, ($j > i$). The signum function is defined as:

$$signum(x_j - x_i) = \begin{cases} 1, & \text{if } x_j - x_i > 0 \\ 0, & \text{if } x_j - x_i = 0 \\ -1, & \text{if } x_j - x_i < 0 \end{cases} \qquad \text{(Eq. 2)}$$

For n ≥ 10, the statistic S approximately follows a normal distribution with its mean and variance given by:

$$mean(S) = 0 \qquad \text{(Eq. 3a)}$$

$$variance(S) = \frac{n(n-1)(2n+5) - \sum_{k=1}^{m} t_k(t_k - 1)(2t_k + 5)}{18} \qquad \text{(Eq. 3b)}$$

where n is the number of observations, m is the number of tied groups, and t_k the number of ties in the k^{th} group. The test statistic (S) is then normalized to compute its standard normal deviate, Z:

$$Z = \begin{cases} \dfrac{S-1}{\sqrt{variance(S)}} & if\ S > 0 \\ 0 & if\ S = 0 \\ \dfrac{S+1}{\sqrt{variance(S)}} & if\ S < 0 \end{cases} \qquad \text{(Eq. 4)}$$

We rejected the null hypothesis if $|Z| > 1.96$ (for 95% significance level).

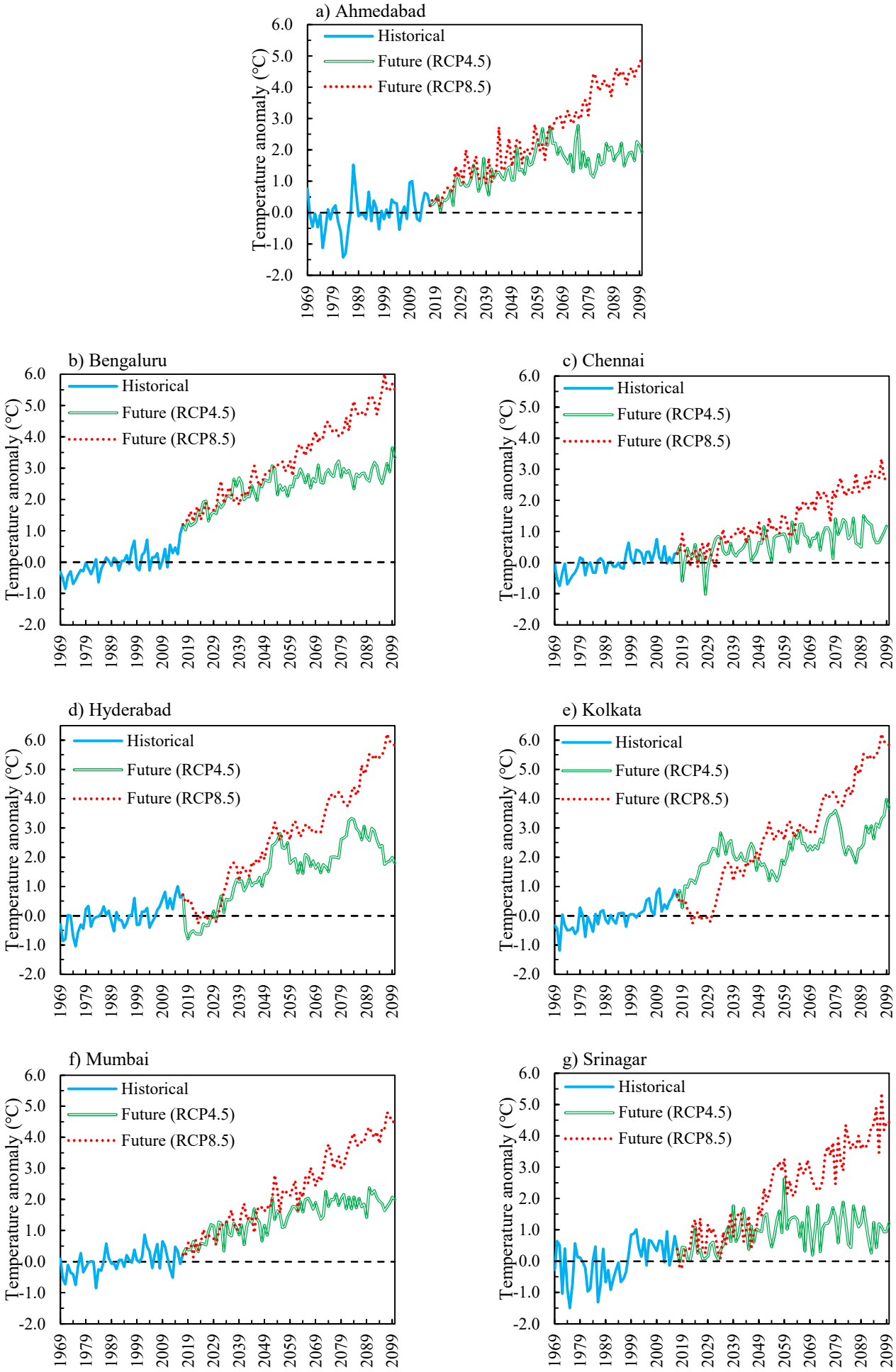

Figure AI2: Historical and future anomalies in annual mean temperatures in a) Ahmedabad, b) Bengaluru, c) Chennai, d) Hyderabad, e) Kolkata, f) Mumbai, and g) Srinagar.

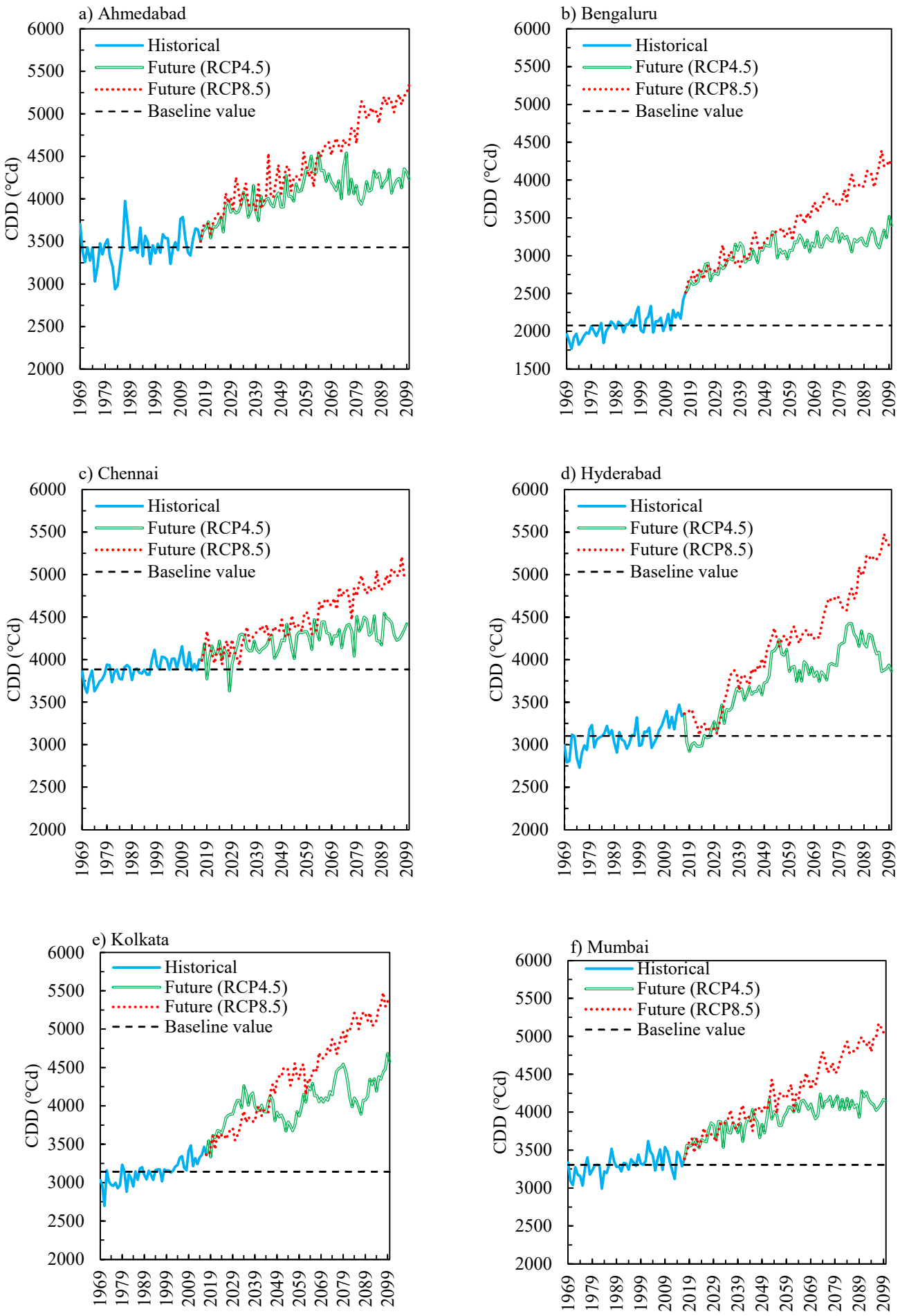

Figure AI3: Historical and future cooling degree days (CDDs) in a) Ahmedabad, b) Bengaluru, c) Chennai, d) Hyderabad, e) Kolkata, and f) Mumbai.

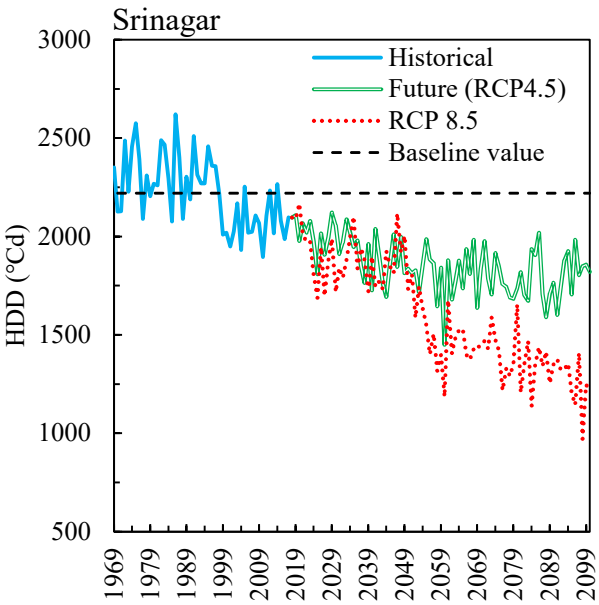

Figure AI4: Historical and future heating degree days (HDDs) in Srinagar.

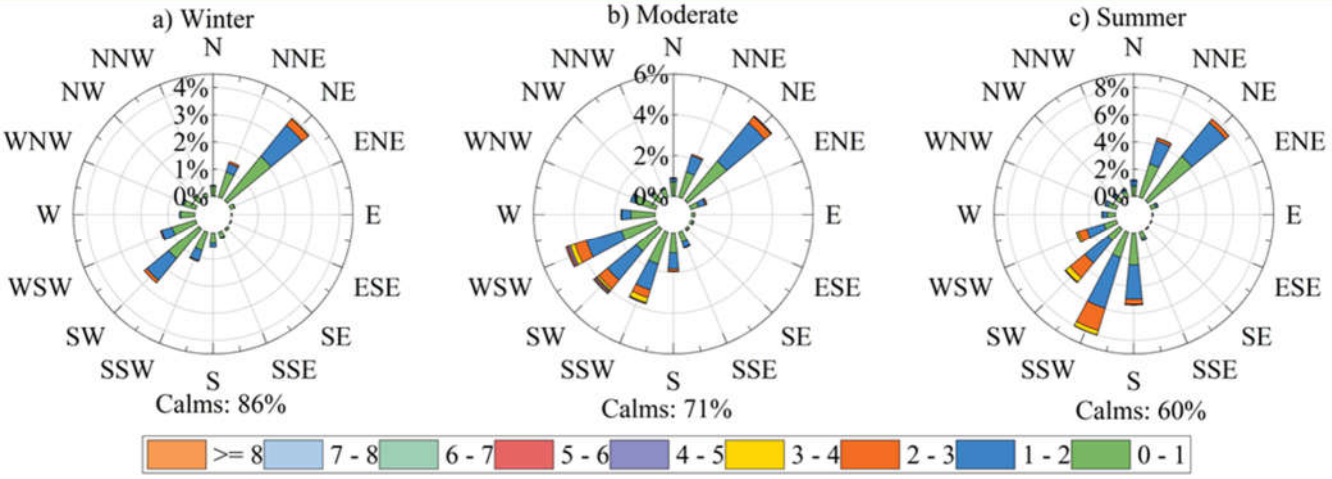

Figure AII1: Measured wind speed (m/s) and direction (degree).

.

Table AII1: Monthly value of the ground surface temperature.

Month	Ground surface temperature (°C)
January	12.0
February	16.9
March	25.9
April	28.8
May	30.9
June	32.4
July	31.6
August	30.5
September	28.0
October	25.8
November	19.1
December	14.0

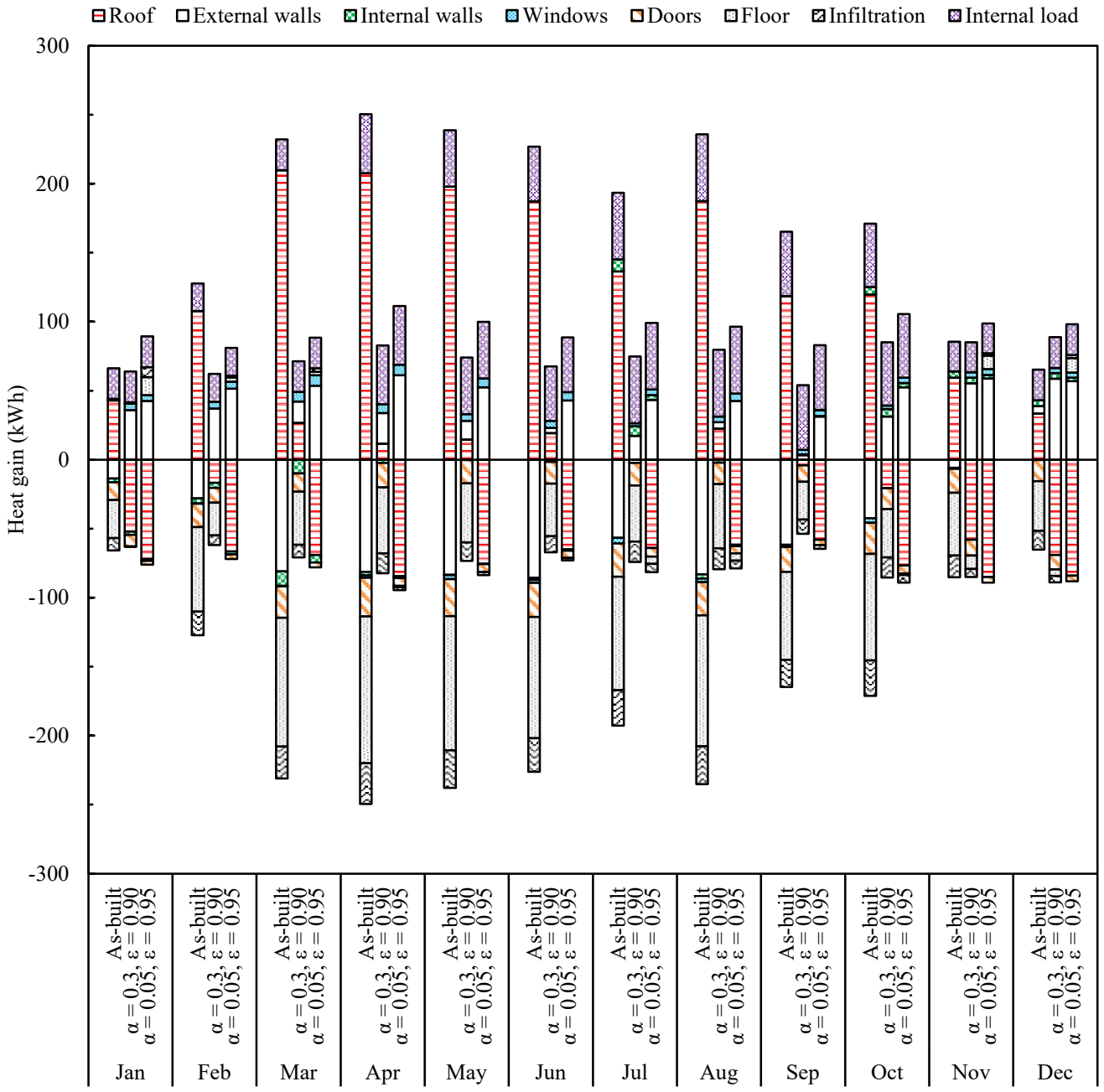

Figure AII2: Contributions of different building elements to the rooms's monthly heat gains and losses for the as-built construction and those with cool/super-cool roofs.

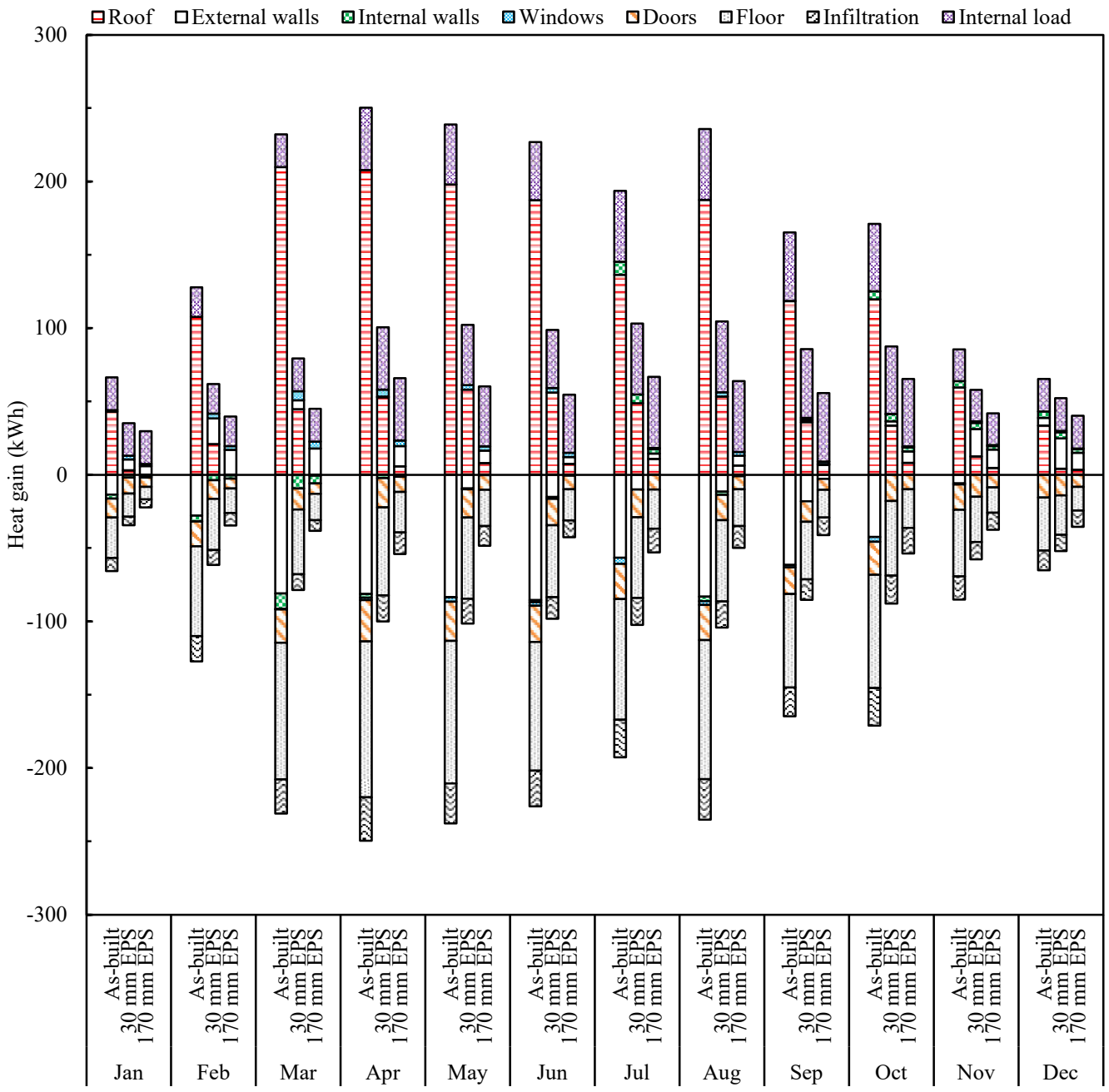

Figure AII3: Contributions of different building elements to the rooms's monthly heat gains and losses for the as-built construction and those with different roof insulation levels.

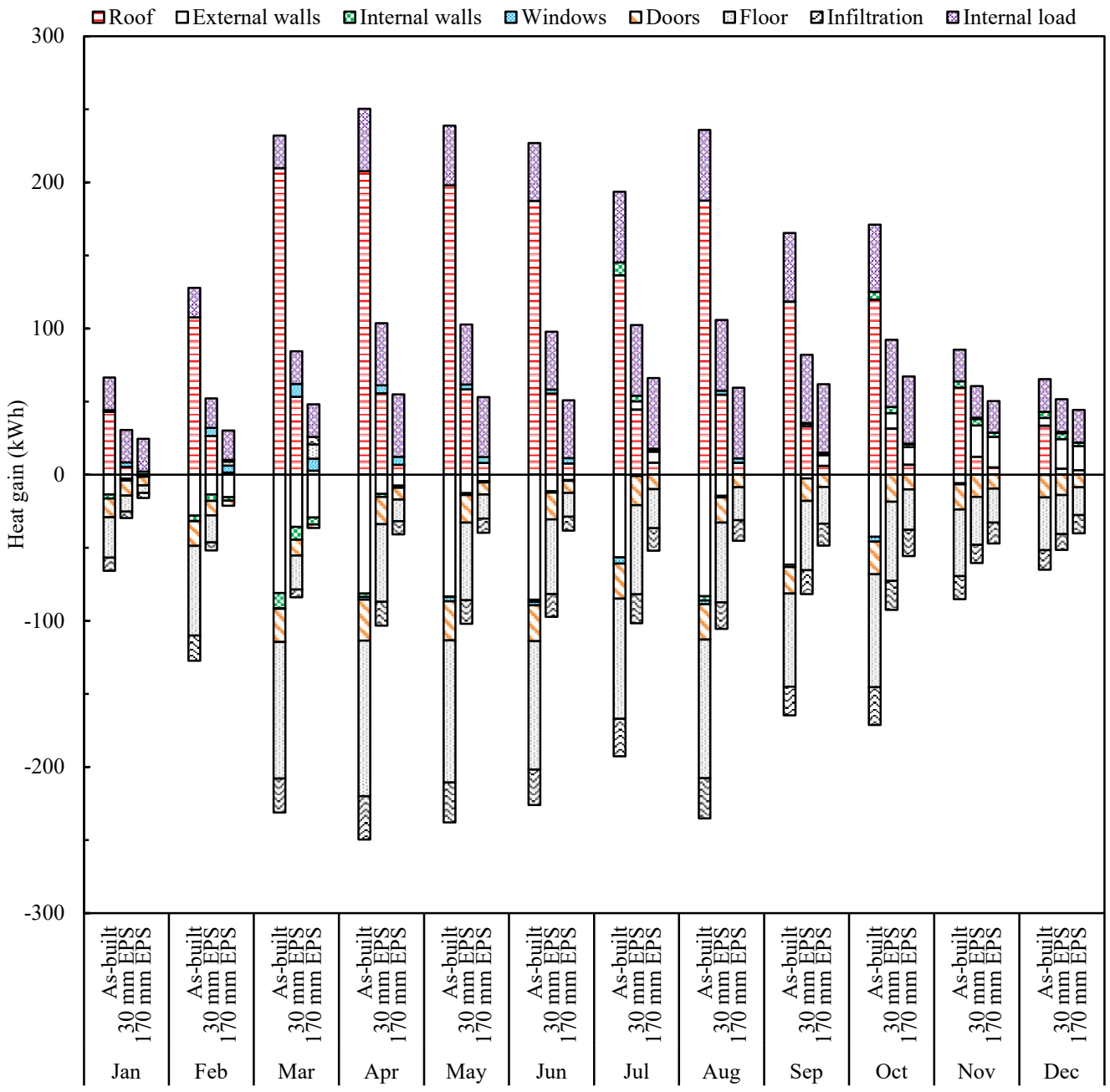

Figure AII4: Contributions of different building elements to the rooms's monthly heat gains and losses for the as-built construction and those with different envelope (wall and roof) insulation levels.

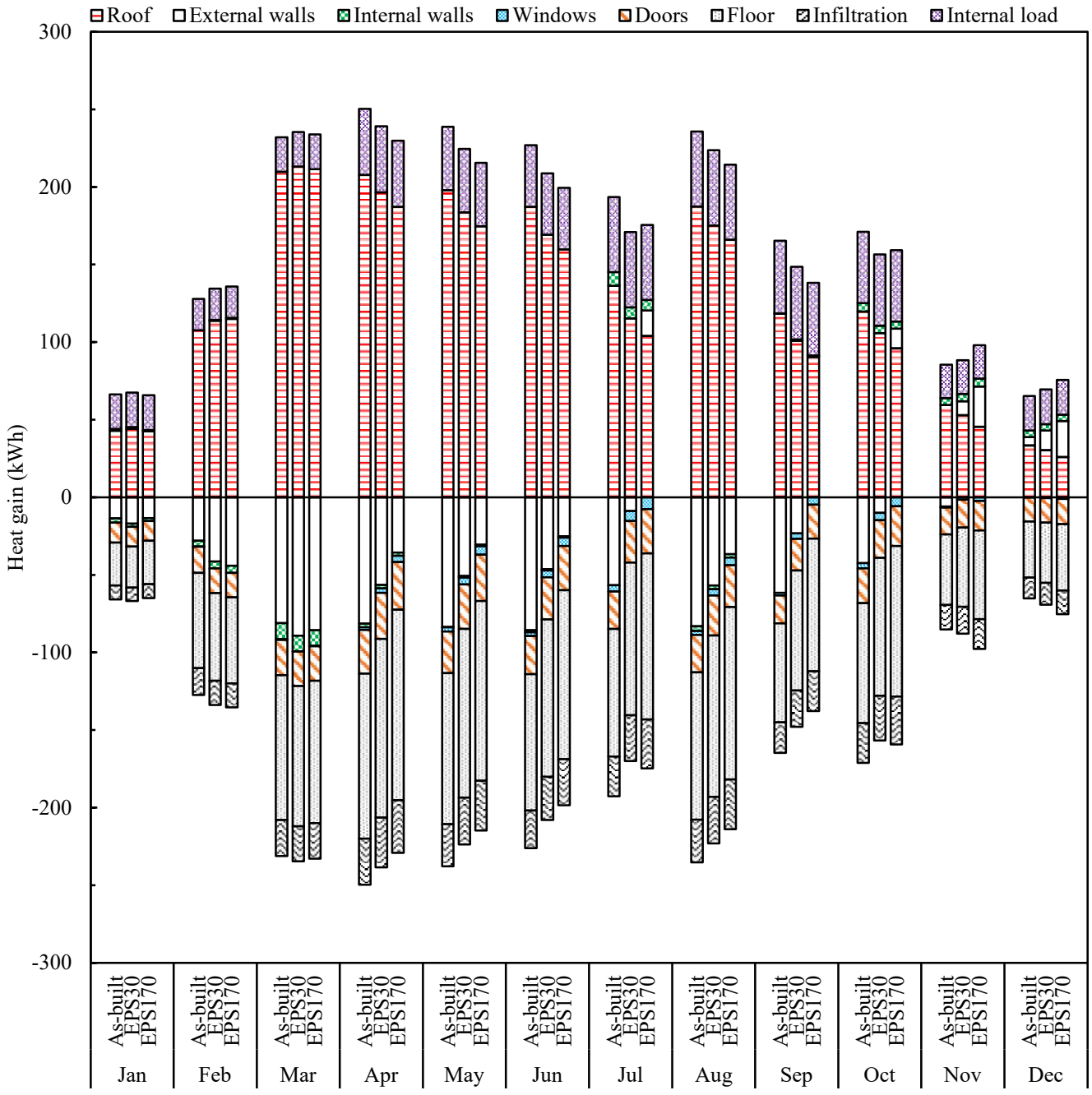

Figure AII5: Contributions of different building elements to the rooms's monthly heat gains and losses for the as-built construction and those with different wall insulation levels.

Peer Reviewed International Journals Publication

1. **Rahul Ukey,** and Aakash Cand Rai (2021) "Impact of global warming on heating and cooling degree days in major Indian cities" **Energy and Buildings, Elsevier.** (SCI/Q1/I.F.: 6.7). https://doi.org/10.1016/j.enbuild.2021.111050

2. **Rahul Ukey,** and Aakash Cand Rai (2024) "Envelope retrofits for enhancing thermal comfort in detached houses in hot semi-arid climatic conditions: a year-long monitoring and simulation study" **Building and Environment, Elsevier.** (SCI/Q1/I.F.: 7.4). https://doi.org/10.1016/j.buildenv.2024.111536

About the Candidate (Rahul Ukey)

Rahul Ukey graduated with Bachelor of Engineering (B.E.) in Mechanical Engineering from Swami Vivekanand College of Engineering, Indore, in 2008 and post-graduated with master's in engineering (M.E.) in Mechanical Engineering (Design and Thermal) from the Institute of Engineering & Technology, Indore, in 2012. He has more than five years of teaching experience. He joined the Department of Mechanical Engineering at BITS Pilani, Pilani campus, as a Ph.D. research scholar in January 2018. During his doctoral research, he has published one research paper to international journals and has another research paper currently under review. His research includes improving indoor comfort and energy efficiency in residential buildings. His research addresses climate change's impact on heating and cooling needs and explores retrofitting options for enhancing indoor thermal comfort.

His web page is https://www.bits-pilani.ac.in/research_scholars/rahul-ukey/

About the Supervisor (Dr. Aakash Chand Rai)

Dr. Aakash Chand Rai is B.Tech. in Mechanical Engineering from the Indian Institute of Technology (IIT) Kharagpur, India, and Ph.D. in Mechanical Engineering from Purdue University, USA. He has more than 08 years of teaching and research experience. He joined IIT Kanpur (IITK) as a faculty in 2022. Before joining IITK, he served as faculty in BITS Pilani and research fellow at the University of Surrey in UK, General Electric (GE), and DRDO in India. He is a recipient of prestigious national and international awards, including the ASHRAE Grant-in-Aid award, BITS OPERA award, and early career research award. His research interest includes energy-efficient buildings, the impact of climate change on the heating and cooling of buildings, indoor air quality, airborne infection transmission, and air pollution. He has more than 19 publications in international journals and international conferences. He is guiding five Ph.D. students, over 4 PG, and UG theses.

His web page is https://home.iitk.ac.in/~aakashrai/

About the Co-Supervisor (Prof. Shyam Sunder Yadav)

Prof. Shayam Shyam Sunder Yadav is an Associate Professor in the Department of Mechanical Engineering at BITS Pilani, Rajasthan. He received a Ph.D. in 2015 from the Indian Institute of Science Bangalore (IISc Bengaluru). Prior to that, he completed his B. Tech. in Mechanical Engineering from the National Institute of Technology Kurukshetra in 2004 and M.E. from the Indian Institute of Science Bangalore in 2010. He has over 07 years of teaching and research experience at graduate and post-graduate levels, in addition, he has 04 of industry experience. He works in the areas of computational fluid dynamics of multiphase flows, two-phase electrohydrodynamic flows, high-performance scientific computing, etc., mostly with open-source codes for scientific computing. He has published more than 20 research papers in national, international journals and proceedings. He also has two research projects for DST India and the National Supercomputing Mission.

His web page is https://www.bits-pilani.ac.in/pilani/shyam-sunder-yadav/